1 **Major perturbations in the global carbon cycle and photosymbiont-bearing**

2 **planktic foraminifera during the early Eocene**

3

4

5 Valeria Luciani[1], Gerald R. Dickens[2,3], Jan Backman [2], Eliana Fornaciari[4], Luca Giusberti[4],

6 Claudia Agnini[4], Roberta D'Onofrio[1]

7

8

9 [1]Department of Physics and Earth Sciences, Ferrara University, Polo Scientifico Tecnologico, via G.

10 Saragat 1, 44100, Ferrara, Italy

11 [2]Department of Geological Sciences, Stockholm University, SE-10691 Stockholm, Sweden

12 [3]Department of Earth Science, Rice University, Houston, TX 77005, USA

13 [4]Department of Geosciences, Padova University, via G. Gradenigo 6, 35131, Padova, Italy

14

15

16 *Correspondence to:* V. Luciani (valeria.luciani@unife.it)

17

18

19   **Abstract.** A marked switch in the abundance of the planktic foraminiferal genera

20   *Morozovella* and *Acarinina* occurred at low-latitude sites near the start of the Early Eocene

21   Climatic Optimum (EECO), a multi-million-year interval when Earth surface temperatures

22   reached their Cenozoic maximum. Stable carbon and oxygen isotope data of bulk sediment

23   are presented from across the EECO at two locations: Possagno in northeast Italy, and DSDP

24   Site 577 in the northwest Pacific. Relative abundances of planktic foraminifera are presented

25   from these two locations, as well as from ODP Site 1051 in the northwest Atlantic. All three

26   sections have good stratigraphic markers, and the δ^{13}C records at each section can be

27   correlated amongst each other and to δ^{13}C records at other locations across the globe. These

28   records show that a series of negative carbon isotope excursions (CIEs) occurred before,

29   during and across the EECO, which is defined here as the interval between the "J" event and

30   the base of *Discoaster sublodoensis*. Significant though ephemeral modifications in planktic

31   foraminiferal assemblages coincide with some of the short-term CIEs, which were marked by

32   increases in the relative abundance of acarininids, similar to what happened across

33   established hyperthermal events in Tethyan settings prior to the EECO. Most crucially, a

34   temporal link exists between the onset of the EECO, carbon cycle changes during this time,

35   and the decline of morozovellids. Possible causes are multiple, and may include temperature

36   effects on photosymbiont-bearing planktic foraminifera and changes in ocean chemistry.

37

38

39

40

41

42

43

44

1 Introduction

Cenozoic Earth surface temperatures attained their warmest long-term state during the Early Eocene Climatic Optimum (EECO). This was a 2-4 Myr time interval (discussed below) centered at ca. 51 Ma (**Figure 1**), when average high latitude temperatures exceeded those at present-day by at least 10°C (Zachos et al., 2008; Huber and Caballero, 2011; Hollis et al., 2012; Pross et al., 2012; Inglis et al., 2015). Several short-term (<200 kyr) global warming events (**Figure 1**) occurred before the EECO. The Paleocene Eocene Thermal Maximum (PETM) provides the archetypical example: about 55.9 Ma (Vandenberghe et al., 2012; Hilgen et al., 2015) temperatures soared an additional 5-6°C relative to background conditions (Sluijs et al., 2006, 2007; Dunkley Jones et al., 2013). Evidence exists for at least two other significant Eocene warming events (Cramer et al., 2003; Lourens et al., 2005; Röhl et al., 2005; Thomas et al., 2006; Nicolo et al., 2007; Agnini et al., 2009; Coccioni et al., 2012; Lauretano et al., 2015; Westerhold et al., 2015): one ca. 54.1 Ma and named H-1 or Eocene Thermal Maximum 2 (ETM-2, also referred as the ELMO event), and one at 52.8 Ma and variously named K, X, or ETM-3 (hereafter called K/X). However, additional brief warming events may have spanned the early Eocene (above references; Kirtland-Turner et al., 2014), and the EECO may comprise a series of successive events (Slotnick et al., 2012). Both long-term and short-term intervals of warming corresponded to major changes in global carbon cycling, although the precise timing between these parameters remains insufficiently resolved.

In benthic foraminiferal stable isotope records for the early Paleogene (**Figure 1**), $\delta^{18}O$ serves as a proxy for deep-water temperature, while $\delta^{13}C$ relates to the composition of deep-water dissolved inorganic carbon (DIC). The highest $\delta^{13}C$ values of the Cenozoic occurred at ca. 58 Ma. From this Paleocene Carbon Isotope Maximum (PCIM), benthic foraminiferal

3

70 $\delta^{13}C$ values plunge by approximately 2.5 ‰ to reach a near Cenozoic minimum at or near the

71 start of the EECO, and subsequently rise by approximately 1.5 ‰ across this interval (Zachos

72 et al., 2001, 2008; Cramer et al., 2009). Benthic foraminiferal $\delta^{13}C$ records also exhibit

73 prominent negative carbon isotope excursions (CIEs) across the three hyperthermals

74 mentioned above (Kennett and Stott, 1991; Littler et al., 2014; Lauretano et al., 2015).

75 Crucially, at least from the late Paleocene to the start of the EECO, similar $\delta^{13}C$ records occur

76 in other carbon-bearing phases, such as bulk marine carbonate, planktic foraminifera, and

77 various marine and terrestrial organic carbon compounds (Shackleton, 1986; Schmitz et al.,

78 1996; Lourens et al., 2005; Nicolo et al., 2007; Agnini et al., 2009, submitted; Leon-

79 Rodriguez and Dickens, 2010; Abels et al., 2012; Coccioni et al., 2012; Sluijs and Dickens,

80 2012; Slotnick et al. 2012, 2015a; Clyde et al., 2013). This strongly suggests that observed

81 changes in $\delta^{13}C$, both long-term trends as well as short-term perturbations, represent

82 variations in the input and output of ^{13}C-depleted carbon to the exogenic carbon cycle

83 (Shackleton, 1986; Dickens et al., 1995; Dickens, 2000; Kurtz et al., 2003; Komar et al.,

84 2013).

85   Significant biotic changes occur in terrestrial and marine environments during times

86 when the early Paleogene $\delta^{18}O$ and $\delta^{13}C$ records show major variations. This has been

87 recognized for the PETM, where land sections exhibit a prominent mammal turnover

88 (Gingerich 2001, 2003; McInerney and Wing, 2011; Clyde et al., 2013), and where marine

89 sections reveal a profound benthic foraminiferal extinction (Thomas, 1998), turnovers in

90 calcareous nannoplankton, ostracods, corals and larger benthic foraminifera (Raffi and De

91 Bernardi, 2008; Scheibner and Speijer, 2008; Yamaguchi and Norris, 2012; Agnini et al.,

92 2014), and appearances of excursion taxa in calcareous nannoplankton, dinoflagellates and

93 planktic foraminifera (Kelly et al., 1996, 1998; Crouch et al., 2001; Sluijs et al., 2006; Self-

94 Trail et al., 2012). Major plant and mammal turnovers also occurred on land during the longer

95   EECO (Wing et al., 1991; Zonneveld et al., 2000; Wilf et al., 2003; Falkowski et al., 2005;

96   Woodbourne et al., 2009; Figueirido et al., 2012). In the marine realm, evolutionary trends

97   across the EECO have been noted, in particular the inception of modern calcareous

98   nannofossil community structure (Agnini et al., 2006, 2014; Schneider et al., 2011; Shamrock

99   et al., 2012) and possibly the same for diatoms (Sims et al., 2006; Oreshkina, 2012). These

100   observations, both from continents and the oceans, support an overarching hypothesis that

101   climate change drives biotic evolution, at least in part (Ezard et al., 2011).

102   Planktic foraminiferal assemblages are abundant in carbonate bearing marine sediments

103   and display distinct evolutionary trends that often can be correlated to climate variability

104   (Schmidt et al., 2004; Ezard et al., 2011; Fraass et al., 2015). This is especially true in the

105   early Paleogene, even though the relationship between climate variability and planktic

106   foraminiferal evolution remains insufficiently known. At the beginning of the Eocene,

107   planktic foraminifera had evolved over ca. 10 Myr following the Cretaceous-Paleogene mass

108   extinction event. Several early Paleogene phylogenetic lines evolved, occupying different

109   ecological niches in the upper water column. Subsequently, a major diversification occurred

110   during the early Eocene, which resulted in a peak of planktic foraminiferal diversity during

111   the middle Eocene (Norris, 1991; Schmidt et al., 2004; Pearson et al., 2006; Aze et al., 2011;

112   Ezard et al., 2011; Fraass et al., 2015).

113   In this study, we focus on the evolution of two planktic foraminiferal genera:

114   morozovellids and acarininids (**Figure 1**). These two genera belong to the "muricate group",

115   a term derived from the muricae that form layered pustules on the test wall. These two genera

116   are of particular interest because of their dominance among tropical and subtropical

117   assemblages of the early Paleogene oceans, and because these genera show a major turnover

118   in taxonomic diversity close to the beginning of the EECO, one that comprises species

119   reduction among morozovellids and species diversification among acarininids (Lu and

120   Keller, 1995; Lu et al., 1998; Pearson et al., 2006; Aze et al., 2011).

121   Numerous lower Eocene sedimentary sections from lower latitudes contain well-

122   preserved (albeit often recrystallized) planktic foraminiferal tests. Changes in foraminiferal

123   assemblages presumably reflect relationships between climate and carbon cycling across the

124   EECO. The present problem is that no section examined to date provides counts of

125   foraminiferal assemblages, detailed stable isotope records and robust planktic foraminiferal

126   biostratigraphies across the entire EECO. Indeed, at present, only a few sites have detailed

127   and interpretable stable isotope records across much of the EECO (Slotnick et al., 2012,

128   2015a; Kirtland-Turner et al., 2014). Furthermore, the EECO lacks formal definition. As a

129   consequence, any relationship between climatic perturbations during the EECO and the

130   evolution of planktic foraminifera remains speculative. Here, we add new data from three

131   locations: the Possagno section from the western Tethys, DSDP Site 577 from the tropical

132   Pacific Ocean, and ODP Site 1051 from the subtropical Atlantic Ocean **(Figure 2)**. These

133   sections hence represent a wide longitudinal span of low latitude locations during the early

134   Paleogene. By comparing stable isotope and planktic foraminiferal records at these three

135   locations, we provide a new foundation for understanding why the abundances of acarininids

136   and morozovellids changed during the EECO.

137

138   **2 The Early Eocene Climatic Optimum**

139

140   Evidence for extreme Earth surface warmth during a multi-million year time interval of the

141   early Eocene is overwhelming, and comes from many studies, utilizing both marine and

142   terrestrial sequences, and both fossil and geochemical proxies (Huber and Caballero, 2011;

143   Hollis et al., 2012; Pross et al., 2012). However, a definition for the EECO, including the

144   usage of "optimum", endures as a perplexing problem. This is for several reasons, including

145   the basic facts that: (i) proxies for temperature should not be used to define a time increment,

146   (ii) clearly correlative records across the middle of the early Eocene with temporal resolution

147   less than 50 kyr remain scarce, and (iii) absolute ages across the early Eocene have changed

148   significantly (Berggren et al., 1995; Vandenberghe et al., 2102). As a consequence, various

149   papers discussing the EECO give different ages and durations spanning from 2 to 4 Myr long

150   sometime between circa 49 and 54 Ma (e.g., Yapp, 2004; Lowenstein and Demicco, 2006;

151   Zachos et al., 2008; Woodburne et al., 2009; Bijl et al., 2009; Smith et al., 2010; Hollis et al.,

152   2012; Slotnick et al., 2012; Puljalte et al., 2015).

153   The EECO, at least as presented in many papers, refers to the time of minimum $\delta^{18}O$

154   values in "stacked" benthic foraminifera stable isotope curves (**Figure 1**). These curves were

155   constructed by splicing together multiple $\delta^{18}O$ records generated at individual locations onto

156   a common age model (originally Berggren et al., 1995). However, the stacked curves (Zachos

157   et al., 2001, 2008; Cramer et al., 2009), while they can be adjusted to different time scales,

158   show significant variance in $\delta^{18}O$ across the middle to late early Eocene. Some of this

159   variance belies imprecisely calibrated records at individual sites, where cores do not align

160   properly in the depth domain (Dickens and Backman, 2013). Some of this variance probably

161   reflects a dynamic early Eocene climate regime, where average temperatures and atmospheric

162   pCO_2 across Earth changed significantly, perhaps on orbital time scales (Smith et al., 2010;

163   Slotnick et al., 2012, 2015a; Kirtland-Turner et al., 2014).

164   There is also the root problem as to where EECO starts and ends. At a basic level, the

165   interval characterized by the lowest Cenozoic benthic foraminiferal $\delta^{18}O$ values begins at a

166   time that closely corresponds with a long-term minimum in $\delta^{13}C$ values (**Figure 1**). This is

167   important for stratigraphic reasons because the two stable isotope curves were generated

168   using the same benthic foraminiferal samples, but $\delta^{13}C$ records at different locations should

169   necessarily correlate in the time domain (unlike $\delta^{18}O$ and temperature). The rationale for such

170   carbon isotope stratigraphy lies in the rapid cycling of carbon across Earth's surface

171   (Shackleton, 1986; Dickens, 2000).

172   The Eocene minimum in $\delta^{13}C$ corresponds to the K/X event (**Figure 1**), which happened

173   in polarity chron C24n.1n and approximately 3 Myr after the PETM (Agnini et al., 2009;

174   Leon-Rodriguez and Dickens, 2010; Slotnick et al., 2012; Dallanave et al., 2015; Lauretano

175   et al., 2015; Westerhold et al., 2015). However, in several detailed studies spanning the early

176   Eocene, changes in long-term trends appear to have occurred about 400 kyr before the K/X

177   event, and at an event called "J" (after Cramer et al., 2003), which happened near the

178   boundary of polarity chrons C24n.2r and C24n.3n (Slotnick et al., 2015a; Lauretano et al.,

179   2015). Notably, the long-term late Paleocene-early Eocene decrease in detailed benthic

180   foraminiferal $\delta^{18}O$ records at Site 1262 on Walvis Ridge ceases at the J event (Lauretano et

181   al., 2015).

182   The end of the EECO has received limited attention from a stratigraphic perspective. In

183   Paleogene continental slope sections now uplifted and exposed in the Clarence River Valley,

184   New Zealand, a major lithologic change from limestone to marl coincides with the J event

185   (Slotnick et al., 2012, 2015a; Dallanave et al., 2015). The marl-rich unit, referred to as

186   "Lower Marl", has been interpreted to reflect enhanced terrigenous supply to a continental

187   margin because of greater temperature and enhanced seasonal precipitation. It has been

188   suggested further that Lower Marl expresses the EECO (Slotnick et al., 2012; Dallanave et

189   al., 2015). The top of Lower Marl, and a return to limestone deposition, lies within the upper

190   part of polarity chron C22n (Dallanave et al., 2015). This is interesting because it

191   approximates the time when general long-term Cenozoic cooling initiates at several locations

192   that have records of polarity chrons and proxies for temperature (Hollis et al., 2012; Pross et

193   al., 2012). It is also useful from a stratigraphic perspective because the end of the EECO thus

194   lies close to a well documented and widespread calcareous nannofossil biohorizon, the base

195 of *Discoaster sublodoensis*. This marks the base of CP10, NP12 or CNE4, depending on the

196 chosen calcareous nannofossil zonal scheme (Okada and Bukry, 1080; Martini, 1971; Agnini

197 et al., 2014).

198 Without an accepted definition in the literature, we tentatively present the EECO as the

199 duration of time between the J event and the base of *D. sublodoensis*. This interval thus

200 begins at about 53 Ma and ends at about 49 Ma on the 2012 Time Scale (GTS; Vandenberghe

201 et al., 2012). However, while the EECO was characterized by generally warm conditions,

202 numerous fluctuations in average temperature likely occurred during the 4 Myr interval.

203

204 **3 Sites and stratigraphy**

205

206 **3.1 Possagno, Venetian Prealps, Tethys**

207

208 An Upper Cretaceous through Miocene succession crops out at the bottom of the Monte

209 Grappa Massif in the Possagno area, about 60 km northwest of Venice. The lower to middle

210 Eocene, of primary focus to this study, is represented by the Scaglia beds. These

211 sedimentary rocks represent pelagic and hemipelagic sediment that accumulated at middle to

212 lower bathyal depths (Cita, 1975; Thomas, 1998) in the western part of the Belluno Basin, a

213 Mesozoic–Cenozoic paleogeographic unit of the Southern Alps (Bosellini, 1989). The basin

214 very likely was an embayment connected to the western Tethys, with a paleolatitude of ca.

215 42° during the early Eocene (**Figure 2**).

216 A quarry at 45°51.0' N and 11°51.6' E exposed in 2002-2003 a 66 m thick section of

217 the Scaglia beds (Figure 3), although it is at present largely covered and inaccessible. This

218 section was examined for its stratigraphy (Agnini et al., 2006; Luciani and Giusberti, 2014),

219 and shown to extend from just below the PETM to within lower Chron C20r in the lower

220 middle Eocene. Like other lower Paleogene sections of the Venetian Pre-alps (Giusberti et

221 al., 2007; Agnini et al., submitted), a Clay Marl Unit (CMU) with a prominent negative CIE

222 marks the PETM.

223   The Possagno section appears to be continuous, but with an important decrease in

224 sedimentation rate (to below 1.4 m/Myr) between 14.66 m and 15.51 m (Agnini et al., 2006).

225 This interval lies within Chron C23r and near the start of the EECO, and predates the onset

226 of a major increase in discoaster abundance (Agnini et al., 2006).

227

228 **3.2 Site 577, Shatsky Rise, Western Pacific**

229

230 Deep Sea Drilling Project (DSDP) Leg 86 drilled Site 577 at 32°26.5' N, 157°43.4' E, and

231 2680 m water depth, on Shatsky Rise, a large igneous plateau in the NW Pacific with a

232 relatively thin veneer of sediment (Shipboard Scientific Party 1985). During the early

233 Eocene, this site was located closer to 15° N (**Figure 2**), and probably at a slightly shallower

234 water depth (Ito and Clift, 1998).

235   Two primary holes were drilled at Site 577. Both Hole 577* and Hole 577A recovered

236 portions of a nominally 65 m thick section of Upper Cretaceous through lower Eocene

237 nannofossil ooze. Similar to the Possagno section, the lower Paleogene interval has

238 biomagnetostratigraphic information (Bleil, 1985; Monechi et al., 1985; Backman, 1986; Lu

239 and Keller, 1995; Dickens and Backman, 2013). Stable isotope records of bulk carbonate

240 have been generated for sediment from several cores at low sample resolution (Shackleton,

241 1986), and for much of Cores 577*-9H and 577*-10H at fairly high sample resolution

242 (Cramer et al. 2003).

243   The composition and relative abundances of planktic foraminifera were nicely

244 documented at Site 577 (Lu, 1995; Lu and Keller, 1995), and show a marked turnover

245 between morozovellids and acaraninids during the early Eocene. These data, however, have

246 remained on an out-dated view for the stratigraphy at this location, where cores were not

247 originally aligned to account for gaps and overlaps (Dickens and Backman, 2013). As will

248 become obvious later, the main phase of the EECO spans Cores 577*-8H and 577A-8H,

249 where detailed stable isotope records have not been generated previously.

250

251 **3.3 Site 1051, Blake Nose, Western Atlantic**

252

253 The Blake Nose is a gentle ramp extending from 1000 m to 2700 m water depth east of

254 Florida (Norris et al, 1998). The feature is known for a relatively thick sequence of middle

255 Cretaceous through middle Eocene sediment with minimal overburden. Ocean Drilling

256 Program (ODP) Leg 171B drilled and cored this sequence at several locations, including Site

257 1051 at 30°03.2' N, 76°21.5' W, and 1994 m water depth (Shipboard Scientific Party 1998).

258 The site was located slightly to the south during the early Eocene (**Figure 2**). Benthic

259 foraminiferal assemblages indicate a lower bathyal depth (1000-2000 m) during the late

260 Paleocene and middle Eocene (Norris et al., 1998), although Bohaty et al. (2009) estimated a

261 paleodepth of about 2200 m for sedimentation ca. 50 Ma.

262   Sediments from 452.24 to 353.10 meters below sea floor (mbsf) at Site 1051 consist of

263 lower to middle Eocene carbonate ooze and chalk (Shipboard Scientific Party, 1998). The

264 site comprises two holes (1051A and 1051B), with core gaps and core overlaps existing at

265 both (Shipboard Scientific Party, 1998). However, the impact of these depth offsets upon

266 age is less than at Site 577, because of higher overall sedimentation rates.

267   The Eocene section at Site 1051 has good sediment recovery, except an interval between

268 382 mbsf and 390 mbsf, which contains significant chert. Stratigraphic markers across the

269 Eocene interval include polarity chrons (Ogg and Bardot, 2001), calcareous nannofossil

270 biohorizons (Mita, 2001), and planktic foraminiferal biohorizons (Norris et al., 1998; Luciani

271 and Giusberti, 2014). As first noted by Cramer et al. (2003), though, there is a basic

272 stratigraphic problem with the labelling of the polarity chrons. The intervals of normal

273 polarity between approximately 388 and 395 mbsf, and between approximately 412 and 420

274 mbsf were tentatively assigned to C22n and C23n, respectively (Ogg and Bardot, 2001). This

275 age assignment was assumed to be correct by Luciani and Giusberti (2014), who therefore

276 considered the last occurrence of *Morozovella subbotinae* as happening near the top of C23n,

277 an assumption that was also made for the revision of Eocene foraminiferal biozones (Wade et

278 al., 2011).

279   These age assignments, however, cannot be correct, because calcareous nannofossil

280 biohorizons that lie below or within C22n (top of *T. orthostylus*, top of *Toweius*, base of *D.*

281 *sublodoensis*) occur above 388 mbsf (Mita, 2001). Instead, there must be a significant hiatus

282 or condensed interval at the chert horizon, and the above noted intervals of normal polarity

283 are C23n and C24n.1n.

284

285 **4 Methods**

286

287 **4.1 Samples for isotopes and foraminifera**

288

289 The three sites provide a good stratigraphic background and key existing data for

290 understanding the temporal link between the EECO, carbon isotope perturbations and

291 planktic foraminiferal evolution. Our analytical aim was to obtain comparable data sets

292 across the sites. More specifically, a need existed to generate stable isotope and planktic

293 foraminiferal assemblage records at the Possagno section, to generate stable isotope records

294 at DSDP Site 577, and to generate planktic foraminiferal assemblage records at ODP Site

295   1051.

296   In total, 298 samples were collected from the originally exposed Possagno section in

297   2002-2003 for isotope analyses. The sampling interval was 2 to 5 cm for the basal 0.7 m, and

298   at variable spacing from 20 to 50 cm for the interval between 0.7 m and 66 m. Bulk sediment

299   samples previously were examined for their calcareous nannofossil assemblages (Agnini et

300   al., 2006). One hundred and ten of these samples were selected for the foraminiferal study.

301   Aliquots of the 110 samples were weighed, and then washed to obtain foraminifera using

302   two standard procedures, depending on lithology. For the indurated marly limestones and

303   limestones, the cold-acetolyse technique was used (Lirer, 2000; Luciani and Giusberti, 2014).

304   This method disaggregates strongly lithified samples, in which foraminifera otherwise can be

305   analyzed only with thin sections (Fornaciari et al., 2007; Luciani et al., 2007). For the marls,

306   samples were disaggregated using 30 % hydrogen peroxide and subsequently washed and

307   sieved at 63 μm. In most cases, gentle ultrasonic treatment (e.g., low-frequency at 40 kHz for

308   30–60 seconds) improved the cleaning of the tests.

309   Relative abundance data of planktic foraminiferal samples were generated for 65 samples

310   at Site 577 (Lu, 1995; Lu and Keller, 1995). We collected new samples for stable isotope

311   measurements that span their previous effort.

312   Fifty samples of Eocene sediment were obtained from Hole 1051A between 452 to 353

313   mbsf. Sample spacing varied from 2.0 m to 0.5 m. As the samples are ooze and chalk, they

314   were prepared using disaggregation using distilled water and washing over 38 μm and 63 μm

315   sieves. Washed residues were dried at <50°C.

316

317   **4.2 Stable Isotopes**

318

319   Carbon and oxygen stable isotope data of bulk sediment samples from the Possagno section

320   and Site 577 were analysed using a Finnigan MAT 252 mass spectrometer equipped with a

321   Kiel device at Stockholm University. Precision is within ±0.06 ‰ for carbon isotopes and

322   within ±0.07 ‰ for oxygen isotopes. Stable isotope values were calibrated to the Vienna Pee

323   Dee Belemnite standard (VPDB) and converted to conventional delta notation (δ^{13}C and

324   δ^{18}O).

325

326   **4.3 Foraminifera analyses**

327

328   The mass percent of the >63 μm size fraction relative to the mass of the bulk sample,

329   typically 100 g/sample was calculated for the 110 Possagno samples. This is referred to as the

330   weight percent coarse fraction, following many previous works. Due to the consistent

331   occurrence of radiolarians at Site 1051, the coarse fraction cannot give information on

332   foraminiferal productivity.

333   Relative abundances for both Possagno and Site 1051 have been determined from about

334   300 complete specimens extracted from each of the 110 samples investigated in the >63 μm

335   size fraction from random splits.

336   The degree of dissolution, expressed as the fragmentation index (F index) was evaluated

337   according to Petrizzo et al. (2008) on ca. 300 elements, by counting planktic foraminiferal

338   fragments or partially dissolved tests versus complete tests. These data are expressed in

339   percentages. Fragmented foraminifera include specimens showing missing chambers and

340   substantial breakage. The taxonomic criteria for identifying planktic foraminifera follows the

341   work by Pearson et al. (2006).

342

343   **5 Results**

344

345   **5.1 Carbon isotopes**

346

347   *Possagno*

348   Carbon isotopes of bulk carbonate at Possagno vary between +1.8 and -0.3 ‰ (**Figure 4,**

349   **Table S1**). Overall, $\delta^{13}C$ decreases from 1.8 ‰ at the base of the section to about 0.6 ‰ at 14

350   m. Generally, values then increase to 1.5 ‰ at 24 m, and remain between 1.5 ‰ and 0.8 ‰

351   for the remainder of the studied interval.

352   Superimposed on these trends are a series of negative CIEs. The most prominent of these

353   (~1.5 ‰) occurs at the 0 m level, and marks the PETM (Agnini et al., 2009). However, other

354   negative CIEs lie above this marker and within the lowermost 21.4 m, albeit some are only

355   defined by one data point (**Figure 4, Table S1**). The lower two at ~8 m and ~12.5 m probably

356   represent the H-1/ETM-2 and J event, respectively, as they lie at the appropriate stratigraphic

357   horizons in relation to polarity chrons. The K/X event may lie at 14.8 m, although this height

358   marks the start of the condensed interval.

359   The complex interval between 15.5 m and 24 m broadly corresponds to all of Chron

360   C23n and the bottom half of Chron C22r. A series of CIEs occur in that interval on the order

361   of 1.4 ‰, superimposed on a background trend of increasing $\delta^{13}C$ values (about 0.7 ‰). We

362   tentatively label these CIEs with even numbers for internal stratigraphic purposes (**Figure 4**),

363   as will become obvious below; their magnitudes range between 0.9 and 0.3 ‰ (**Table S1**).

364   However, the sample spacing through this interval varies from 20 to 50 cm. The precise

365   magnitudes and positions certainly could change with higher sample resolution, given the

366   estimated compacted sedimentation rate of ~0.5 cm/kyr for this part of the section (Agnini et

367   al., 2006).

368   Above Chron C22r, the Possagno $\delta^{13}C$ record contains additional minor CIEs (**Figure 4**).

369   The most prominent of these CIEs, at least relative to baseline values (~1.2 ‰), occurs within

370 Chron C21n. More important to understanding the EECO, a ~0.6 ‰ CIE nearly coincides

371 with the base of *D. sublodoensis* within the lower part of Chron C22n.

372

373 <u>*DSDP Site 577*</u>

374 The δ^{13}C record of bulk carbonate at DSDP Site 577 from just below the PETM through

375 Chron C22n ranges between 2.3 and 0.6 ‰ (**Figure 5; Table S2**). Overall, δ^{13}C decreases

376 from 1.4 ‰ at 84.5 mcd to about 0.6 ‰ at ~76 mcd. Values then generally increase to 2.1 ‰

377 at ~68 mcd, and remain between 2.3 ‰ and 1.6 ‰ for the rest of the studied interval. Thus,

378 the ranges and general trends in δ^{13}C for the two sections are similar, but skewed at DSDP

379 Site 577 relative to Possagno by about +0.6 ‰.

380   Like at Possagno, the early Eocene δ^{13}C record at DSDP Site 577 exhibits a series of

381 CIEs (**Figure 5**). The portion of this record from the PETM through the K/X event has been

382 documented and discussed elsewhere (Cramer et al., 2003; Dickens and Backman, 2013). The

383 new portion of this record, from above the K/X event through Chron C22n, spans the

384 remainder of the EECO. Within this interval, where background δ^{13}C values rise by ~1.5 ‰,

385 there again occur a series of minor CIEs with magnitudes between 0.3 and 0.5 ‰ (**Table S2**).

386 Here, however, multiple data points define most of the CIEs. We again give these an internal

387 numerical labelling scheme. A ~0.4 ‰ CIE also nearly coincides with the base of *D.*

388 *sublodoensis* within the lower part of C22n.

389

390 **5.2 Oxygen isotopes**

391

392 <u>*Possagno*</u>

393 Oxygen isotopes of bulk carbonate at Possagno range between -3.3 and 0.8 ‰ with a mean

394 value of -1.7 ‰ (**Figure 4, Table S1**). In general, considerable scatter exists across the data

395   set with respect to depth, as adjacent samples often display a difference in $\delta^{18}O$ that exceeds

396   0.5 ‰. Nonetheless, some of the more prominent lows in $\delta^{18}O$ show a clear correspondence

397   with negative $\delta^{13}C$ values (CIEs) and vice versa. This correspondence occurs across the

398   PETM and other known hyperthermals, as well as within and after the EECO. Indeed, the

399   main phase of the EECO corresponds with a broad has the lowest $\delta^{18}O$ values.

400

401   *DSDP Site 577*

402   The $\delta^{18}O$ record at Site 577 noticeably deviates from that at Possagno (**Figure 5, Table S2**).

403   This is because values range between -1.1 ‰ and 0.2 with an average value of -0.4 ‰. Thus,

404   relative to Possagno, the record at Site 577 has less scatter, and an overall shift of about -1.3

405   ‰. There is exists again a modest correlation between decreases in $\delta^{18}O$ and negative $\delta^{13}C$

406   values, as well as a general low in $\delta^{18}O$ across the main phase of the EECO.

407

408   **5.3 Coarse fraction**

409

410   The coarse fraction of samples from Possagno shows two distinct trends (**Figure 6, Table**

411   **S3**). Before the EECO, values are 10.4 % ± 2.67 %. However, from the base of the EECO

412   and up through the section, values decrease to 5.3 ± 1.3 %.

413

414   **5.4 Foraminiferal preservation and fragmentation**

415

416   Planktic foraminifera are consistently present and diverse throughout the studied intervals at

417   Possagno and at ODP Site 1051. Preservation of the tests at Possagno varies from moderate

418   to fairly good (Luciani and Giusberti, 2014). However, planktic foraminiferal tests at

419   Possagno are recrystallized and essentially totally filled with calcite. Planktic foraminifera

420 from samples at Site 1051 are readily recognizable throughout the studied interval. Planktic

421 foraminifera from Site 577, at least as illustrated by published plates (Lu and Keller, 1995),

422 show a very good state of preservation (albeit possibly recrystallized).

423   The *F* index record at Possagno (**Figure 6, Table S3**) displays large amplitude variations

424 throughout the investigated interval. The highest values, up to 70 %, were observed between

425 16 and 22 m. In general, highs in *F* index values correspond to lows in the $\delta^{13}C$ record.

426   The *F* index record at Site 1051 (**Figure 8, Table S4**) shows less variability compared to

427 that at Possagno, although some of this may reflect the difference in the number of samples

428 examined at the two locations. A maximum value of 60 % is found in Zone E5, just below an

429 interval of uncertain magnetostratigraphy (Norris et al., 1998), but corresponding to the J

430 event (Cramer et al., 2003). Relatively high *F* index values, around 50 %, also occur in

431 several samples below this horizon. The interval across the EECO generally displays low *F*

432 index values (<20 %).

433

434 **5.5 Planktic foraminiferal quantitative analysis**

435

436 *Possagno*

437 Planktic foraminiferal assemblages at Possagno show significant changes across the early to

438 early middle Eocene (**Figure 6, Table S3**). Throughout the entire section, the mean relative

439 abundance of *Acarinina* is about 46 % of the total assemblage. However, members of this

440 genus ~~show~~ exhibit peak abundances of 60-80 % of the total assemblage ~~occur~~ across several

441 intervals, often corresponding to CIEs. Particularly prominent is the broad abundance peak of

442 *Acarinina* coincident with the main phase of the EECO.

443   The increases in acarininid relative abundance typically are counterbalanced by transient

444 decreases of subbotinids (**Figure 6**). This group also shows a general increase throughout the

18

445   section. Below the EECO the relative abundances of subbotinids average ~24 %. Above the

446   EECO, this average rises to ~36 %.

447   The trends of acarininids and subbotinids contrast with that of morozovellids (**Figure 6**),

448   which exhibit a major and permanent decline within Zone E5. This group collapses from

449   mean abundances ~24 % in the 0-15 m interval to <6 % above 15 m. Qualitative examination

450   of species shows that, in the lower part of Zone E5, where relatively high morozovellids

451   abundances are recorded, there is no dominance of any species. *M. marginodentata*, *M.*

452   *subbotinae* and *M. lensiformis* are each relatively common, and *M. aequa, M. aragonensis,*

453   *M. formosa* and *M. crater* are each less common. By contrast, in the upper part of Zone E5,

454   where low abundances of morozovellids occur, *M. aragonensis, M. formosa, M. crater* and

455   *M. caucasica* are the most common species. The general decrease of morozovellids

456   abundances appears unrelated to the disappearance of a single, dominant species.

457   At Possagno, morozovellids never recover to their pre-EECO abundances. This is true

458   even if one includes the morphologically and ecologically comparable genus *Morozovelloides*

459   (Pearson et al., 2006), which first appears in samples above 36 m.

460   Other planktic foraminiferal genera are always less than 15 % of the total assemblages

461   throughout the studied interval at Possagno (**Figure S1, Table S3**).

462

463   *ODP Site 577*

464   Samples from Site 577 were disaggregated in water and washed through a >63 sieve (Lu,

465   1995; Lu and Keller, 1995). They determined relative abundances of planktic foraminifera

466   from random splits of about 300 specimens (Lu, 1995; Lu and Keller, 1995). The resulting

467   data are shown in **Figure 7**, placed onto the composite depth scale by Dickens and Backman

468   (2013). Major changes in planktic foraminiferal assemblages are comparable to those

469   recorded at Possagno. Such changes include indeed a distinct decrease of morozovellids

470 within Zone E5. The decrease at Site 577 is from mean values of 26.6 % to 6.7 % (**Table S4**).

471 This marked drop occurs at ca. 78 mcd close to the J event and at the start of the EECO. Like

472 at Possagno, morozovellids never recover to their pre-EECO abundances.

473   The morozovellids decrease is counter balanced by the trend of acarininid abundances

474 that increase from mean values of 30.4 % to 64.8 % in correspondence to the level of the

475 morozovellid collapse. Subbotinids fluctuate in abundance throughout the interval

476 investigated from 1 % to 18 %, with a mean value of ca. 8 %.

477

478 *ODP Site 1051*

479 Planktic foraminifera show distinct changes in abundance at Site 1051 (**Figure 8, Table S5**).

480 The changes of the main taxa are similar to the variations observed at Possagno. The genus

481 *Acarinina* displays an increase in mean relative abundance from 35 % (base to ca. 450 mbsf)

482 to around 50 % (ca. 430 mbsf), with maximum values of about 60 %. The relatively low

483 resolution used here does not permit comparison to the early Eocene CIEs at Site 1051

484 (Cramer et al., 2003), or how the relative abundance of planktic foraminiferal genera varies

485 with respect to CIEs.

486   The abundance of subbotinids shows ~~little~~ small variations around mean values of 20 %

487 at Site 1051. Like at Possagno, samples from Site 1051 also record a slight increase in

488 abundance toward the end of the EECO and above.

489   The major change in planktic foraminiferal assemblages at Site 1051 includes a distinct

490 decrease of *Morozovella*, from mean values around 40 % to 10 % in the middle part of Zone

491 E5 (**Figure 7**). Similar to Possagno, the lower part of Zone E5 with the higher percentages of

492 morozovellids does not record the dominance of selected species, but at Site 1051 *M.*

493 *aragonensis* and *M. formosa* besides *M. subbotinae* are relatively common whereas *M.*

494 *marginodentata* is less frequent. Within the interval of low morozovellids abundances, *M.*

495 *aragonensis* and *M. formosa* are the most common taxa. The general decline of

496 morozovellids does not appear therefore related, both at Possagno and at Site 1051, to the

497 extinction or local disappearance of a dominant species.

498

499 **6 Discussion**

500

501 **6.1 Dissolution, recrystallization, and bulk carbonate stable isotopes**

502

503 The bulk carbonate stable isotope records within the lower Paleogene sections at Possagno

504 and at Site 577 need thought, considering how such records are produced and modified in

505 much younger strata dominated by pelagic carbonate. In open ocean environments, carbonate

506 preserved on the seafloor principally consists of calcareous tests of nannoplankton

507 (coccolithophores) and planktic foraminifera (Bramlette and Riedel, 1954; Berger, 1967;

508 Vincent and Berger, 1981). However, the total amount of carbonate and its microfossil

509 composition can vary considerably across locations because of differences in deep-water

510 chemistry and in test properties (e.g., ratio of surface area to volume; mineralogical

511 composition). For regions at low to mid latitudes, a reasonable representation of carbonate

512 components produced in the surface water accumulates on the seafloor at modest (<2000 m)

513 water depth. By contrast, microfossil assemblages become heavily modified in deeper water,

514 because of increasingly significant carbonate dissolution (Berger, 1967). Such dissolution

515 preferentially affects certain tests, such as thin-walled, highly porous planktic foraminifera

516 (Berger, 1970; Bé et al., 1975; Thunell and Honjo, 1981).

517 The stable isotope composition of modern bulk carbonate ooze reflects the mixture of its

518 carbonate components, which mostly record water temperature and the composition of

519 dissolved inorganic carbon (DIC) within the mixed layer (<100 m water depth). The stable

520   isotope records are imperfect, though, because of varying proportions of carbonate

521   constituents, and "vital effects", which impact stable isotope fractionation for each

522   component (Anderson and Cole, 1975; Reghellin et al., 2015). Nonetheless, the stable isotope

523   composition of bulk carbonate ooze on the seafloor can be related to overlying temperature

524   and chemistry of surface water (Anderson and Cole, 1975; Reghellin et al., 2015).

525   Major modification of carbonate ooze occurs during sediment burial. This is because,

526   with compaction and increasing pressure, carbonate tests begin to dissolve and recrystallize

527   (Schlanger and Douglas, 1974; Borre and Fabricus, 1998). Typically within several hundred

528   meters of the seafloor, carbonate ooze becomes chalk and, with further burial, limestone

529   (Schlanger and Douglas, 1974; Kroencke et al., 1991; Borre and Fabricus, 1998). Carbonate

530   recrystallization appears to be a local and nearly closed system process, such that mass

531   transfer occurs over short distances (i.e., less than a few meters) (above references and Matter

532   et al., 1975; Arthur et al., 1984; Frank et al., 1999).

533   In pelagic sequences with appreciable carbonate content and low organic carbon content,

534   bulk carbonate $\delta^{13}C$ records typically give information of paleoceanographic significance

535   (Scholle and Arthur, 1980; Frank et al., 1999). Even when transformed to indurated

536   limestone, the $\delta^{13}C$ value for a given sample should be similar to that originally deposited on

537   the seafloor. This is because, for such sediments, almost all carbon within small ~~sedimentary~~

538   volumes exists as carbonate. Bulk carbonate $\delta^{18}O$ records are a different matter, especially in

539   indurated marly limestones and limestones (Marshall, 1992; Schrag et al., 1995; Frank et al.,

540   1999). This is because pore water dominates the total amount of oxygen within an initial

541   parcel of sediment, and oxygen isotope fractionation depends strongly on temperature. Thus,

542   during dissolution and recrystallization of carbonate, significant exchange of oxygen isotopes

543   occurs. At first, carbonate begins to preferentially acquire ^{18}O, because shallowly buried

544   sediment generally has lower temperatures than surface water. However, with increasing

545 burial depth along a geothermal gradient, carbonate begins to preferentially acquire ^{16}O

546 (Schrag et al., 1995; Frank et al., 1999).

547

548 **6.2 Carbon isotope stratigraphy through the EECO**

549

550 Stratigraphic issues complicate direct comparison of various records from Possagno and Site

551 577. The two sections have somewhat similar multi-million year sedimentation rates across

552 the early Eocene. However, the section at Possagno contains the condensed interval, where

553 much of C23r spans a very short distance (Agnini et al., 2006), and the section at Site 577 has

554 a series of core gaps and core overlaps (Dickens and Backman, 2013).

555   An immediate issue to amend is the alignment of Cores 8H and 9H in Hole 577* and

556 Core 8H in Hole 577A (**Figure 5**). On the basis of GRAPE density records for these cores,

557 Dickens and Backman (2013) initially suggested a 2.6 m core gap between Cores 8H* and

558 9H*. However, a 3.5 m core gap also conforms to all available stratigraphic information. The

559 newly generated δ^{13}C (and δ^{18}O) records across these three cores show the latter to be correct.

560   Once sedimentation rate differences at Possagno are recognized and coring problems at

561 Site 577 are rectified, early Eocene δ^{13}C records at both locations display similar trends and

562 deviations in relation to polarity chrons and key microfossil events (**Figures 4, 5**). Moreover,

563 the δ^{13}C variations seemingly can be correlated in time to those found in bulk carbonate δ^{13}C

564 records at other locations, including Site 1051 (**Figure 8**) and Site 1258 (**Figure 9**). As noted

565 previously, such correlation occurs because the bulk carbonate δ^{13}C signals reflect past global

566 changes in the composition of surface water DIC, even after carbonate recrystallization.

567   For the latest Paleocene and earliest Eocene, nominally the time spanning from the base

568 of C24r through the middle of C24n, detailed stable carbon isotope records have been

569 generated at more than a dozen locations across the globe (Cramer et al., 2003; Agnini et al.,

570   2009; Galeotti et al., 2010; Zachos et al., 2010; Slotnick et al., 2012; Littler et al., 2014;

571   Agnini et al., in review). These records can be described consistently as a long-term drop in

572   $\delta^{13}C$ superimposed with a specific sequence of prominent CIEs that include those

573   corresponding to the PETM, H-1, and J events. In continuous sections with good

574   magnetostratigraphy and biostratigraphy, there is no ambiguity in the assignment of CIEs

575   (Zachos et al., 2010; Littler et al., 2014; Slotnick et al., 2012, 2105a; Lauretano et al., 2015).

576   This "$\delta^{13}C$ template" can be found at the Possagno section and at Site 577 (**Figure 9**); it is

577   found at Site 1051 for the depth interval where carbon isotopes have been determined

578   (**Figure 8**).

579   After the J event and across the EECO, very few detailed $\delta^{13}C$ records have been

580   published (Slotnick et al., 2012, 2015a; Kirtland-Turner et al., 2014). Moreover, the available

581   records are not entirely consistent. For example, the K/X event in Clarence River valley

582   sections manifests as a prominent CIE within a series of smaller $\delta^{13}C$ excursions (Slotnick et

583   al., 2012, 2015a), whereas the event has limited expression in the $\delta^{13}C$ record at Site 1258

584   (Kirtland-Turner et al., 2014; **Figure 9**).

585   The new records from Possagno and Site 577 emphasize an important finding regarding

586   bulk carbonate $\delta^{13}C$ records across the EECO. Between the middle of C24n and the upper

587   part of C23r, there appears to be a sequence of low amplitude, low frequency CIEs. (Note

588   that this portion of the record is missing at Possagno because of the condensed interval;

589   **Figure 9**). However, near the C23r/C23n boundary, a long-term rise in $\delta^{13}C$ begins, but with

590   a series of relatively high amplitude, high frequency CIEs (Kirtland-Turner et al., 2014;

591   Slotnick et al., 2014). The number, relative magnitude and precise timing of CIEs within this

592   interval remain uncertain. For example, the CIE labelled "4" appears to occur near the top of

593   C23r at Site 577 but near the bottom of C23n.2n at Site 1258 and at Possagno. Additional

594   $\delta^{13}C$ records across this interval are needed to resolve the correct sequence of CIEs and to

595 derive an internally consistent labelling scheme for these perturbations. It is also not clear

596 which of these CIEs during the main phase of the EECO specifically relate to significant

597 increases in temperature, as clear for the "hyperthermals" in the earliest Eocene. Nonetheless,

598 numerous CIEs, as well as an apparent change in the mode of these events, characterize the

599 EECO (Kirtland-Turner et al., 2014; Slotnick et al., 2014).

600   The causes of δ^{13}C changes during the early Paleogene lie at the crux of considerable

601 research and debate (Dickens et al., 1995, 1997; Zeebe et al., 2009; Dickens, 2011; Lunt et

602 al., 2011; Sexton et al., 2011; De Conto et al., 2012; Lee et al., 2013; Kirtland Turner et al.,

603 2014). Much of the discussion has revolved around three questions: (1) what are the sources

604 of ^{13}C-depleted carbon that led to prominent CIEs, especially during the PETM? (2) does the

605 relative importance of different carbon sources vary throughout this time interval? and, (3)

606 are the geologically brief CIEs related to the longer secular changes in δ^{13}C? One might

607 suggest, through several papers, a convergence of thought as to how carbon cycled across

608 Earth's surface during the early Paleogene, at least between the late Paleocene and the K/X

609 event (Cramer et al., 2003; Lourens et al., 2005; Galeotti et al., 2010; Hyland et al., 2013;

610 Zachos et al., 2010; Lunt et al. 2011; Littler et al., 2014; Lauretano et al., 2015; Westerhold et

611 al., 2015). Changes in tectoniesm, volcanism, and weathering drove long-term changes

612 atmospheric pCO$_2$ (Vogt, 1979; Raymo and Ruddiman, 1992; Sinton and Duncan, 1998;

613 Demicco, 2004; Zachos et al., 2008), which was generally high throughout the early

614 Paleogene, but increased toward the EECO (Pearson and Palmer, 2000; Fletcher et al., 2008;

615 Lowenstein and Demicco, 2006; Smith et al., 2010; Hyland and Sheldon, 2013). However, as

616 evident from the large range in δ^{13}C across early Paleogene stable isotope records, major

617 changes in the storage and release of organic carbon must have additionally contributed to

618 variability in atmospheric pCO$_2$ and ocean DIC concentrations (Shackleton, 1986; Kurtz et

619 al., 2003; Komar et al., 2013). When long-term increases in pCO$_2$, perhaps in conjunction

620   with orbital forcing, pushed temperatures across some threshold, such as the limit of sea-ice

621   formation (Lunt et al., 2011), rapid inputs of ^{13}C-depleted organic carbon from the shallow

622   geosphere served as a positive feedback to abrupt warming (Dickens et al., 1995; Bowen et

623   al., 2006; DeConto et al., 2012).

624   Our new δ^{13}C records do not directly address the above questions and narrative

625   concerning early Paleogene carbon cycling. However, they do highlight two general and

626   related problems when such discussion includes the EECO. First, surface temperatures appear

627   to stay high across an extended time interval when the δ^{13}C of benthic foraminifer (**Figure 1**)

628   and bulk carbonate (**Figure 9**) increase. Second, numerous brief CIEs mark this global long-

629   term rise in δ^{13}C. Whether the aforementioned views need modification or reconsideration

630   (Kirtland Turner et al., 2014) is an outstanding issue, one that depends on how long-term and

631   short-term δ^{13}C changes relate across the entire early Paleogene.

632   The overall offset between bulk carbonate δ^{13}C values at Possagno and Site 577 may hint

633   at an important constraint to any model of early Paleogene carbon cycling. Throughout the

634   early Eocene, δ^{13}C values at Site 577 exceed those at Possagno by nominally 0.8 ‰ (**Figure**

635   **9**). This probably does reflect recrystallization or lithification, because similar offsets appear

636   across numerous records independent of post-depositional history but dependent on location

637   (Schmitz et al., 1996; Cramer et al., 2003; Slotnick et al., 2012, 2015a; Agnini et al.,

638   submitted). In general, absolute values of bulk carbonate δ^{13}C records increase from the

639   North Atlantic and western Tethys (low), through the South Atlantic and eastern

640   Tethys/Indian, to the Pacific (high), although suggestively with a latitudinal component to

641   this signature.

642

643   **6.3 Stable oxygen isotope stratigraphy across the EECO**

644

645   Bulk carbonate δ^{18}O values for Holocene sediment across the Eastern Equatorial Pacific

646   relate to average temperatures in the mixed layer (Shackleton and Hall, 1995; Reghellin et al.,

647   2015). Indeed, values are close to those predicted from water chemistry (δ^{18}O$_w$) and

648   equilibrium calculations for calcite precipitation (e.g., Bemis et al., 1998) if vital effects in

649   the dominant nannoplankton increase δ^{18}O by nominally 1‰ (Reghellin et al., 2015).

650   Site 577 was located at about 15°N latitude in the eastern Pacific during the early

651   Paleogene. Given that sediment of this age remains "nannofossil ooze" (Shipboard Scientific

652   Party, 1985), one might predict past mixed layer temperatures from the δ^{18}O values with

653   three assumptions: early Paleogene δ^{18}O$_w$ was 1.2 ‰ less than that at present-day to account

654   for an ice-free world; local δ^{18}O$_w$ was equal to average seawater, similar to modern chemistry

655   at this off-Equator location (LeGrande and Schmidt, 2006); and, Paleogene nannoplankton

656   also fractionated δ^{18}O by 1.0 ‰. With commonly used equations that relate the δ^{18}O of

657   calcite to temperature (Bemis et al., 1998), these numbers render temperatures of between

658   16°C and 21°C for the data at Site 577. Such temperatures seem too cold by at least 10°C,

659   given other proxy data and modelling studies (e.g., Pearson et al., 2007; Huber and Caballero,

660   2011; Hollis et al., 2012; Pross et al., 2012; Inglis et al., 2015). At low latitudes, bottom

661   waters are always much colder than surface waters. Even during the EECO, deep waters

662   probably did not exceed 12°C (Zachos et al., 2008). The calculated tepid temperatures likely

663   indicate partial recrystallization of bulk carbonate near the seafloor. Examinations of

664   calcareous nannofossils in Paleogene sediment at Site 577 show extensive calcite

665   overgrowths (Shipboard Scientific Party, 1985; Backman, 1986). Relatively low δ^{18}O values

666   mark the H-1 and K/X events, as well as the main phase of the EECO (**Figure 5**). Both

667   observations support the idea that the bulk carbonate δ^{18}O at Site 577 represents the

668   combination of a primary surface water δ^{18}O signal and a secondary shallow pore water δ^{18}O

669   signal.

670   Lithification should further impact bulk carbonate $\delta^{18}O$ records (Marshall, 1992; Schrag

671   et al., 1995; Frank et al., 1999). Because this process occurs well below the seafloor, where

672   temperatures approach or exceed those of surface water, the $\delta^{18}O$ values of pelagic marls and

673   limestones should be significantly depleted in ^{18}O relative to partially recrystallized

674   nannofossil ooze. This explains the nominal 2‰ offset in average $\delta^{18}O$ between correlative

675   strata at Possagno and at Site 577. While temperature calculations using the $\delta^{18}O$ record at

676   Possagno render reasonable surface water values for a mid-latitude location in the early

677   Paleogene (26-31°C, using the aforementioned approach), any interpretation in these terms

678   more than likely reflects happenstance. The fact that planktic foraminifera are completely

679   recrystallized and totally filled with calcite at Possagno supports this inference.

680   One might suggest, at least for the Possagno section, that meteoric water might have also

681   impacted the $\delta^{18}O$ record. This is because rainwater generally has a $\delta^{18}O$ composition less

682   than that of seawater. However, samples were collected at Possagno in 2002-2003 from fresh

683   quarry cuts.

684   As observed at Site 577, however, horizons of lower $\delta^{18}O$ at Possagno may represent

685   times of relative warmth in surface water. This includes the broad interval between 16 and

686   22.5 m, which marks the main phase of the EECO, as well as many of the brief CIEs, at least

687   one that clearly represents the PETM (**Figure 4**). That is, despite obvious overprinting of the

688   original $\delta^{18}O$ signal, early to early middle Eocene climate variations appear manifest in the

689   data.

690

691   **6.4 The EECO and planktic foraminiferal abundances**

692

693   Bulk carbonate $\delta^{13}C$ records, especially in conjunction with other stratigraphic markers,

694   provide a powerful means to correlate early Paleogene sequences from widely separated

695   locations (**Figure 9**). They also allow for placement of planktic foraminiferal assemblage

696   changes into broader context.

697   The most striking change in planktic foraminiferal assemblages occurred near the start of

698   the EECO. Over a fairly short time interval and at multiple widespread locations, the relative

699   abundance of acarininids increased significantly whereas the relative abundance of

700   morozovellids decreased significantly. This switch, best defined by the decline in

701   morozovellids, happened just before the condensed interval at Possagno (**Figure 6**), just

702   above the J event at Site 577 (**Figure 7, Table S4**), and during the J event at Site 1051

703   (**Figure 8**). At the Farra section, cropping out in the same geological setting of Possagno at

704   50 km NE of the Carcoselle quarry, it also appears to have occurred close to the J event

705   (**Figure 10**). Indeed, the maximum turnover in relative abundances may have been coincident

706   with the J event at all locations. Importantly, the relative abundance of subbotinids only

707   changed marginally during this time.

708   The morozovellid decline across the start of the EECO did not rebound afterward. At

709   Possagno, at Site 1051, and at Site 577, it was coupled with the gradual disappearances of

710   several species, including *M. aequa, M. gracilis, M. lensiformis, M. marginodentata,* and *M.*

711   *subbotinae*. Furthermore, the loss of morozovellids was not counterbalanced by the

712   appearance of the *Morozovelloides* genus, which shared with *Morozovella* the same

713   ecological preferences. This latter genus appeared in C21r, near the Ypresian/Lutetian

714   boundary, and well after the EECO (Pearson et al., 2006; Aze et al., 2011), including at

715   Possagno (Luciani and Giusberti, 2014; **Figure 6**). Though *Morozovelloides* were

716   morphologically similar to *Morozovella*, they probably evolved from *Acarinina* (Pearson et

717   al., 2006; Aze et al., 2011; **Figure 1**).

718   At Possagno, higher abundances of acarininids also correlate with pronounced negative

719    $\delta^{13}C$ perturbations before and after the EECO (**Figure 6**). This includes the H-1 event, as well

720   as several unlabelled CIEs during C22n, C21r and C21n. Such increases in the relative

721   abundances of acarininids have been described for the PETM interval at the nearby Forada

722   section (Luciani et al., 2007), and for the K/X event at the proximal Farra section (Agnini et

723   al., 2009). Unlike for the main switch near the J event, however, these changes are transient,

724   so that relative abundances in planktic foraminiferal genera are similar before and after the

725   short-term CIEs.

726

727   **6.5 The impact of dissolution**

728

729   Carbonate dissolution at or near the seafloor presents a potential explanation for observed

730   changes in foraminifera assemblages. Some studies of latest Paleocene to initial Eocene age

731   sediments, including laboratory experiments, suggest a general ordering of dissolution

732   according to genus, with acarininds more resistant than morozovellids, and the latter more

733   resistant than subbotinids (Petrizzo et al., 2008; Nguyen et al., 2009, 2011).

734   Carbonate solubility horizons that impact calcite preservation and dissolution on the

735   seafloor (i.e., the CCD and lysocline) also shoaled considerably during various intervals of

736   the early Eocene. The three most prominent hyperthermals that occurred before the main

737   phase of the EECO (PETM, H-1, K/X) were clearly marked by pronounced carbonate

738   dissolution at multiple locations (Zachos et al., 2005; Agnini et al., 2009; Stap et al., 2009;

739   Leon-Rodriguez and Dickens, 2010). A multi-million year interval characterized by a

740   relatively shallow CCD also follows the K/X event (Leon-Rodriguez and Dickens, 2010;

741   Pälike et al., 2012; Slotnick et al., 2015b).

742   Should changes in carbonate preservation primarily drive the observed planktic

743   foraminiferal assemblages, it follows that the dominance of acarininids during the EECO and

744   multiple CIEs could represent a taphonomic artefact. Limited support for this idea comes

745   from our records of fragmentation (*F* index). In general, intervals with relatively high

746   abundances of acarininids (and low $\delta^{13}C$) correspond to intervals of fairly high fragmentation

747   at Possagno and at Site 1051 (**Figures 6, 8**). This can suggest carbonate dissolution, because

748   this process breaks planktic foraminifera into fragments (Berger, 1967; Hancock and

749   Dickens, 2005).

750   Carbonate dissolution can cause the coarse fraction of bulk sediment to decrease (Berger

751   et al., 1982; Broecker et al., 1999; Hancock and Dickens, 2005). This happens because whole

752   planktic foraminiferal tests typically exceed 63 μm, whereas the resulting fragments often do

753   not exceed 63 μm. The decrease in CF values at the start of the EECO at Possagno (**Figure 6**)

754   may therefore further indicate loss of foraminiferal tests. However, relatively low CF values

755   continue to the top of the section, independent of changes in the *F* index. The CF record

756   parallels the trend of morozovellids abundance, and thus might also suggest a loss of larger

757   morozovellids rather than carbonate dissolution.

758   The cause of the long-term rise in carbonate dissolution horizons remains perplexing, but

759   may relate to reduced inputs of ^{13}C-depleted carbon into the ocean and atmosphere (Leon-

760   Rodriguez and Dickens, 2010; Komar et al., 2013). Should the morozovellids decline and

761   amplified *F* index at the Possagno section mostly represent dissolution, it would imply

762   considerable shoaling of these horizons in the western Tethys, given the inferred deposition

763   in middle to lower bathyal setting. As with open ocean sites (Slotnick et al., 2015b), further

764   studies on the Eocene lysocline and CCD are needed from Tethyan locations. One idea is that

765   remineralization of organic matter intensified within the water column, driven by augmented

766   microbial metabolic rates at elevated temperatures during the EECO; this may have decreased

767   pH at intermediate water column depths (Brown et al., 2004; Olivarez Lyle and Lyle, 2006;

768   O'Connor et al., 2009; John et al., 2013, 2014).

769   Despite evidence for carbonate dissolution, this process probably only amplified primary

770   changes in planktic foraminiferal assemblages. The most critical observation is the similarity

771   of the abundance records for major planktic foraminiferal genera throughout the early Eocene

772   at multiple locations (**Figures 6-8**). This includes the section at Site 1051, where carbonate

773   appears only marginally modified by dissolution according to the *F* index values (**Figure 7**).

774   Subbotinid abundance also remains fairly high throughout the early Eocene. One explanation

775   is that, in contrast to laboratory experiments (Nguyen et al., 2009, 2011), subbotinids are

776   more resistant to dissolution than morozovellids (Boersma and Premoli Silva, 1983; Berggren

777   and Norris, 1997), at least once the EECO has transpired. In the proximal middle-upper

778   Eocene section at Alano, Luciani et al. (2010) documented a dominance of subbotinids within

779   intervals of high fragmentation (*F* index) and enhanced carbonate dissolution. The degree of

780   dissolution across planktic foraminiferal assemblages may have varied through the early

781   Paleogene, as distinct species within each genus may respond differently (Nguyen et al.,

782   2011). So far, data on dissolution susceptibility for different species and genera are limited

783   for early and early middle Eocene times (Petrizzo et al., 2008).

784   There is also recent work from the Terche section (ca. 28 km NE of Possagno) to

785   consider. This section is located in the same geological setting as Possagno, but across the H-

786   1, H-2 and I1 events, there are very low *F* index values and marked increases of acarininids

787   coupled with significant decreases of subbotinids (D'Onofrio et al., 2014). Therefore,

788   although the Possagno record may be partially altered by dissolution, an increase of warm

789   water acarininids concomitant with decrease of subbotinids seems to be a robust finding

790   during early Paleogene warming events in Tethyan settings.

791

792   **6.6 A record of mixed water change**

793

794   The switch in abundance between morozovellids and acaraninids at the start of the EECO

795 supports a hypothesis whereby environmental change resulted in a geographically widespread

796 overturn of planktic foraminiferal genera. During the PETM and K/X events, acarininids

797 became dominant over morozovellids in a number of Tethyan successions. This has been

798 interpreted as signifying enhanced eutrophication of surface waters near continental margins

799 (Arenillas et al., 1999; Molina et al., 1999; Ernst et al., 2006; Guasti and Speijer, 2007;

800 Luciani et al., 2007; Agnini et al., 2009), an idea consistent with evidence for elevated (albeit

801 more seasonal) riverine discharge during these hyperthermals (Schmitz and Pujalte, 2007;

802 Giusberti et al., 2007; Schulte et al., 2011; Slotnick et al., 2012; Pułjalte et al., 2015).

803 Increased nutrient availability may also have occurred at Possagno during the early part of the

804 EECO, given the relatively high concentration of radiolarians, which may reflect

805 eutrophication (Hallock, 1987).

806   However, the fact that the major switch at the start of the EECO can be found at Sites

807 1051 (western Atlantic) and Site 577 (central Pacific) suggests that local variations in

808 oceanographic conditions, such as riverine discharge, was not the primary causal mechanism.

809 Rather, the switch must be a consequence of globally significant modifications related to the

810 EECO, most likely sustained high temperatures, elevated pCO$_2$, or both. Given model

811 predictions for our Earth in the coming millennia (IPCC, 2014), indirect effects also could

812 have contributed, especially including increased ocean stratification and decreased pH.

813   An explanation for the shift may lie in habitat differences across planktic foraminifera

814 genera. Although both morozovellids and acaraninids likely had photsymbionts,

815 morozovellids may have occupied a shallower surface habitat than the latter genus as

816 indicated by minor variations in their stable isotope compositions (Boersma et al., 1987;

817 Pearson et al., 1993; 2001).

818   One important consideration to any interpretation is the evolution of new species that

819 progressively appear during the post-EECO interval. In good agreement with studies of lower

820   Paleogene sediment from other low latitude locations (Pearson et al., 2006), thermocline

821   dwellers such as subbotinids and parasubbotinids seem to proliferate at Possagno (Luciani

822   and Giusberti, 2014). These include *Subbotina corpulenta, S. eocena, S. hagni, S. senni, S.*

823   *yeguanesis, Parasubbotina griffinae,* and *P. pseudowilsoni.* The appearance of the radially-

824   chambered *Parasubbotina eoclava*, considered to be the precursor of the truly clavate

825   chambered *Clavigerinella* (Coxall et al., 2003; Pearson and Coxall, 2014), also occurs at 19.8

826   m, and in the core of the EECO (Luciani and Giusberti, 2014). *Clavigerinella* is the ancestor

827   of the genus *Hantkenina* that successfully inhabited the sub-surface and surface waters during

828   the middle through late Eocene (Coxall et al., 2000).

829   A second consideration is the change in planktic foraminiferal assemblages during the

830   Middle Eocene Climate Optimum (MECO), another interval of anomalous and prolonged

831   warmth ca. 40 Ma (Bohaty and Zachos, 2003). At Alano (**Figure 11**) and other locations

832   (Luciani et al., 2010; Edgar et al., 2012), the MECO involved the reduction in the abundance

833   and test size of large acarininids and *Morozovelloides*. This has been attributed to "bleaching"

834   and the loss of photosymbionts resulting from global warming (Edgar et al., 2012), although

835   related factors, such as a decrease in pH, a decrease in nutrient availability, or changes in

836   salinity, may have been involved (Douglas, 2003; Wade et al., 2008). The symbiotic

837   relationship with algae is considered an important strategy adopted by muricate planktic

838   foraminifera during the early Paleogene (Norris, 1996; Quillévéré et al., 2001). Considering

839   the importance of this relationship in extant species (Bé, 1982; Bé et al., 1982; Hemleben et

840   al., 1989), the loss of photosymbionts may represent a crucial mechanism to explain the

841   relatively rapid decline foraminifera utilizing this strategy, including morozovellids at the

842   start of the EECO.

843   Available data suggest that the protracted conditions of extreme warmth and high pCO_2

844   during the EECO were the key elements inducing a permanent impact on planktic

845 foraminiferal evolution, and the decline of the morozovellids. Even during the PETM, the

846 most pronounced hyperthermal, did not adversely affect the morozovellids permanently.

847 While "excursion taxa" appeared, morozovellids seem to have increased in abundance in

848 open ocean settings (Kelly et al., 1996; 1998, 2002; Lu and Keller, 1995; Petrizzo, 2007);

849 only in some continental margin settings did a transient decrease in abundance occur (Luciani

850 et al., 2007).

851

852 **6.7 Post-EECO changes at Possagno**

853

854 Several small CIEs appear in the $\delta^{13}C$ record at Possagno during polarity chrons C22n, C21r,

855 and C21n. Some of these post-EECO excursions coincide with planktic foraminiferal

856 assemblage changes similar to those recorded in lower strata. Specifically, there are marked

857 increases of acarininids (**Figure 6**). These "post-EECO" CIEs are concomitant with $\delta^{18}O$

858 excursions and coupled to distinct modifications in the planktic foraminiferal assemblages

859 comparable to those recorded across known hyperthermals in Tethyan settings (Luciani et al.,

860 2007; Agnini et al., 2009; D'Onofrio et al., 2014). Additional hyperthermals, although of less

861 intensity and magnitude, may extend through the entirety of the early and middle Eocene, as

862 suggested previously (Sexton et al., 2006; 2011; Kirtland-Turner et al., 2014). Whether these

863 imply different forcing and feedback mechanisms compared to the PETM remains an open

864 discussion.

865

866 **7 Summary and conclusions**

867   The symbiont-bearing planktic foraminiferal genera *Morozovella* and *Acarinina* were

868 among the most important calcifiers of the early Paleogene tropical and subtropical oceans.

869 However, a remarkable and permanent switch in the relative abundance of these genera

870   happened in the early Eocene, an evolutionary change accompanied by species reduction of

871   *Morozovella* and species diversification of *Acarinina*. We show here that this switch probably

872   coincided with a carbon isotope excursion (CIE) presently coined J. Although the Early

873   Eocene Climatic Optimum (EECO), a multi-million year interval of extreme Earth surface

874   warmth, lacks an accepted definition, we propose that the EECO is best defined as the

875   duration of time between the J event and the base of *D. sublodoensis* (about 53 Ma to 49 Ma

876   on the 2012 GTS).

877   Our conclusion that the planktic foraminferal switch coincides with the start of the

878   EECO derives from the generation of new records and collation of old records concerning

879   bulk sediment stable isotopes and planktic foraminiferal abundances at three sections. These

880   sections span a wide longitude range of the low latitude Paleogene world: the Possagno

881   section from the western Tethys, DSDP Site 577 from the central Pacific Ocean, and ODP

882   Site 1051 from the western Atlantic Ocean. Importantly, these locations have robust

883   calcareous nannofossils and polarity chron age markers, although the stratigraphy required

884   amendment at Sites 577 and 1051.

885   An overarching problem is that global carbon cycling was probably very dynamic during

886   the EECO. The interval appears to have been characterized not only by numerous CIEs, but

887   also a major switch in the timing and magnitude of these perturbations. Furthermore, there

888   was a rapid shoaling of carbonate dissolution horizons in the middle of the EECO. A key

889   finding of our study is that the major switch in planktic foraminiferal assemblages happened

890   at the start of the EECO. Significant, though ephemeral, modifications in planktic

891   foraminiferal assemblages coincide with numerous short-term CIEs, before, during and after

892   the EECO. Often, there are marked increases in the relative abundance of acarininids, similar

893   to what happened permanently across the start of the EECO.

894   Although we show for the first time that the critical turnover in planktic foraminifera

895   clearly coincided with the start of the EECO, the exact cause for the switch (aka the decline

896   of morozovellids) remains elusive. Possible causes are multiple, and may include temperature

897   effects on photosymbiont-bearing planktic foraminifera, changes in ocean chemistry, or even

898   interaction with other microplankton groups such as radiolarians, diatoms or dinoflagellates

899   that represented possible competitors in the use of symbionts or as symbiont providers. For

900   some reason, a critical threshold was surpassed at the start the EECO, and this induced an

901   unfavourable habitat for continued morozovellid diversification and proliferation but a

902   favourable habitat for the acarinids.

903

920 significantly.

921

922 **References**

923

924

925 Abels, H. A., Clyde, W. C., Gingerich, P. D., Hilgen, F. J., Fricke, H. C., Bowen, G. J., and
926   Lourens, L. J.: Terrestrial carbon isotope excursions and biotic change during Palaeogene
927   hyperthermals, Nat. Geosci., 5, 326-329, doi: 10.1038/ngeo1427, 2012.

928 Agnini, C., Muttoni, G., Kent, D. V., and Rio, D.: Eocene biostratigraphy and magnetic
929   stratigraphy from Possagno, Italy: the calcareous nannofossils response to climate
930   variability, Earth Planet. Sci. Lett., 241, 815-830, 2006.

931 Agnini, C., Macrì, P., Backman, J., Brinkhuis, H., Fornaciari, E., Giusberti, L., Luciani, V.,
932   Rio, D., Sluijs, A., and Speranza, F.: An early Eocene carbon cycle perturbation at 52.5
933   Ma in the Southern Alps: chronology and biotic response, Paleoceanography, 24,
934   PA2209. doi: 10.1029/2008PA001649, 2009.

935 Agnini, C., Fornaciari, E., Raffi, I., Catanzariti, R., Pälike, H., Backman, J., and Rio, D.:
936   Biozonation and biochronology of Paleogene calcareous nannofossils from low to middle
937   latitudes, News. Strat., 47, 131-181, 2014.

938 Agnini, C., Spofforth, D. J. A., Dickens, G. R., Rio, D., Pälike, H., Backman, J., Muttoni, G.,
939   and Dallanave, E.: Stable isotope and calcareous nannofossil assemblage records for the
940   Cicogna section: toward a detailed template of late Paleocene and early Eocene global
941   carbon cycle and nannoplankton evolution, Clim. Past, sumbitted.

942 Anderson, T. F., and Cole, S. A.: The stable isotope geochemistry of marine coccoliths: a
943   preliminary comparison with planktonic foraminifera, J. Foram. Res., 5 (3), 188-192,
944   1975.

945 Arthur , M. A., Dean, W. E., Bottjer, D., and Schole, P. A.: Rhythmic bedding in Mesozoic-
946   Cenozoic pelagic carbonate sequences: the primary and diagenetic origin of
947   Milankovitch like cycles, in: Milankovitch and Climate, A. Berger, J. Imbrie, J. Hays, G.
948   Kucla, B. Satzman (eds.), 191-222, D. Reidel Publ. Company, Dordrecht, Holland,
949   1984.

950 Arenillas, I., Molina, E., and Schmitz, B.: Planktic foraminiferal and $\delta^{13}C$ isotopic changes
951   across the Paleocene/Eocene boundary at Possagno (Italy), Int. J. Earth Sc., 88, 352–364,

952   1999.

953   Aze, T., Ezard, T. H. G., Purvis, A., Coxall, H. K., Stewart, D. R. M, Wade, B. S., and

954   Pearson, P. N.: A phylogeny of Cenozoic macroperforate planktonic foraminifera from

955   fossil data, Biol. Rev., 86, 900-927. 900 doi: 10.1111/j.1469-185X.2011.00178.x, 2011.

956   Backman, J.: Late Paleocene to middle Eocene calcareous nannofossil biochronology from

957   the Shatsky Rise, Walvis Ridge and Italy, Palaeogeogr. Palaeoclimatol. Palaeoecol., 57

958   (1), 43-59, 1986.

959   Bé, A. W. H.: Biology of planktonic foraminifera, in: Foraminifera: notes for a short course,

960   Broadhead T., Stud. Geol., 6, Univ. Knoxville, Tenn., 51-92, 1982.

961   Bé, A. W. H., John, W. M., and Stanley, M. H.: Progressive dissolution and ultrastructural

962   breakdown of planktic foraminifera, Cushman Foundation for Foraminiferal Research

963   Special Publication, 13, 27-55, 1975.

964   Bé, A. W. H., Spero, H. J., and Anderson O. R.: Effects of symbiont elimination and

965   reinfection on the life processes of the planktonic foraminifer *Globigerinoides sacculifer,*

966   Marine Biol. 70, 73-86, 1982.

967   Bemis, B. E., Spero, H. J., Bijma, J., and Lea, D. W.: Reevaluation of the oxygen isotopic

968   composition of planktonic foraminifera: Experimental results and revised

969   paleotemperature equations, Paleoceanography, 13 (2), 150-160, 1998.

970   Berger, W. H.: Foraminiferal ooze: Solution at depth, Science, 156: 383-385, 1967.

971   Berger, W. H.: Planktonic foraminifera - selective solution and lysocline, Marine Geol., 8(2),

972   111-138, 1970.

973   Berger, W. H., Bonneau, M.-C., and. Parker, F. L.: Foraminifera on the deep-sea floor:

974   lysocline and dissolution rate, Oceanol. Acta, 5 (2), 249-258, 1982.

975   Berggren, W. A., and Norris, R. D.: Biostratigraphy, phylogeny and systematics of Paleocene

976   trochospiral planktic foraminifera, Micropaleont., 43 (Suppl. 1), 1-116, 1997.

977   Berggren, W. A., and Pearson, P. N.: A revised tropical to subtropical Paleogene planktic

978   foraminiferal zonation: J. Foram. Res., v. 35, p. 279-298, 2005.

979   Berggren, W. A., Kent, D. V., Swisher, C. C. III, and Aubry, M-P.: A revised Cenozoic

980   geochronology and chronostratigraphy, in: Berggren W. A, Kent D. V., Aubry M-P.,

981   Hardenbol J. (Eds.), Geochronology, time scales and global stratigraphic correlation.

982   SEPM Special Publication 54, 129-212, 1995.

983   Bijl, P. K., Schouten, S., Sluijs, A., Reichart, G.-J., Zachos, J. C., and Brinkhuis, H.: Early

984   Paleogene temperature evolution of the southwest Pacific Ocean. Nature, 461, 776–

985   779, doi:10.1038/nature08399, 2009.

986 Bleil, U.: The magnetostratigraphy of northwest Pacific sediments, Deep Sea Drilling Project
987   Leg 86, Initial Reports Deep Sea Drilling Project, 86, 441-458.

988 Boersma, A., and Premoli Silva, I.: Paleocene planktonic foraminiferal biogeography and the
989   paleoceanography of the Atlantic-Ocean, Micropaleont., 29, 355-381, 1983.

990 Boersma, A., Premoli Silva, I., and Shackleton, N.: Atlantic Eocene planktonic foraminiferal
991   biogeography and stable isotopic paleoceanography, Paleoceanography, 2, 287-331,
992   1987.

993 Bohaty, S. M., and J. C. Zachos: A significant Southern Ocean warming event in the late
994   middle Eocene, Geology, 31, 1017–1020, doi:10.1130/G19800.1, 2003.

995 Bohaty, S. M., Zachos, J. C., Florindo, F., and Delaney, M. L.: Coupled greenhouse warming
996   and deep-sea acidification in the middle Eocene, Paleoceanography, 24, PA2207,
997   doi:10.1029/2008PA001676, 2009.

998 Bolli, H. M.: Monografia micropaleontologica sul Paleocene e sull'Eocene di Possagno,
999   Provincia di Treviso, Italia. Mémoires Suisses de Paléontologie 97: 222 pp., 1975.

1000 Borre, M. and Fabricus, I.L.: Chemical and mechanical processes during burial diagenesis of
1001   chalk: an interpretation based on specific surface data of deep-sea sediments,
1002   Sedimentology, 45, 755-769, 1998.

1003 Bosellini, A.: Dynamics of Tethyan carbonate platform, in: Controls on Carbonate Platform
1004   and Basin Platform, Crevello, P.D., Wilson, J.L., Sarg, J.F., Read, J.F., (Eds.), SEPM
1005   Spec. Publ., 44, 3-13, 1989.

1006 Bowen, G. J., Bralower, T. J., Delaney, M. R., Dickens, G. R., Kelly, D. C., Koch, P. L.,
1007   Kump, L. R., Meng, J., Sloan, L. C., Thomas, E., Wing, S. L., and Zachos, J. C.: Eocene
1008   Hyperthermal Event Offers Insight Into Greenhouse Warming, EOS, 87 (17), 165-169,
1009   DOI: 10.1029/2006EO170002, 2006.

1010 Braga G.: L'assetto tettonico dei dintorni di Possagno (Trevigiano occidentale). Rendiconti
1011   dell'Accademia Nazionale dei Lincei, 8/48: 451-455, 1970.

1012 Bramlette, M. N., and Riedel, W. R.: Stratigraphic value of discoasters and some other
1013   microfossils related to recent coccolithophores, J. Paleont., 28: 385-403, 1954.

1014 Broecker, W. S., Clark, E., McCorkle D. C., Peng, T-H., Hajadas, I., and Bonani, G.:
1015   Evidence of a reduction in the carbonate ion content of the deep see during the course of
1016   the Holocene, Paleoceanography, 14 (6), 744-752, 1999.

1017 Brown, J. H., Gillooly, J. F., Allen, A. P., Savage, V. M., and West, G. B.: Toward a
1018   metabolic theory of ecology, Ecology, 85(7), 1771-1789, 2004.

1019 Cita, M. B.: Stratigrafia della Sezione di Possagno, in: Bolli, H. M. (Ed.), Monografia

1020   Micropaleontologica sul Paleocene e l'Eocene di Possagno, Provincia di Treviso, Italia,

1021   Schweiz. Palaeontol. Abhandl., 97, 9–33, 1975.

1022 Clyde, W. C., Gingerich, P. D., Wing, S. L., Röhl, U., Westerhold, T., Bowen, G., Johnson,

1023   K., Baczynski, A. A., Diefendorf, A., McInerney, F., Schnurrenberger, D., Noren, A.,

1024   Brady, K., and the BBCP Science Team: Bighorn Basin Coring Project (BBCP): A

1025   continental perspective on early Paleogene hyperthermals, Scientific Drilling, 16, 21-31,

1026   2013.

1027 Coccioni, R., Bancalà, G., Catanzariti, R., Fornaciari, E., Frontalini, F., Giusberti, L., Jovane,

1028   L., Luciani, V., Savian, J., and Sprovieri, M.: An integrated stratigraphic record of the

1029   Palaeocene–lower Eocene at Gubbio (Italy): new insights into the early Palaeogene

1030   hyperthermals and carbon isotope excursions, Terra Nova, 24, 380-386, 2012.

1031 Coxall, H. K., Pearson, P. N., Shackleton, N.J., Hall, M.A.: Hantkeninid depth adaptation: An

1032   evolving life strategy in a changing ocean, Geology, 28, 87-90, doi:10.1130/0091-

1033   7613(2000)28<87:HDAAEL>2.0.CO;2, 2000.

1034 Coxall, H. K., Huber, B. T., and Pearson, P. N.: Origin and morphology of the Eocene

1035   planktic foraminifera *Hantkenina,* J. Foram. Res., 33, 237-261, 2003.

1036 Cramer, B. S., Wright, J. D., Kent, D. V., and Aubry, M.-P.: Orbital climate forcing of δ^{13}C

1037   excursions in the late Paleocene–early Eocene (chrons C24n–C25n), Paleoceanography,

1038   18, 21-1. doi:10.1029/2003PA000909, 2003.

1039 Cramer, B. S., Toggweiler, J. R., Wright, M. E., Katz, J. D., and Miller, K. G.: Ocean

1040   overturning since the Late Cretaceous: Inferences from a new benthic foraminiferal

1041   isotope compilation, Paleoceanography, 24, PA4216, doi:10.1029/2008PA001683, 2009.

1042 Crouch, E. M., Heilmann-Clausen, C., Brinkhuis, H., Morgans, H. E. G, Rogers, K.

1043   M., Egger, H., and Schmitz, B.: Global dinoflagellate event associated with the late

1044   Paleocene thermal maximum, Geology, 29(4), 315-318, 2001.

1045 D'Onofrio, R., Luciani V., Giusberti L., Fornaciari E., and Sprovieri, M.: Tethyan planktic

1046   foraminiferal record of the early Eocene hyperthermal events ETM2, H2 and I1 (Terche

1047   section, northeastern Italy), Rendiconti Online della Società Geologica Italiana, 31, 66-

1048   67, doi: 10.3301/ROL.2014.48, 2014.

1049 Dallanave, E., Agnini, C., Bachtadse, V., Muttoni, G., Crampton J. S., Strong, C. P., Hines,

1050   B. H., Hollis, C. J., and Slotnick, B. S.: Early to middle Eocene magneto-biochronology

1051   of the southwest Pacific Ocean and climate influence on sedimentation: Insights from the

1052   Mead Stream section, New Zealand, Geol. Soc. Am. Bull., 127 (5-6), 643-660, 2015.

1053 DeConto, R. M., Galeotti, S., Pagani, M., Tracy, D., Schaefer, K., Zhang, T., Pollard, D., and

Beerling, D. J.: Past extreme warming events linked to massive carbon re-lease from thawing permafrost, Nature, 484, 87-92, http://dx.doi.org/10.1038/nature10929, 2012.

Demicco, R. V.: Modeling seafloor-spreading rates through time, Geology, 32, 485-488, 2004.

Dickens, G. R.: Methane oxidation during the Late Palaeocene Thermal Maximum, B. Soc. Geol. Fr., 171 (1), 37-49, 2000.

Dickens, G. R.: Down the Rabbit Hole: toward appropriate discussion of methane release from gas hydrate systems during the Paleocene–Eocene thermal maximum and other past hyperthermal events. Clim. Past, 7, 831-846. http://dx.doi.org/10.5194/cp-7-831-2011, 2011.

Dickens, G. R., and Backman J.: Core alignment and composite depth scale for the lower Paleogene through uppermost Cretaceous interval at Deep Sea Drilling Project Site 577, Newsl. Stratigr., 46, 47-68, 2013.

Dickens, G. R., O'Neil, J. R., Rea, D. K., and Owen, R. M.: Dissociation of oceanic methane hydrate as a cause of the carbon isotope excursion at the end of the Paleocene, Paleoceanography, 10, 965-971, doi:10.1029/95PA02087, 1995.

Dickens, G. R., Castillo, M. M., and Walker, J. C. G.: A blast of gas in the latest Paleocene: simulating first-order effects of massive dissociation of oceanic methane hydrate, Geology, 25, 259-262, 1997.

Dunkley Jones, T., Lunt, D. J., Schmidt, D. N., Ridgwell, A., Sluijs, A., Valdez, P. J., and Maslin, M. A.: Climate model and proxy data constraints on ocean warming across the Paleocene–Eocene Thermal Maximum, Earth Sci. Rev., 125, 123-145, 2013.

Edgar, K. M., Bohaty, S. M., Gibbs, S. J., Sexton, P. F., Norris, R. D., and Wilson, P. A.: Symbiont 'bleaching' in planktic foraminifera during the Middle Eocene Climatic Optimum, Geology, 41, 15-18, doi:10.1130/G33388.1, 2012.

Ernst, S.R., Guasti, E., Dupuis, C., and Speijer, R.P.: Environmental perturbation in the southern Tethys across the Paleocene/Eocene boundary (Dababiya, Egypt): foraminiferal and clay mineral records. Mar. Micropaleont., 60, 89–111, 2006.

Ezard, T. H. G., Aze, T., Pearson, P.N., and Purvis, A: Interplay between changing climate and species' ecology drives macroevolutionary dynamics, Science, 332, 349-351, 2011.

Falkowski, P. G., Katz, M. E., Milligan, A. J., Fennel, K., Cramer, B. S., Aubry, M. P., Berner, R. A., Novacek, M. J., Zapol, W. M.: Mammals evolved, radiated, and grew in size as the concentration of oxygen in Earth's atmosphere increased during the past 100 million years, Science, 309 (5744), 2202-2204, 2005.

1088   Figueirido, B., Janis, C. M., Pérez-Claros, J. A., De Renzi, M., and Palmqvist, P.: Cenozoic
1089   climate change influences mammalian evolutionary dynamics, Proc. Natl. Acad. Sci.
1090   USA, 109 (3), 722-727, 2012.

1091   Fletcher, B. J., Brentnall, S. J., Anderson, C. W., Berner, R. A., and Beerling, D.J.:
1092   Atmospheric carbon dioxide linked with Mesozoic and early Cenozoic climate change,
1093   Nature Geoscience, 1, 43-48, 2008.

1094   Fornaciari, E., Giusberti, L., Luciani, V., Tateo, F., Agnini, C., Backman, J., Oddone, M., and
1095   Rio, D.: An expanded Cretaceous–Tertiary transition in a pelagic setting of the Southern
1096   Alps (central–western Tethys), Palaeogeogr. Palaeoclimatol. Palaeoecol., 255, 98-131,
1097   2007.

1098   Fraass, A. J., Kelly, D. K., and. Peters, S. E.: Macroevolutionary history of the planktic
1099   foraminifera, Annual Review of Earth and Planetary Sciences, 43, 139-66, doi:
1100   10.1146/annurev-earth-060614-105059, 2015.

1101   Frank, T. D., Arthur, M. A., and Dean, W. E.: Diagenesis of Lower Cretaceous pelagic
1102   carbonates, North Atlantic: paleoceanographic signals obscured, J. Foramin. Res., 29,
1103   340-351, 1999.

1104   Galeotti, S., Krishnan, S., Pagani, M., Lanci, L., Gaudio, A., Zachos, J. C., Monechi, S.,
1105   Morelli, G., and Lourens, L. J.: Orbital chronology of early Eocene hyperthermals from
1106   the Contessa Road section, central Italy, Earth Planet. Sci. Lett., 290(1-2), 192-200, doi:
1107   10.1016/j.epsl.2009.12.021, 2010.

1108   Gingerich, P. D.: Rates of evolution on the time scale of the evolutionary process, Genetica,
1109   112-113, 127-144, 2001.

1110   Gingerich, P. D.: Mammalian response to climate change at the Paleocene–Eocene boundary:
1111   Polecat Bench record in the northern Bighorn Basin, Wyoming, Geol. Soc. Am. Spec.
1112   Pap., 369, 463-478, 2003.

1113   Giusberti, L., Rio, D., Agnini, C., Backman, J., Fornaciari, E., Tateo, E., and Oddone, M.:
1114   Mode and tempo of the Paleocene–Eocene thermal maximum in an expanded section
1115   from the Venetian pre-Alps, Geol. Soc. Am. Bull., 119, 391-412, 2007.

1116   Guasti, E., and Speijer, R.P.: The Paleocene–Eocene thermal maximum in Egypt and
1117   Jordan: an overview of the planktic foraminiferal record. Geol. Soc. Spec. Pap., 424, 53–
1118   67, 2007.

1119   Hallock, P.: Fluctuations in the trophic resource continuum: a factor in global diversity
1120   cycles? Paleoceanography, 2, 457–471, 1987.

1121   Hancock, H. J. L., and Dickens, G. R.: Carbonate dissolution episodes in Paleocene and

Eocene sediment, Shatsky Rise, west-central Pacific, Proc. Ocean Drill. Progr., Sci. Results 198, 24 pp., doi:10.2973/odp.proc.sr.198.116., 2005.

Hemleben, C, Spindler, M., and Anderson, O. R (Eds.).: Modern planktonic foraminifera, Springer-Verlag, New York, 1-363, ISBN-13: 9780387968155, 1989.

Hilgen, F. J., Abels, H. A., Kuiper, K. F., Lourens, L. J., and Wolthers, M.: Towards a stable astronomical time scale for the Paleocene: aligning Shatsky Rise with the Zumaia – Walvis Ridge ODP Site 1262 composite, Newsl. Stratigr., 48, 91-110, doi: 10.1127/nos/2014/0054, 2015.

Hollis, C. J., Taylor, K. W. R., Handley, L., Pancost, R. D., Huber, M., Creech, J. B., Hines, B. R., Crouch, E. M., Morgans, H. E. G., Crampton, J. S., Gibbs, S., Pearson, P. N., and Zachos, J. C.: Early Paleogene temperature history of the Southwest Pacific Ocean: Reconciling proxies and models: Earth Planet. Sci. Lett., 349-350, 53–66, doi: 10.1016/j.epsl.2012.06.024, 2012.

Huber, M., and Caballero, R.: The early Eocene equable climate problem revisited. Clim. Past, 7, 603-633, 2011.

Hyland, E. G., and Sheldon, N. D.: Coupled CO_2-climate response during the Early Eocene Climatic Optimum, Palaeogeogr. Palaeoclimatol. Palaeoecol., 369, 125-135, 2013.

Hyland, E. G., Sheldon, N. D., and Fan, M.: Terrestrial paleoenvironmental reconstructions indicate transient peak warming during the early Eocene climatic optimum, Geol. Soc. Am. Bull., 125 (7-8), 1338-1348, 2013.

IPCC, 2014: Climate Change 2014: Synthesis Report. Contribution of Working Groups I, II and III to the Fifth Assessment Report of the Intergovernmental Panel on Climate Change [Core Writing Team, R.K. Pachauri and L.A. Meyer (eds.)]. IPCC, Geneva, Switzerland, 151 pp, 2014.

Inglis, G. N., Farnsworth, A., Lunt, D., Foster, G. L., Hollis, C. J., Pagani, M., Jardine, P. E., Pearson, P. N., Markwick, P., Galsworthy, A. M. J., Raynham, L., Taylor, K. W. R., and Pancost, R. D.: Descent toward the icehouse: Eocene sea surface cooling inferred from GDGT distributions. Paleoceanography, 30 (7), 100-1020, 10.1002/2014PA002723, 2015.

Ito, G., and Clift, P. D.: Subsidence and growth of Pacific Cretaceous plateaus. Earth Plant. Sci. Lett., 161, 85-100, 1998.

John E. H., Pearson P. N., Coxall H. K., Birch H., Wade B. S., and Foster G. L.: Warm ocean processes and carbon cycling in the Eocene, Phil. Trans. R. Soc., A, 371, 20130099, 2013.

1156   John E. H., Wilson J. D., Pearson P. N., and Ridgwell, A.: Temperature-dependent
1157   remineralization and carbon cycling in the warm Eocene oceans, Palaeogeogr.
1158   Palaeoclimatol. Palaeoecol., 413, 158-166, 2014.

1159   Kelly, D. C., Bralower, T. J., Zachos, J. C., Premoli Silva, I., and Thomas, E.: Rapid
1160   diversification of planktonic foraminifera in the tropical Pacific (ODP Site 865) during
1161   the late Paleocene thermal maximum, Geology 24, 423-426, 1996.

1162   Kelly, D. C., Bralower, T. J., and Zachos, J. C.: Evolutionary consequences of the latest
1163   Paleocene thermal maximum for tropical planktonic foraminifera, Palaeogeogr.,
1164   Palaeoclimatol., Palaeoecol., 141, 139-161, 1998.

1165   Kennett, J. P., and Stott, L. D.: Abrupt deep-sea warming, palaeoceanographic changes and
1166   benthic extinctions at the end of the Palaeocene, Nature 353, 225-229, 1991.

1167   Kirtland-Turner, S., Sexton P. F., Charled C. D., and Norris R. D.: Persistence of carbon
1168   release events through the peak of early Eocene global warmth, Nature Geoscience, 7,
1169   748-751, doi: 10.1038/NGEO2240, 2014.

1170   Komar, N., Zeebe, R. E., and Dickens, G. R.: Understanding long-term carbon cycle trends:
1171   the late Paleocene through the early Eocene, Paleoceanography, 28, 650-662, doi:
1172   10.1002/palo.20060, 2013.

1173   Kroenke, L. W., Berger, W. H., Janecek, T. R., et al.: Ontong Java Plateau, Leg 130: synopsis
1174   of major drilling results, Proceedings of the Ocean Drilling Program, Initial Reports, 130,
1175   497-537, 1991.

1176   Kurtz, A. C., Kump, L. R., Arthur, M. A., Zachos, J. C., and Paytan, A.: Early Cenozoic
1177   decoupling of the global carbon and sulfur cycles, Paleoceanography, 18, 1090, doi:
1178   10.1029/2003PA000908, 2003.

1179   Lauretano, V., Littler, K., Polling, M., Zachos, J. C., and Lourens, L. J.: Frequency,
1180   magnitude and character of hyperthermal events at the onset of the Early Eocene
1181   Climatic Optimum, Clim. Past, 11, 1313-1324, doi: 10.5194/cp-11-1313-2015, 2015.

1182   Lee C. T., Shen B., Slotnick B. S., Liao K., Dickens G. R., Yokoyama Y., Lenardic A.,
1183   Dasgupta R., Jellinek M., Lackey J. S., Schneider T., and Tice M. M.: Continental arc-
1184   island arc fluctuations, growth of crustal carbonates, and long-term climate change,
1185   Geosphere, 9, 21-36, 2013.

1186   LeGrande, A. N. and Schmidt, G. A.: Global gridded data set of the oxygen isotopic
1187   composition in seawater, Geophys. Res. Lett., 33, L12604, doi: 10.1029/2006GL026011,
1188   2006.

1189   Leon-Rodriguez, L. and Dickens, G. R.: Constraints on ocean acidification associated with

1190   rapid and massive carbon injections: The early Paleogene record at ocean drilling

1191   program site 1215, equatorial Pacific Ocean, Palaeogeogr. Palaeoclimatol. Palaeoecol.,

1192   298 (3-4), 409-420, doi: 10.1016/j.palaeo.2010.10.029, 2010.

1193   Lirer, F.: A new technique for retrieving calcareous microfossils from lithified lime deposits.

1194   Micropaleontol., 46, 365–369, 2000.

1195   Littler, K., Röhl, U., Westerhold, T., and Zachos, J. C.: A high-resolution benthic stable-

1196   isotope for the South Atlantic: implications for orbital-scale changes in Late Paleocene-

1197   early Eocene climate and carbon cycling, Earth Planet. Sci. Lett., 401, 18-30.

1198   http://dx.doi.org/10.1016/j.epsl.2014.05.054, 2014.

1199   Lourens, L. J., Sluijs, A., Kroon, D., Zachos, J. C., Thomas, E., Röhl, U., Bowles, J., and

1200   Raffi, I.: Astronomical pacing of late Palaeocene to early Eocene global warming events,

1201   Nature, 7045, 1083-1087, 2005.

1202   Lowestein, T. K., and Demicco R. V.: Elevated Eocene atmospheric CO_2 and its subsequent

1203   decline, Science, 313 (5795), doi: 10.1126/science.1129555, 2006.

1204   Lu, G.: Paleocene-Eocene transitional events in the ocean: Faunal and isotopic analyses of

1205   planktic foraminifera, Ph.D. Thesis, Princeton University, pp. 1-284, 1995.

1206   Lu, G., and Keller, G.: Planktic foraminiferal faunal turnovers in the subtropical Pacific

1207   during the late Paleocene to early Eocene, J. Foramin. Res., 25 (2), 97-116, 1995.

1208   Lu, G., Keller, G. and Pardo, A.: Stability and change in Tethyan planktic foraminifera across

1209   the Paleocene-Eocene transition, Mar. Micropaleont., 35 (3-4), 203-233, 1998.

1210   Luciani, V., Giusberti, L., Agnini, C., Backman, J., Fornaciari, E., and Rio., D.: The

1211   Paleocene–Eocene Thermal Maximum as recorded by Tethyan planktonic foraminifera

1212   in the Forada section (northern Italy), Mar. Micropaleont., 64, 189-214, 2007.

1213   Luciani, V., Giusberti, L., Agnini, C., Fornaciari, E., Rio, D., Spofforth, D. J. A., and Pälike

1214   H.: Ecological and evolutionary response of Tethyan planktonic foraminifera to the

1215   middle Eocene climatic optimum (MECO) from the Alano section (NE Italy),

1216   Palaeogeogr. Palaeoclimatol. Palaeoecol., 292, 82-95, doi: 10.1016/j.palaeo.2010.03.029,

1217   2010.

1218   Luciani, V., and Giusberti, L.: Reassessment of the early–middle Eocene planktic

1219   foraminiferal biomagnetochronology: new evidence from the Tethyan Possagno section

1220   (NE Italy) and Western North Atlantic Ocean ODP Site 1051, J. Foram. Res., 44, 2, 187-

1221   201, 2014.

1222   Lunt, D. J., Ridgwell, A., Sluijs, A., Zachos, J., Hunter, S., and Haywood, A.: A model for

1223   orbital pacing of methane hydrate destabilization during the Palaeogene, Nat. Geosc., 4,

1224   775-778, doi: 10.1038/NGEO1266, 2011.

1225 Marshall, J. D.: Climatic and oceanographic isotopic signals from the carbonate rock records

1226   and their preservation, Geol. Mag., 129, 143-160, 1992.

1227 Matter, A., Douglas, R. G., and Perch-Nielsen, K: Fossil preservation, geochemistry and

1228   diagenesis of pelagic carbonates from Shatsky Rise, northwest Pacific, Initial Reports

1229   Deep Sea Drilling Project, 32, 891-922, doi: 10.2973/dsdp.proc.32.137, 1975.

1230 Martini, E.: Standard Tertiary and Quaternary calcareous nannoplankton zonation. In:

1231   Farinacci, A., Ed., Proceedings of the 2nd Planktonic Conference, 739–785. Roma:

1232   Edizioni Tecnoscienza, vol. 2, 1971.

1233 McInerney, F. A. and Wing, S. L.: The Paleocene–Eocene thermal maximum: a perturbation

1234   of carbon cycle, climate, and biosphere with implications for the future, Ann. Rev. Earth

1235   Planet. Sci., 39, 489-516, doi: 10.1146/annurev-earth-040610-133431, 2011.

1236 Mita, I.: Data Report: Early to late Eocene calcareous nannofossil assemblages of Sites 1051

1237   and 1052, Blake Nose, Northwestern Atlantic Ocean, Proc. Ocean Drilling Program, Sci.

1238   Results, 171B, 1-28, 2001.

1239 Molina, E., Arenillas, I., Pardo, A.: High resolution planktic foraminiferal biostratigraphy

1240   and correlation across the Palaeocene Palaeocene/Eocene boundary in the Tethys, B.

1241   Soc. Géol. Fr., 170, 521–530, 1999.

1242 Monechi, L., Bleil, U., and Backman, J.: Magnetobiochronology of Late Cretaceous-

1243   Paleogene and late Cenozoic pelagic sedimentary sequences from the northwest Pacific

1244   (Deep Sea Drilling Project, Leg 86, Site 577. Proceedings of the Ocean Drilling Program

1245   86, Initial Reports, Ocean Drilling Program, College Station, TX,

1246   doi:10.2973/dsdp.proc.86.137.1985.

1247 Nguyen, T. M. P., Petrizzo, M.-R., and Speijer, R. P.: Experimental dissolution of a fossil

1248   foraminiferal assemblage (Paleocene–Eocene Thermal Maximum, Dababiya, Egypt):

1249   implications for paleoenvironmental reconstructions, Mar. Micropaleont., 73 (3-4), 241-

1250   258, doi: 10.1016/j.marmicro.2009.10.005, 2009.

1251 Nguyen, T. M. P., Petrizzo, M.-R., Stassen, P., and Speijer, R. P.: Dissolution susceptibility

1252   of Paleocene–Eocene planktic foraminifera: Implications for palaeoceanographic

1253   reconstructions, Mar. Micropaleont., 81, 1-21, 2011.

1254 Nicolo, M. J., Dickens, G. R., Hollis, C. J., and Zachos, J. C.: Multiple early Eocene

1255   hyperthermals: their sedimentary expression on the New Zealand continental margin and

1256   in the deep sea, Geology, 35, 699-702, 2007.

1257 Norris, R.D.: Biased extinction and evolutionary trends, Paleobiology, 17 (4), 388-399, 1991.

1258   Norris, R.: Symbiosis as an evolutionary innovation in the radiation of Paleocene planktic
1259   foraminifera, Paleobiology, 22, 461-480, 1996.

1260   Norris, R. D., Kroon, D., and Klaus, A.: Proceedings of the Ocean Drilling Program, Initial
1261   Reports, 171B, Proc. Ocean Drill. Progr. Sci. Results, 1-749, 1998.

1262   O'Connor, M., Piehler, M. F., Leech, D. M., Anton, A., and Bruno, J. F.: Warming and
1263   resource availability shift food web structure and metabolism, PLOS Biol., 7(8), 1-6. doi:
1264   10.1371/journal.pbio.1000178, 2009.

1265   Ogg, J. G., and Bardot, L.: Aptian through Eocene magnetostratigraphic correlation of the
1266   Blake Nose Transect (Leg 171B), Florida continental margin, Proc. Ocean Drill. Progr.,
1267   Sci. Results, 171B, 1-58, doi: 10.2973/odp.proc.sr.171B.104.2001

1268   Okada, H. and Bukry, D.: Supplementary modification and introduction of code numbers to
1269   the low-latitude coccolith biostratigraphic zonation (Bukry, 1973;1975). Mar.
1270   Micropaleont., 5, 321-325, 1980.

1271   Olivarez Lyle, A., and Lyle, M. W.: Missing organic carbon in Eocene marine sediments: Is
1272   metabolism the biological feedback that maintains end-member climates?
1273   Paleoceanography, 21, PA2007, doi: 10.1029/2005PA001230, 2006.

1274   Oreshkina, T. V.: Evidence of late Paleocene - early Eocene hyperthermal events in
1275   biosiliceous sediments of Western Siberia and adjacent areas, Austrian Journal of Earth
1276   Science, 105, 145-153, 2012.

1277   Pälike, H., Lyle, M. W., Nishi, H., Raffi, I., Ridgwell, A., Gamage, K., Klaus, A., Acton, G.,
1278   Anderson, L., Backman, J., Baldauf, J., Beltran, C., Bohaty S. M., Bown, P., Busch, W.
1279   Channell, J. E. T., Chun, C. O. J., Delaney, M., Dewangan, P., Dunkley Jones, T., Edgar,
1280   K. M., Evans, H., Fitch, P. L., Foster, G. L., Gussone, N., Hasegawa, H., Hathorne, E. C.,
1281   Hayashi, H., Herrle, J. O., Holbourn, A., Hovan, S., Hyeong, K., Iijima, K., Ito, T.,
1282   Kamikuri, S., Kimoto, K., Kuroda, J., Leon-Rodriguez, L., Malinverno, A., Moore, T. C.,
1283   Brandon, H., Murphy, D. P., Nakamura, H., Ogane, K., Ohneiser, C. Richter, C.,
1284   Robinson, R., Rohling, E. J., Romero, O., Sawada, K., Scher, H., Schneider, L., Sluijs,
1285   A., Takata, H., Tian, J., Tsujimoto, A., Wade, B. S., Westerhold, T., Wilkens, R.,
1286   Williams, T., Wilson, P. A., Yamamoto, Y., Yamamoto, S., Yamazaki, T., and Zeebe, R.
1287   E.: Cenozoic record of the equatorial Pacific carbonate compensation depth, Nature, 488,
1288   609-614, doi: 10.1038/nature11360, 2012, 2012.

1289   Pearson P.N., Coxall H.K.: Origin of the Eocene planktonic foraminifer *Hantkenina* by
1290   gradual evolution, Palaeontology, 57, 243-267, 2014.

1291   Pearson, P. N., and Palmer, M. R.: Atmospheric carbon dioxide concentrations over the past

1292   60 million years, Nature, 406, 695-699, doi: 10.1038/35021000, 2000.

1293   Pearson, P. N., Shackleton, N.J., Hall, M.A.: Stable isotope paleoecology of middle Eocene

1294   planktonic foraminifera and multi-species isotope stratigraphy, DSDP Site 523, south

1295   Atlantic, J. Foram. Res., 23, 123-140, 1993.

1296   Pearson, P.N., Ditchfield, P.W, Singano, J., Harcourt-Brown, K.G., Nicholas, C.J., Olsson,

1297   R.K, Shackleton, N.J., Hall, M.A.: Warm tropical sea surface temperatures in the Late

1298   Cretaceous and Eocene epochs, Nature, 413, 481-487, 2001. doi:10.1038/35097000,

1299   2001.

1300   Pearson, P. N., Olsson, R. K., Huber, B. T., Hemleben, C., and Berggren, W.A. (Eds.): Atlas

1301   of Eocene planktonic foraminifera, Cushman Found. Foram. Res., Spec. Publ., 41, 1-514,

1302   2006.

1303   Pearson, P. N., Van Dongen, B. E., Nicholas, C. J., Pancost, R. D., Schouten, S., Singano, J.

1304   M. and Wade, B. S.: Stable warm tropical climate through the Eocene Epoch, Geology,

1305   35, 211-214, 2007.

1306   Petrizzo, M.R.: The onset of the Paleocene–Eocene Thermal Maximum (PETM) at Sites 1209

1307   and 1210 (Shatsky Rise, Pacific Ocean) as recorded by planktonic foraminifera, Mar.

1308   Micropaleont., 63, 187–200, 2007.

1309   Petrizzo, M.-R., Leoni, G., Speijer, R. P., De Bernardi, B., and Felletti, F.: Dissolution

1310   susceptibility of some Paleogene planktonic foraminifera from ODP Site 1209 (Shatsky

1311   Rise, Pacific Ocean), J. Foram. Res. 38, 357-371, 2008.

1312   Pross, J., Contreras, L., Bijl, P. K., Greenwood, D. R., Bohaty, S. M., Schouten, S., Bendle J.

1313   A., Röhl, U., Tauxe, L., Raine, J. I., Claire E., Huck, C. E., van de Flierdt, T., Stewart S.

1314   R. Jamieson, S. S. R., Stickley, C. E., van de Schootbrugge, B., Escutia, C., and

1315   Brinkhuis, H.: Persistent near-tropical warmth on the Antarctic continent during the early

1316   Eocene Epoch: Nature, v. 488, 73-77, doi: 10 .1038 /nature11300, 2012.

1317   Pujalte, V., Baceta, J. G., and Schmitz, B.: A massive input of coarse-grained siliciclastics in

1318   the Pyrenean Basin during the PETM: the missing ingredient of a coeval abrupt change

1319   in hydrological regime, Clim. Past, Climatic and biotic events of the Paleogene, Special

1320   issue, G. R. Dickens, V. Luciani, and A. Sluijs, (Eds.), 11, 1653-1672, doi:10.5194/cp-

1321   11-1653-2015, 2015.

1322   Quillévéré, F., Norris, R. D., Moussa, I., and Berggren, W. A.: Role of photosymbiosis and

1323   biogeography in the diversification of early Paleogene acarininids (planktonic

1324   foraminifera), Paleobiology, 27, 311-326, 2001.

1325   Raffi, I., and De Bernardi, B.: Response of calcareous nannofossils to the Paleocene-Eocene

1326   Thermal Maximum: observations on composition, preservation and calcification in

1327   sediments from ODP Site 1263 (Walvis Ridge-SW Atlantic). Mar. Micropaleont. 69,

1328   119–138, 2008.

1329   Raymo, M. E., and Ruddiman W. F.: Tectonic forcing of late Cenozoic climate, Nature, 359,

1330   117-122, 1992.

1331   Reghellin, D., Coxall, H. K., Dickens, G. R., and Backman, J.: Carbon and oxygen isotopes

1332   of bulk carbonate in sediment deposited beneath the eastern equatorial Pacific over the

1333   last 8 million years. Paleoceanography, 30: 1261-1286. doi: 10.1002/2015PA002825,

1334   2015.

1335   Röhl, U., Westerhold, T., Monechi, S., Thomas, E., Zachos, J. C., and Donner, B.: The third

1336   and final early Eocene Thermal Maximum: characteristics, timing, and mechanisms of

1337   the "X" event, Geol. Soc. Am. Abstracts with Program, 37(7), 264, 2005.

1338   Schlanger, S.O. and Douglas, R.G.: The pelagic ooze-chalk-limestone transition and its

1339   implications for marine stratigraphy, In: Pelagic Sediments: on Land and under the Sea,

1340   K.J. Hsü and H.C. Jenkyns (Eds.), Spec. Publs. Ass. Sediment., 1, 117–148, 1974.

1341   Scholle, P. A., and Arthur, M. A.: Carbon isotope fluctuations in Cretaceous pelagic

1342   limestones: potential stratigraphic and petroleum exploration tool, American Association

1343   of Petroleum Geologists Bulletin, 64, 67-87, 1980.

1344   Schmitz, B., and Puljate, V.: Abrupt increase in seasonal extreme precipitation at the

1345   Paleocene-Eocene boundary, Geology, 35, 215-218, 2007.

1346   Schmidt, D. N., Thierstein, H. R., and Bollmann, J.: The evolutionary history of size variation

1347   of planktic foraminiferal assemblages in the Cenozoic, Palaeogeogr. Palaeoclimatol.

1348   Palaeoecol., 212, 159-180, doi: 10.1016/j.palaeo.2004.06.002, 2004.

1349   Scheibner, C., and Speijer, R.P.: Decline of coral reefs during the late Paleocene to early

1350   Eocene global warming, eEarth, 3, 19-26, www.electronic-earth.net/3/19/2008/, 2008.

1351   Schneider, L. J. Bralower, T. J., and Kump, L. J.: Response of nannoplankton to early Eocene

1352   ocean destratification, Palaeogeogr. Palaeoclimatol. Palaeoecol., 310, 152-162, 2011.

1353   Schulte, P., Scheibner, C. and Speijer, R.C.: Fluvial discharge and sea-level changes

1354   controlling black shale deposition during the Paleocene–Eocene Thermal Maximum in

1355   the Dababiya Quarry section, Egypt, Chem. Geol., 285, 167-183,

1356   doi:10.1016/j.chemgeo.2011.04.004, 2011.

1357   Schrag, D. P., DePaolo, D. J., and Richter, F. M.: Reconstructing past sea surface

1358   temperatures: correcting for diagenesis of bulk marine carbonate, Geochim. Cosmochim.

1359   Ac., 59, 2265-2278, 1995.

1360   Schmitz, B., Speijer, R. P., and Aubry M.-P.: Latest Paleocene benthic extinction event on

1361   the southern Tethyan shelf (Egypt): Foraminiferal stable isotopic (δ^{13}C, δ^{18}O) records,

1362   Geology, 24, 347-350, 1996.

1363   Self-Trail, J. M., Powars, D. S., Watkins, D. K., Wandless, G. A.: Calcareous nannofossil

1364   assemblage changes across the Paleocene–Eocene Thermal Maximum: Evidence from a

1365   shelf setting, Mar. Micropaleont., 92–93, 61–80, 2012.

1366   Sexton, P.F., Wilson, P.A., Norris, R.D.: Testing the Cenozoic multisite composite δ^{18}O and

1367 δ^{13}C curves: New monospecific Eocene records from a single locality, Demerara Rise

1368   (Ocean Drilling Program Leg 207), Paleoceanography, 21, PA2019, 2006.

1369   Sexton, P. F., Norris R. D., Wilson, P. A., Pälike, H., Westerhold, T., Röhl, U., Bolton, C. T.,

1370   and Gibbs, S.: Eocene global warming events driven by ventilation of oceanic dissolved

1371   organic carbon, Nature 471, 349-353, doi: 10.1038/nature09826, 2011.

1372   Shackleton, N. J.: Paleogene stable isotope events. Palaeogeogr. Palaeoclim. Palaeoecol., 57,

1373   91-102, 1986.

1374   Shackleton, N. J., and Hall, M. A.: Stable isotope records in bulk sediments (Leg 138), Proc.

1375   Ocean Drill. Progr. Sci. Results, 138, 797-805, doi:10.2973/odp.proc.sr.138.150.1995.

1376   Shamrock, J. L., Watkins, D. K., and Johnston, K. W.: Eocene bio-geochronology of ODP

1377   Leg 122 Hole 762C, Exmouth Plateau (northwest Australian Shelf), Stratigraphy, 9, 55-

1378   76, 2012.

1379   Shipboard Scientific Party, 1985, Site 577: Initial Reports Deep Sea Drilling Project, 86, in:

1380   Heath, G.R., Burckle, L.H., et al. (Eds.), Washington (U.S. Government Printing Office),

1381   91–137. doi:10.2973/dsdp.proc.86.104.1985, 1995.

1382   Shipboard Scientific Party, 1998, Site 1051: Proceeding Ocean Drilling Program, Initial

1383   Reports, 171B, in: Norris, R.D., Kroon, D., Klaus, A., et al (Eds.), Ocean Drilling

1384   Program, College Station, TX, 171–239. doi:10.2973/odp.proc.ir.171b.105.1998, 1998.

1385   Sims, P. A., Mann, D. G., and Medlin, L. K.: Evolution of the diatoms: insights from fossil,

1386   biological and molecular data, Phycologia, 45, 361-402, 2006.

1387   Sinton, C. W., and Duncan R. A.: ^{40}Ar-^{39}Ar ages of lavas from the southeast Greenland

1388   margin, ODP Leg 152, and the Rockall Plateau, DSDP Leg 81, Ocean Drill. Progr., Sci.

1389   Res., 152, 387-402, doi:10.2973/odp.proc.sr.152.234.1998, 1998.

1390   Slotnick, B. S., Dickens, G. R., Nicolo, M. J., Hollis, C. J., Crampton, J. S., Zachos, J. C., and

1391   Sluijs, A.: Large-amplitude variations in carbon cycling and terrestrial weathering during

1392   the latest Paleocene and earliest Eocene: The Record at Mead Stream, New Zealand, J.

1393   Geol., 120, 487-505, 2012.

1394 Slotnick, B. S., Dickens, G. R., Hollis, C. J., Crampton, J. S., Percy Strong, C., and Zachos, J.

1395   C.: Extending lithologic and stable carbon isotope records at Mead Stream (New

1396   Zealand) through the middle Eocene, in: Dickens G.R., Luciani V. eds. Climatic and

1397   biotic events of the Paleogene 2014 CBEP 2014 Volume 31, Roma, Società Geologica

1398   Italiana, 201-202, 2014.

1399 Slotnick, B. S., Dickens, G. R., Hollis, C. J., Crampton, J. S., Strong, P. S. and Phillips, A.:

1400   The onset of the Early Eocene Climatic Optimum at Branch Stream, Clarence River

1401   valley, New Zealand, New Zeal. J. Geol. Geop., doi: 10.1080/00288306.2015.1063514,

1402   2015a.

1403 Slotnick, B. S., Laurentano, V., Backman, J., Dickens, G. R., Sluijs, A., and Lourens, L.:

1404   Early Paleogene variations in the calcite compensation depth: new constraints using old

1405   borehole sediments from across Ninetyeast Ridge, central Indian Ocean, Clim. Past, 11,

1406   472-493, 2015b.

1407 Sluijs, A., and Dickens, G. R.: Assessing offsets between the $\delta^{13}C$ of sedimentary

1408   components and the global exogenic carbon pool across early Paleogene carbon cycle

1409   perturbations, Global Biogeochem. Cy., 26 (4), GB4019, doi: 10.1029/2011GB004094,

1410   2012.

1411 Sluijs, A., Schouten, S., Pagani, M., Woltering, M., Brinkhuis, H., Sinninghe Damsté, J. S.,

1412   Dickens, G. R., Huber, M., Reichart, G., Stein, R., Matthiessen, J., Lourens, L. J.,

1413   Pedentchouk, N., Backman, J., Moran, K., and the Expedition 302 Scientists: Subtropical

1414   Arctic Ocean temperatures during the Palaeocene/Eocene thermal maximum, Nature,

1415   441, 610-613, doi: 10.1038/nature04668, 2006.

1416 Sluijs, A., Bowen, G. J., Brinkhuis, H., Lourens, L. J., and Thomas, E.: The Paleocene–

1417   Eocene thermal maximum super greenhouse: biotic and geochemical signatures, age

1418   models and mechanisms of global change, in: Deep-Time Perspectives on Climate

1419   Change, Williams, M., Haywood, A. M., Gregory, F. J., and Schmidt, D. N., (Eds.),

1420   Micropalaeont. Soc. Spec. Publ., Geological Society, London, 323-350, 2007.

1421 Smith, R. Y., Greenwood, D. R., and Basinger, J. F.: Estimating paleoatmospheric pCO_2

1422   during the Early Eocene Climatic Optimum from stomatal frequency of Ginkgo,

1423   Okanagan Highlands, British Columbia, Canada, Palaeogeogr. Palaeoclimatol.

1424   Palaeoecol., 293, 120-131, 2010.

1425 Stap, L., Sluijs, A., Thomas, E., and Lourens L. J.: Patterns and magnitude of deep sea

1426   carbonate dissolution during Eocene Thermal Maximum 2 and H2, Walvis Ridge,

1427   southeastern Atlantic Ocean, Paleoceanography, 24, 1211, doi: 10.1029/2008PA001655,
1428   2009.

1429 Thomas, E.: Biogeography of the late Paleocene benthic foraminiferal extinction, in: Late
1430   Paleocene-early Eocene climatic and biotic events in the marine and terrestrial Records,
1431   Aubry, M.-P., Lucas, S., and Berggren, W. A., (Eds.), Columbia University Press, New
1432   York, 214-243, 1998.

1433 Thomas, E., Brinkhuis, H., Huber, M., and Röhl, U.: An ocean view of the early Cenozoic
1434   Greenhouse world, Oceanography, 19, 94-103, 2006.

1435 Thunell R. C. and Honjo, S.: Calcite dissolution and the modification of planktonic
1436   foraminiferal assemblages, Mar. Micropaleont., 6, 169-182, 1981.

1437 Vandenberghe N., Hilgen F. J., Speijer R. P., Ogg J. G., Gradstein F. M., Hammer O., Hollis
1438   C. J., and Hooker J. J.: The Paleogene Period, in: Gradstein, F., Ogg, J.G., Schmitz,
1439   M.D., Ogg, G.M., (Eds.), The Geologic Time Scale 2012, 855-921, Elsevier,
1440   Amsterdam, 2012.

1441 Vincent, E., and Berger, W. H: Planktonic foraminifera and their use in paleoccanography;
1442   in: Emiliani. C (Ed.), The Sea, 7 (25), New York, 1025-1119, 1981.

1443 Vogt, P. R.: Global magmatic episodes: New evidence and implications for the steady state
1444   mid-oceanic ridge, Geology, 7, 93-98, 1979.

1445 Wade, B. S.: Planktonic foraminiferal biostratigraphy and mechanisms in the extinction of
1446   *Morozovella* in the late Middle Eocene, Mar. Micropaleont., 51, 23–38, 2004.

1447 Wade, B. S., Al-Sabouni, N., Hemleben, C., and Kroon, D.: Symbiont bleaching in fossil
1448   planktonic foraminifera, Evol. Ecol., 22, 253-265. doi: 10.1007/s10682-007-9176-6,
1449   2008.

1450 Wade, B. S., Pearson, P. N., Berggren, and W. A., Pälike, H.: Review and revision of
1451   Cenozoic tropical planktonic foraminiferal biostratigraphy and calibration to the
1452   geomagnetic polarity and astronomical time scale, Earth Sci. Rev., 104, 111-142, doi:
1453   10.1016/j.earscirev.2010.09.003, 2011.

1454 Wade, B.S., Fucek, V.P., Kamikuri, S.-I., Bartol, M., Luciani, V., Pearson, P.N.: Successive
1455   extinctions of muricate planktonic foraminifera (*Morozovelloides* and *Acarinina*) as a
1456   candidate for marking the base Priabonian, Newsl. Stratigr., 45 (3) 245-262, 2012.

1457 Westerhold, T., Röhl, U., Frederichs, T., Bohaty, S. M., and Zachos, J. C.: Astronomical
1458   calibration of the geological timescale: closing the middle Eocene gap, Clim. Past, 11,
1459   1181–1195, doi: 10.5194/cp-11-1181-2015, 2015.

1460 Wilf, P., Cúneo, R. N., Johnson, K. R., Hicks, J. F., Wing, S. L., and Obradovich, J. D.: High

1461   plant diversity in Eocene South America: evidence from Patagonia, Science, 300, 122-

1462   125, 2003.

1463 Wing, S. L., Bown, T. M., and Obradovich, J. D.: Early Eocene biotic and climatic change in

1464   interior western North America, Geology 19, 1189-1192, 1991.

1465 Woodbourne, M. O., Gunnell, G. F., and Stucky, R. K.: Climate directly influences Eocene

1466   mammal faunal dynamics in North America, P. Natl. Acad. Sci. USA, 106 (32), 13399-

1467   13403, 2009.

1468 Yapp, C. J.: Fe(CO_3)OH in goethite from a mid-latitude North American Oxisol: Estimate of

1469   atmospheric CO_2 concentration in the early Eocene "climatic optimum". Geochim.

1470   Cosmochim. Ac., 68(5), 935-947. doi: 10.1016/j.gca.2003.09.002, 2004.

1471 Yamaguchi, T., and Norris R. D.: Deep-sea ostracode turnovers through the Paleocene-

1472   Eocene thermal maximum in DSDP Site 401, Bay of Biscay, North Atlantic, Mar.

1473   Micropaleont., 86-87, 32-44, 2012.

1474 Zachos, J. C., Pagani, M., Sloan, L., Thomas, E., and Billups, K.: Trends, rhythms, and

1475   aberrations in global climate 65 Ma to Present, Science, 292, 686-693, 2001.

1476 Zachos, J. C., Röhl, U., Schellenberg, S. A., Sluijs, A., Hodell, D. A., Kelly, D. C., Thomas,

1477   E., Nicolo, M., Raffi, I., Lourens, L. J., McCarren, H., and Kroon, D.: Rapid acidification

1478   of the ocean during the Paleocene–Eocene thermal maximum, Science, 308, 1611-161,

1479   2005.

1480 Zachos, J. C., Dickens, G. R., and Zeebe, R. E.: An early Cenozoic perspective on

1481   greenhouse warming and carbon-cycle dynamics, Nature, 451, 279-283, 2008.

1482 Zachos, J. C., McCarren, H., Murphy, B., Röhl, U., and Westerhold, T.: Tempo and scale of

1483   late Paleocene and early Eocene carbon isotope cycles: Implications for the origin of

1484   hyperthermals, Earth Planet. Sci. Lett., 299, 242-249, doi: 10.1016/j.epsl.2010.09.004,

1485   2010.

1486 Zeebe, R. E., Zachos, J. C., Dickens, G. R.: Carbon dioxide forcing alone insufficient to

1487   explain Palaeocene–Eocene Thermal Maximum warming. Nat. Geosci.2 (8), 576-580,

1488   http://dx.doi.org/10.1038/ngeo578, 2009.

1489 Zonneveld, J. P., Gunnell, G. F., and Bartels, W. S.: Early Eocene fossil vertebrates from the

1490   southwestern Green River Basin, Lincoln and Uinta Counties, Wyoming, Journal of

1491   Vertebrate Paleontology, 20, 369-386, 2000.

1492

1493 **Figure Captions**

1494

1495   **Figure 1.** Evolution of climate, carbon cycling, and planktic foraminifera across the middle

1496   Paleogene on the GPTS 2012 time scale. Left side shows polarity chrons, and smoothed

1497   oxygen and carbon isotope records of benthic foraminifera, slightly modified from

1498   Vandenberghe et al. (2012). Original oxygen and carbon isotope values come from

1499   compilations by Zachos et al. (2008) and Cramer et al. (2009). Middle of the figure indicates

1500   planktic foraminiferal biozones by Wade et al. (2011) with three modifications. The lower

1501   boundary for Zone E7a is now based on the first occurrence of *Astrorotalia palmerae* due to

1502   diachroneity in the first appearance of the previously selected marker *Acarinina*

1503   *cuneicamerata* (Luciani and Giusberti, 2014). The base of Zone E5, identified by the first

1504   appearance of *Morozovella aragonensis,* occurs within the middle of C24n instead of lower

1505   C23r (see text). A question marks the top of *Morozovella subbotinae* because there is

1506   diachroneity for this occurence (see text). Right side shows a partial view of morozovellid

1507   and acarininid evolution as envisioned by Pearson et al. (2006) and Aze et al. (2011). It does

1508   not include several "root taxa" that disappear in the earliest Eocene (e.g., *M. velascoensis*) or

1509   "excursion taxa" that appear during the Paleocene-Eocene Thermal Maximum (PETM) (e.g.,

1510   *M. allisonensis*). Superimposed on these records are key intervals of climate change,

1511   including the Early Eocene Climatic Optimum (EECO), the Middle Eocene Climatic

1512   Optimum (MECO) and the three well documented early Eocene hyperthermal events. The

1513   extent of the EECO is not precise, because of stratigraphic issues (see text). Red and blue

1514   triangles= top and base of the morozovellid and acarininid zonal markers.

1515

1516   **Figure 2.** Approximate locations of the three sites discussed in this work during the early

1517   Eocene. Also shown is Site 1258, which has a bulk carbonate $\delta^{13}C$ record spanning the

1518   EECO. Base map is from http://www.odsn/de/services/paleomap.html.

1519

1520 **Figure 3**. The Possagno section. Upper panel: geological map (modified from Braga, 1970).

1521 1 = Quaternary deposits; 2, 3 = Calcarenite di Castelcucco (Miocene); 4 = glauconitic

1522 arenites (Miocene); 5 = siltstones and conglomerates (upper Oligocene-lower Miocene); 6 =

1523 Upper Marna di Possagno (upper Eocene); 7 = Formazione di Pradelgiglio (upper Eocene); 8

1524 = Marna di Possagno (upper Eocene); 9 = Scaglia Cinerea (middle-upper Eocene); 10 =

1525 Scaglia Rossa (upper Cretaceous-lower Eocene); 11 = faults; 12 = traces of stratigraphic

1526 sections originally studied by Bolli (1975); red circle = the Carcoselle quarry. Lower panel:

1527 the exposed quarry face during Summer 2002 (Photo by Luca Giusberti).

1528

1529 **Figure 4.** Lithology, stratigraphy, and bulk sediment stable-isotope composition of the

1530 Possagno section aligned according to depth. Lithololologic key: 1 = limestone; 2 = marly

1531 limestone and calcareous marl; 3 = cyclical marl-limestone alternations, 4 = marl; 5= Clay

1532 Marl unit (CMU). Planktic foraminiferal biozones follow those of Wade et al. (2011), as

1533 modified by Luciani and Giusberti (2014). Magnetostratigraphy and key calcareous

1534 nannofossil events come from Agnini et al. (2006); NP-zonation is from Martini (1971).

1535 Nannofossil events are shown as red triangles (tops), blue triangles (bases), and purple

1536 diamonds (evolutionary crossovers); *S. rad*. = *Sphenolithus radians*; T.c./T.o. = *Tribrachiatus*

1537 *contortus/ Tribrachiatus orthostylus; D. lod*. = *Discoaster lodoensis*; Tow. =*Toweius*; *T. orth*.

1538 = *Tribrachiatus orthostylus*; *D. sublod*. = *Discoaster sublodoensis*. Stable isotope records

1539 determined in this study. Established early Eocene "events" are superimposed in light red;

1540 suggested carbon isotope excursions (CIEs) within the EECO are shown with numbers.

1541

1542 **Figure 5.** Cores, stratigraphy, and bulk sediment stable isotope composition for the early

1543 Eocene interval at Deep-Sea Drilling Project (DSDP) Site 577 aligned according to

composite depth (Dickens and Backman, 2013). Note the increased length for the gap

between Core 577*-8H and Core 577*-9H (see text). The Wade et al. (2011) E-zonation,

partly modified by Luciani and Giusberti (2014), has been applied to Site 577 given

assemblages presented by Lu (1995) and Lu and Keller (1995). Note that: (a) the base of

Zone E3 (top of *Morozovella velascoensis*) lies within a core gap; (b) the E4/E5 zonal

boundary (base of M. *aragonensis*) occurs within C24n, in agreement with Luciani and

Giusberti (2014); (c) the E5/E6 zonal boundary is problematic because the top of *M.*

subbotinae occurs in middle C24n, much earlier than the presumed disappearance in the

upper part of C23n (Wade et al., 2011). We have therefore positioned the E5/E6 boundary at

the lowest occurrence of *Acarinina aspensis,* according to the original definition of Zone E5

(Berggren and Pearson, 2005); (d) we cannot differentiate between Zone E6 and Zone E7a

due to the absence of *Astrorotalia palmerae* and to the diachronous appearance of *A.*

cuneicametrata (Luciani and Giusberti, 2014). Magnetostratigraphy and key calcareous

nannofossil events are those summarized by Dickens and Backman (2013). For the latter and

beyond that noted for **Figure 4**: *F.* spp. = *Fasciculithus spp.*; *D. dia.* = *Discoaster diastypus*.

Stable isotope records: black - Cramer et al. (2003), red and blue - this study. Early Eocene

"events" are the same as those in **Figure 4**.

Figure 6. The Possagno section and its δ^{13}C record (**Figure 4**) with measured relative

abundances of primary planktic foraminiferal genera, fragmentation index (*F* index) and

coarse fraction. The subbotinid abundance includes both *Subbotina* and *Parasubbotina*

genera. Note that a significant increase in *Acarinina* abundance marks the EECO and several

carbon isotope excursions (CIEs). Note also the major decline in abundance of *Morozovella*

at the start of the EECO. Filled yellow hexagons show occurrences of abundant radiolarians.

1569   Lithological symbols and early Eocene "events" are the same as those in **Figure 4**.

1570

1571   **Figure 7.** The early Eocene succession at DSDP Site 577 and its δ^{13}C record (**Figure 5**) with

1572   relative abundances of primary planktic foraminiferal genera (Lu, 1995; Lu and Keller,

1573   1995). Note the major switch in *Morozovella* and *Acarinina* abundances approximately

1574   coincides with the J-event, the top of polarity chron C24n, and the start of the EECO. Early

1575   Eocene "events" are the same as those in **Figure 4**.

1576

1577   **Figure 8.** Stratigraphy, bulk sediment δ^{13}C composition, relative abundances of primary

1578   planktic foraminiferal genera, and fragmentation index (*F* index) for the early Eocene interval

1579   at ODP Site 1051. Planktic foraminiferal biozones follow those of Wade et al. (2011), as

1580   modified by Luciani and Giusberti (2014; see **Figure 1** caption). Magnetostratigraphy and

1581   positions of key calcareous nannofossil events come from Ogg and Bardot (2001) and Mita

1582   (2001), but with an important modification to polarity chron labelling (see text and Cramer et

1583   al., 2003). Calcareous nannofossil horizons are the same as in previous figures. Foraminferal

1584   information comes from this study; subbotinids include both *Subbotina* and *Parasubbotina*.

1585   Early Eocene "events" are the same as those in **Figure 4**.

1586

1587   **Figure 9.** Carbon isotope and paleomagnetic records across the early Eocene for the

1588   Possagno section, DSDP Site 577, and ODP Site 1258 (Kirtland-Turner et al., 2014). This

1589   highlights the overall framework of carbon cycling in the early Eocene, but also stratigraphic

1590   problems across the EECO at each of the three sites. At Possagno, the coarse resolution of

1591 δ^{13}C records and the condensed interval makes correlations difficult. At ODP Site 1258 the

1592   prominent K/X event seems missing. At DSDP Site 577, the entire record is compressed in

1593   the depth domain. Nonetheless, a major shift in frequency and amplitude of carbon isotope

1594   excursions (CIEs) appears to have happened during the EECO. CIEs that suggestively

1595   correlate within the EECO are shown with numbers.

1596

1597   **Figure 10.** Records of magnetostratigraphy, bulk sediment δ^{13}C, CaCO$_3$ content, *F* index and

1598   abundance patterns for primary planktic foraminiferal taxa at the Farra section, which crops

1599   out 50 km NE of Possagno. All data are from Agnini et al. (2009). Note that the switch in

1600   abundance between *Morozovella* and *Acarinina* occurs close the J event.

1601

1602   **Figure 11**. Records of morozovellids and large acarininids (>200 micron) in the western

1603   Tethyan setting from the Possagno section (this paper) and the Alano section (Luciani et al.,

1604   2010), plotted with generalized δ^{13}C and δ^{18}O curves for benthic foraminiferal on the

1605   GTS2012 time scale (as summarized by Vandenberghe et al., 2012; slightly modified). These

1606   records suggest that the long-lasting EECO and MECO intervals of anomalous warmth mark

1607   two main steps in the decline of morozovellids and acarininids. The plankic foraminferal

1608   biozones follow those presented by Wade et al. (2011), as partly modified by Luciani and

1609   Giusberti (2014).

1610

1611   **Supplementary material**

1612

1613   **Table S1**. Carbon and oxygen isotopes from the Possagno section.

1614

1615   **Table S2**. Carbon and oxygen isotopes from DSDP Site 577.

1616

1617   **Table S3**. Foraminiferal abundances, fragmentation index (%) and coarse fraction (%) from

1618   the Possagno section.

1619

1620   **Table S4**. Foraminiferal abundances from DSDP Site 577.

1621

1622   **Table S5**. Foraminiferal abundances from ODP Site 1051.

1623

1624   **Figure S1.** The Possagno δ^{13}C data and relative abundance of minor planktic foraminiferal

1625   genera and selected species plotted against lithology and fragmentation index (F index) data.

1626   Magnetostratigraphy is from Agnini et al. (2006). The planktic foraminferal biozonal scheme

1627   is from Wade et al. (2011), as modified by Luciani and Giusberti (2014). Various symbols are

1628   the same as in **Figure 4**.

1629

1630   **Appendix A: Taxonomic list of planktic foraminiferal species cited in text and figures**

1631

1632   *Globanomalina australiformis* (Jenkins, 1965)

1633   *Morozovella aequa* (Cushman and Renz, 1942)

1634   *Morozovella gracilis* (Bolli, 1957)

1635   *Morozovella lensiformis* (Subbotina, 1953)*,*

1636   *Morozovella marginodentata* (Subbotina, 1953)

1637   *Morozovella subbotinae* (Morozova, 1939)

1638   *Parasubbotina eoclava* Coxall*,* Huber and Pearson, 2003

1639   *Parasubbotina griffinae* (Blow, 1979)

1640   *Parasubbotina pseudowilsoni* Olsson and Pearson, 2006

1641   *Subbotina corpulenta* (Subbotina, 1953)

1642   *Subbotina eocena* (Gümbel, 1868)

1643   *Subbotina hagni* (Gohrbandt, 1967)

1644   *Subbotina senni* (Beckmann, 1953)

1645   *Subbotina yeguanesis* (Weinzierl and Applin, 1929*)*

1646   *Planoglobanomalina pseudoalgeriana* Olsson & Hemleben, 2006

1647

1648   **Appendix B: Taxonomic list of calcareous nannofossil taxa cited in text and figures**

1649

1650   *Globanomalina australiformis* (Jenkins, 1965)

1651   *Morozovella aequa* (Cushman and Renz, 1942)

1652   *Morozovella gracilis* (Bolli, 1957)

1653   *Morozovella lensiformis* (Subbotina, 1953)*,*

1654   *Morozovella marginodentata* (Subbotina, 1953)

1655   *Morozovella subbotinae* (Morozova, 1939)

1656   *Parasubbotina eoclava* Coxall*,* Huber and Pearson, 2003

1657   *Parasubbotina griffinae* (Blow, 1979)

1658   *Parasubbotina pseudowilsoni* Olsson and Pearson, 2006

1659   *Subbotina corpulenta* (Subbotina, 1953)

1660   *Subbotina eocena* (Gümbel, 1868)

1661   *Subbotina hagni* (Gohrbandt, 1967)

1662   *Subbotina senni* (Beckmann, 1953)

1663   *Subbotina yeguanesis* (Weinzierl and Applin, 1929*)*

1664   *Planoglobanomalina pseudoalgeriana* Olsson & and Hemleben, 2006

1665

1666   **Appendix B: Taxonomic list of calcareous nannofossil taxa cited in text and figures**

1667

1668   *Discoaster diastypus* Bramlette and Sullivan, 1961

1669   *Discoaster lodoensis* Bramlette and Sullivan, 1961

1670   *Discoaster sublodoensis* Bramlette and Sullivan, 1961

1671   *Fasciculithus* Bramlette and Sullivan, 1961

1672   *Fasciculithus tympaniformis* Hay and Mohler in Hay et al., 1967

1673   *Sphenolithus radians* Deflandre in Grassé, 1952

1674   *Toweius* Hay and Mohler, 1967

1675   *Tribrachiatus contortus* (Stradner, 1958) Bukry, 1972

1676   *Tribrachiatus orthostylus* (Bramlette and Riedel, 1954) Shamrai, 1963

1677

1678

1679

1680

1681

1682

1683

1684

1685

1686

1687

1688

1689

1690

1691

1692

1693

1694 **Major perturbations in the global carbon cycle and photosymbiont-bearing**

1695 **planktic foraminifera during the early Eocene**

1696

1697

1698 Valeria Luciani[1], Gerald R. Dickens[2,3], Jan Backman [2], Eliana Fornaciari[4], Luca Giusberti[4],

1699 Claudia Agnini[4], Roberta D'Onofrio[1]

1700

1701

1702 [1]Department of Physics and Earth Sciences, Ferrara University, Polo Scientifico Tecnologico, via G.

1703   Saragat 1, 44100, Ferrara, Italy

1704 [2]Department of Geological Sciences, Stockholm University, SE-10691 Stockholm, Sweden

1705 [3]Department of Earth Science, Rice University, Houston, TX 77005, USA

1706 [4]Department of Geosciences, Padova University, via G. Gradenigo 6, 35131, Padova, Italy

1707

1708

1709 *Correspondence to:* V. Luciani (valeria.luciani@unife.it)

1710

1711

1712 **Abstract.** A marked switch in the abundance of the planktic foraminiferal genera

1713 *Morozovella* and *Acarinina* occurred at low-latitude sites near the start of the Early Eocene

1714 Climatic Optimum (EECO), a multi-million-year interval when Earth surface temperatures

1715 reached their Cenozoic maximum. Stable carbon and oxygen isotope data of bulk sediment

1716 are presented from across the EECO at two locations: Possagno in northeast Italy, and DSDP

1717 Site 577 in the northwest Pacific. Relative abundances of planktic foraminifera are presented

1718 from these two locations, as well as from ODP Site 1051 in the northwest Atlantic. All three

1719 sections have good stratigraphic markers, and the δ^{13}C records at each section can be

1720 correlated amongst each other and to δ^{13}C records at other locations across the globe. These

1721 records show that a series of negative carbon isotope excursions (CIEs) occurred before,

1722 during and across the EECO, which is defined here as the interval between the "J" event and

1723 the base of *Discoaster sublodoensis*. Significant though ephemeral modifications in planktic

1724 foraminiferal assemblages coincide with some of the short-term CIEs, which were marked by

1725 increases in the relative abundance of acarininids, similar to what happened across

1726 established hyperthermal events in Tethyan settings prior to the EECO. Most crucially, a

1727 temporal link exists between the onset of the EECO, carbon cycle changes during this time,

1728 and the ~~demise~~ decline of morozovellids. Possible causes are multiple, and may include

1729 temperature effects on photosymbiont-bearing planktic foraminifera and changes in ocean

1730 chemistry.

1731

1732

1733

1734

1735

1736

1737

1 Introduction

Cenozoic Earth surface temperatures attained their warmest long-term state during the Early

Eocene Climatic Optimum (EECO). This was a 2-4 Myr time interval (discussed below)

centered at ca. 51 Ma (**Figure 1**), when average high latitude temperatures exceeded those at

present-day by at least 10°C (Zachos et al., 2008; Huber and Caballero, 2011; Hollis et al.,

2012; Pross et al., 2012; Inglis et al., 2015). Several short-term (<200 kyr) global warming

events (**Figure 1**) occurred before the EECO. The Paleocene Eocene Thermal Maximum

(PETM) provides the archetypical example: about 55.9 Ma (Vandenberghe et al., 2012;

Hilgen et al., 2015) temperatures soared an additional 5-6°C relative to background

conditions (Sluijs et al., 2006, 2007; Dunkley Jones et al., 2013). Evidence exists for at least

two other significant Eocene warming events (Cramer et al., 2003; Lourens et al., 2005; Röhl

et al., 2005; Thomas et al., 2006; Nicolo et al., 2007; Agnini et al., 2009; Coccioni et al.,

2012; Lauretano et al., 2015; Westerhold et al., 2015): one ca. 54.1 Ma and named H-1 or

Eocene Thermal Maximum 2 (ETM-2, also referred as the ELMO event), and one at 52.8 Ma

and variously named K, X, or ETM-3 (hereafter called K/X). However, additional brief

warming events may have spanned the early Eocene (above references; Kirtland-Turner et al.,

2014), and the EECO may comprise a series of successive events (Slotnick et al., 2012). Both

long-term and short-term intervals of warming corresponded to major changes in global

carbon cycling, although the precise timing between these parameters remains insufficiently

resolved.

In benthic foraminiferal stable isotope records for the early Paleogene (**Figure 1**), $\delta^{18}O$

serves as a proxy for deep-water temperature, while $\delta^{13}C$ relates to the composition of deep-

water dissolved inorganic carbon (DIC). The highest $\delta^{13}C$ values of the Cenozoic occurred at

ca. 58 Ma. From this Paleocene Carbon Isotope Maximum (PCIM), benthic foraminiferal

1764 δ^{13}C values plunge by approximately 2.5 ‰ to reach a near Cenozoic minimum at or near the

1765 start of the EECO, and subsequently rise by approximately 1.5 ‰ across this interval (Zachos

1766 et al., 2001, 2008; Cramer et al., 2009). Benthic foraminiferal δ^{13}C records also exhibit

1767 prominent negative carbon isotope excursions (CIEs) across the three hyperthermals

1768 mentioned above (Kennett and Stott, 1991; Littler et al., 2014; Lauretano et al., 2015).

1769 Crucially, at least from the late Paleocene to the start of the EECO, similar δ^{13}C records occur

1770 in other carbon-bearing phases, such as bulk marine carbonate, planktic foraminifera, and

1771 various marine and terrestrial organic carbon compounds (Shackleton, 1986; Schmitz et al.,

1772 1996; Lourens et al., 2005; Nicolo et al., 2007; Agnini et al., 2009, submitted; Leon-

1773 Rodriguez and Dickens, 2010; Abels et al., 2012; Coccioni et al., 2012; Sluijs and Dickens,

1774 2012; Slotnick et al. 2012, 2015a; Clyde et al., 2013). This strongly suggests that observed

1775 changes in δ^{13}C, both long-term trends as well as short-term perturbations, represent

1776 variations in the input and output of ^{13}C-depleted carbon to the exogenic carbon cycle

1777 (Shackleton, 1986; Dickens et al., 1995; Dickens, 2000; Kurtz et al., 2003; Komar et al.,

1778 2013).

1779   Significant biotic changes occur in terrestrial and marine environments during times

1780 when the early Paleogene δ^{18}O and δ^{13}C records show major variations. This has been

1781 recognized for the PETM, where land sections exhibit a prominent mammal turnover

1782 (Gingerich 2001, 2003; McInerney and Wing, 2011; Clyde et al., 2013), and where marine

1783 sections reveal a profound benthic foraminiferal extinction (Thomas, 1998), turnovers in

1784 calcareous nannoplankton, ostracods, corals and larger benthic foraminifera (Raffi and De

1785 Bernardi, 2008; Scheibner and Speijer, 2008; Yamaguchi and Norris, 2012; Agnini et al.,

1786 2014), and appearances of excursion taxa in calcareous nannoplankton, dinoflagellates and

1787 planktic foraminifera (Kelly et al., 1996, 1998; Crouch et al., 2001; Sluijs et al., 2006; Self-

1788 Trail et al., 2012). Major plant and mammal turnovers also occurred on land during the longer

EECO (Wing et al., 1991; Zonneveld et al., 2000; Wilf et al., 2003; Falkowski et al., 2005; Woodbourne et al., 2009; Figueirido et al., 2012). In the marine realm, evolutionary trends across the EECO have been noted, in particular the inception of modern calcareous nannofossil community structure (Agnini et al., 2006, 2014; Schneider et al., 2011; Shamrock et al., 2012) and possibly the same for diatoms (Sims et al., 2006; Oreshkina, 2012). These observations, both from continents and the oceans, support an overarching hypothesis that climate change drives biotic evolution, at least in part (Ezard et al., 2011).

Planktic foraminiferal assemblages are abundant in carbonate bearing marine sediments and display distinct evolutionary trends that often can be correlated to climate variability (Schmidt et al., 2004; Ezard et al., 2011; Fraass et al., 2015). This is especially true in the early Paleogene, even though the relationship between climate variability and planktic foraminiferal evolution remains insufficiently known. At the beginning of the Eocene, planktic foraminifera had evolved over ca. 10 Myr following the Cretaceous-Paleogene mass extinction event. Several early Paleogene phylogenetic lines evolved, occupying different ecological niches in the upper water column. Subsequently, a major diversification occurred during the early Eocene, which resulted in a peak of planktic foraminiferal diversity during the middle Eocene (Norris, 1991; Schmidt et al., 2004; Pearson et al., 2006; Aze et al., 2011; Ezard et al., 2011; Fraass et al., 2015).

In this study, we focus on the evolution of two planktic foraminiferal genera: morozovellids and acarininids (**Figure 1**). These two genera belong to the "muricate group", a term derived from the muricae that form ~~conical~~ layered pustules on the test wall. These two genera are of particular interest because of their dominance among tropical and subtropical assemblages of the early Paleogene oceans, and because these genera show a major turnover in taxonomic diversity close to the beginning of the EECO, one that comprises ~~and~~ species reduction among morozovellids and species diversification among

1814 acarininids (Figure 1) (Lu and Keller, 1995; Lu et al., 1998; Pearson et al., 2006; Aze et al.,

1815 2011).

1816   Numerous lower Eocene sedimentary sections from lower latitudes contain well-

1817 preserved (albeit often recrystallized) planktic foraminiferal tests. Changes in These

1818 foraminiferal assemblages presumably reflect relationships between climate and carbon

1819 cycling across the EECO. The present problem is that no section examined to date provides

1820 counts of foraminiferal assemblages, detailed stable isotope records and robust planktic

1821 foraminiferal biostratigraphies across the entire EECO. Indeed, at present, only a few sites

1822 have detailed and interpretable stable isotope records across much of the EECO (Slotnick et

1823 al., 2012, 2015a; Kirtland-Turner et al., 2014). Furthermore, the EECO lacks formal

1824 definition. As a consequence, any relationship between climatic perturbations during the

1825 EECO and the evolution of planktic foraminifera remains speculative. Here, we add new data

1826 from three locations: the Possagno section from the western Tethys, DSDP Site 577 from the

1827 tropical Pacific Ocean, and ODP Site 1051 from the subtropical Atlantic Ocean **(Figure 2)**.

1828 These sections hence represent a wide longitudinal span of low latitude locations during the

1829 early Paleogene. By comparing stable isotope and planktic foraminiferal records at these

1830 three locations, we provide a new foundation for understanding why the abundances of

1831 acarininids and morozovellids changed during the EECO.

1832

1833 **2 The Early Eocene Climatic Optimum**

1834

1835 Evidence for extreme Earth surface warmth during a multi-million year time interval of the

1836 early Eocene is overwhelming, and comes from many studies, utilizing both marine and

1837 terrestrial sequences, and both fossil and geochemical proxies (Huber and Caballero, 2011;

1838 Hollis et al., 2012; Pross et al., 2012). However, a definition for the EECO, including the

1839   usage of "optimum", endures as a perplexing problem ~~circa 2015~~. This is for several reasons,

1840   including the basic facts that: (i) proxies for temperature should not be used to define a time

1841   increment, (ii) clearly correlative records across the middle of the early Eocene with temporal

1842   resolution less than 50 kyr remain scarce, and (iii) absolute ages across the early Eocene have

1843   changed significantly (Berggren et al., 1995; Vandenberghe et al., 2102). As a consequence,

1844   various papers discussing the EECO give different ages and durations spanning from 2 to 4

1845   Myr long sometime between circa 49 and 54 Ma (e.g., Yapp, 2004; Lowenstein and

1846   Demicco, 2006; Zachos et al., 2008; Woodburne et al., 2009; Bijl et al., 2009; Smith et al.,

1847   2010; Hollis et al., 2012; Slotnick et al., 2012; Puljalte et al., 2015).

1848   The EECO, at least as presented in many papers, refers to the time of minimum δ^{18}O

1849   values in "stacked" benthic foraminifera stable isotope curves (**Figure 1**). These curves were

1850   constructed by splicing together multiple δ^{18}O records generated at individual locations onto

1851   a common age model (originally Berggren et al., 1995). However, the stacked curves (Zachos

1852   et al., 2001, 2008; Cramer et al., 2009), while they can be adjusted to different time scales,

1853   show significant variance in δ^{18}O across the middle to late early Eocene. Some of this

1854   variance belies imprecisely calibrated records at individual sites, where cores do not align

1855   properly in the depth domain (Dickens and Backman, 2013). Some of this variance probably

1856   reflects a dynamic early Eocene climate regime, where average temperatures and atmospheric

1857 pCO$_2$ across Earth changed significantly, perhaps on orbital time scales (Smith et al., 2010;

1858   Slotnick et al., 2012, 2015a; Kirtland-Turner et al., 2014).

1859   There is also the root problem as to where EECO starts and ends. At a basic level, the

1860   interval characterized by the lowest Cenozoic benthic foraminiferal δ^{18}O values begins at a

1861   time that closely corresponds with a long-term minimum in δ^{13}C values (**Figure 1**). This is

1862   important for stratigraphic reasons because the two stable isotope curves were generated

1863   using the same benthic foraminiferal samples, but δ^{13}C records at different locations should

1864   necessarily correlate in the time domain (unlike $\delta^{18}O$ and temperature). The rationale for such

1865   carbon isotope stratigraphy lies in the rapid cycling of carbon across Earth's surface

1866   (Shackleton, 1986; Dickens, 2000).

1867   The Eocene minimum in $\delta^{13}C$ corresponds to the K/X event (**Figure 1**), which happened

1868   in polarity chron C24n.1n and approximately 3 Myr after the PETM (Agnini et al., 2009;

1869   Leon-Rodriguez and Dickens, 2010; Slotnick et al., 2012; Dallanave et al., 2015; Lauretano

1870   et al., 2015; Westerhold et al., 2015). However, in several detailed studies spanning the early

1871   Eocene, changes in long-term trends appear to have occurred about 400 kyr before the K/X

1872   event, and at an event called "J" (after Cramer et al., 2003), which happened near the

1873   boundary of polarity chrons C24n.2r and C24n.3n (Slotnick et al., 2015a; Lauretano et al.,

1874   2015). Notably, the long-term late Paleocene-early Eocene decrease in detailed benthic

1875   foraminiferal $\delta^{18}O$ records at Site 1262 on Walvis Ridge ceases at the J event (Lauretano et

1876   al., 2015).

1877   The end of the EECO has received limited attention from a stratigraphic perspective. In

1878   Paleogene continental slope sections now uplifted and exposed in the Clarence River Valley,

1879   New Zealand, a major lithologic change from limestone to marl coincides with the J event

1880   (Slotnick et al., 2012, 2015a; Dallanave et al., 2015). The marl-rich unit, referred to as

1881   "Lower Marl", has been interpreted to reflect enhanced terrigenous supply to a continental

1882   margin because of greater temperature and enhanced seasonal precipitation. It has been

1883   suggested further that Lower Marl expresses the EECO (Slotnick et al., 2012; Dallanave et

1884   al., 2015). The top of Lower Marl, and a return to limestone deposition, lies within the upper

1885   part of polarity chron C22n (Dallanave et al., 2015). This is interesting because it

1886   approximates the time when general long-term Cenozoic cooling initiates at several locations

1887   that have records of polarity chrons and proxies for temperature (Hollis et al., 2012; Pross et

1888   al., 2012). It is also useful from a stratigraphic perspective because the end of the EECO thus

1889 lies close to a well documented and widespread calcareous nannofossil biohorizon, the base

1890 of *Discoaster sublodoensis*. This marks the base of CP10, NP12 or CNE4, depending on the

1891 chosen calcareous nannofossil zonal scheme (Okada and Bukry, 1080; Martini, 1971; Agnini

1892 et al., 2014).

1893   Without an accepted definition in the literature, we tentatively present the EECO as the

1894 duration of time between the J event and the base of *D. sublodoensis*. This interval thus

1895 begins at about 53 Ma and ends at about 49 Ma on the 2012 Time Scale (GTS; Vandenberghe

1896 et al., 2012). However, while the EECO was characterized by generally warm conditions,

1897 numerous fluctuations in average temperature likely occurred during the 4 Myr interval.

1898

1899 **3 Sites and stratigraphy**

1900

1901 **3.1 Possagno, Venetian Prealps, Tethys**

1902

1903 An Upper Cretaceous through Miocene succession crops out at the bottom of the Monte

1904 Grappa Massif in the Possagno area, about 60 km northwest of Venice. The lower to middle

1905 Eocene, of primary focus to this study, is represented by the Scaglia beds. These

1906 sedimentary rocks represent pelagic and hemipelagic sediment that accumulated at middle to

1907 lower bathyal depths (Cita, 1975; Thomas, 1998) in the western part of the Belluno Basin, a

1908 Mesozoic–Cenozoic paleogeographic unit of the Southern Alps (Bosellini, 1989). The basin

1909 very likely was an embayment connected to the western Tethys, with a paleolatitude of 42°

1910 during the early Eocene (**Figure 2**).

1911   A quarry at 45°51.0' N and 11°51.6' E exposed in 2002-2003 a 66 m thick section of

1912 the Scaglia beds (Figure 3), although it is at present largely covered and inaccessible. This

1913 section was examined for its stratigraphy (Agnini et al., 2006; Luciani and Giusberti, 2014),

1914 and shown to extend from just below the PETM to within lower Chron C20r in the lower

1915 middle Eocene. Like other lower Paleogene sections of the Venetian Pre-alps (Giusberti et

1916 al., 2007; Agnini et al., submitted), a Clay Marl Unit (CMU) with a prominent negative CIE

1917 marks the PETM.

1918   The Possagno section appears to be continuous, but with an important decrease in

1919 sedimentation rate (to below 1.4 m/Myr) between 14.66 m and 15.51 m (Agnini et al., 2006).

1920 This interval lies within Chron C23r and near the start of the EECO, and predates the onset

1921 of a major increase in discoaster abundance (Agnini et al., 2006).

1922

1923 **3.2 Site 577, Shatsky Rise, Western Pacific**

1924

1925 Deep Sea Drilling Project (DSDP) Leg 86 drilled Site 577 at 32°26.5' N, 157°43.4' E, and

1926 2680 m water depth, on Shatsky Rise, a large igneous plateau in the NW Pacific with a

1927 relatively thin veneer of sediment (Shipboard Scientific Party 1985). During the early

1928 Eocene, this site was located closer to 15° N (**Figure 2**), and probably at a slightly shallower

1929 water depth (Ito and Clift, 1998).

1930   Two primary holes were drilled at Site 577. Both Hole 577* and Hole 577A recovered

1931 portions of a nominally 65 m thick section of Upper Cretaceous through lower Eocene

1932 nannofossil ooze. Similar to the Possagno section, the lower Paleogene interval has

1933 biomagnetostratigraphic information (Bleil, 1985; Monechi et al., 1985; Backman, 1986; Lu

1934 and Keller, 1995; Dickens and Backman, 2013). Stable isotope records of bulk carbonate

1935 have been generated for sediment from several cores at low sample resolution (Shackleton,

1936 1986), and for much of Cores 577*-9H and 577*-10H at fairly high sample resolution

1937 (Cramer et al. 2003).

1938   The composition and relative abundances of planktic foraminifera were nicely

1939 documented at Site 577 (Lu, 1995; Lu and Keller, 1995), and show a marked turnover

1940 between morozovellids and acaraninids during the early Eocene. These data, however, have

1941 remained on an out-dated view for the stratigraphy at this location, where cores were not

1942 originally aligned to account for gaps and overlaps (Dickens and Backman, 2013). As will

1943 become obvious later, the main phase of the EECO spans Cores 577*-8H and 577A-8H,

1944 where detailed stable isotope records have not been generated previously.

1945

1946 **3.3 Site 1051, Blake Nose, Western Atlantic**

1947

1948 The Blake Nose is a gentle ramp extending from 1000 m to 2700 m water depth east of

1949 Florida (Norris et al, 1998). The feature is known for a relatively thick sequence of middle

1950 Cretaceous through middle Eocene sediment with minimal overburden. Ocean Drilling

1951 Program (ODP) Leg 171B drilled and cored this sequence at several locations, including Site

1952 1051 at 30°03.2' N, 76°21.5' W, and 1994 m water depth (Shipboard Scientific Party 1998).

1953 The site was located slightly to the south during the early Eocene (**Figure 2**). Benthic

1954 foraminiferal assemblages indicate a lower bathyal depth (1000-2000 m) during the late

1955 Paleocene and middle Eocene (Norris et al., 1998), although Bohaty et al. (2009) estimated a

1956 paleodepth of about 2200 m for sedimentation ca. 50 Ma.

1957 Sediments from 452.24 to 353.10 meters below sea floor (mbsf) at Site 1051 consist of

1958 lower to middle Eocene carbonate ooze and chalk (Shipboard Scientific Party, 1998).

1959 ~~Although~~ The site comprises two holes (1051A and 1051B), with core gaps and core

1960 overlaps existing at both (Shipboard Scientific Party, 1998). However, the impact of these

1961 depth offsets upon age is less than at Site 577, because of higher overall sedimentation rates.

1962 The Eocene section at Site 1051 has good sediment recovery, except an interval between

1963 382 mbsf and 390 mbsf, which contains significant chert. Stratigraphic markers across the

1964 Eocene interval include polarity chrons (Ogg and Bardot, 2001), calcareous nannofossil

1965 biohorizons (Mita, 2001), and planktic foraminiferal biohorizons (Norris et al., 1998; Luciani

1966 and Giusberti, 2014). ~~However,~~ As first noted by Cramer et al. (2003), though, there is a

1967 basic stratigraphic problem with the labelling of the polarity chrons. The intervals of normal

1968 polarity between approximately 388 and 395 mbsf, and between approximately 412 and 420

1969 mbsf were tentatively assigned to C22n and C23n, respectively (Ogg and Bardot, 2001). ~~The~~

1970 ~~original~~ This age assignment was ~~adopted~~ assumed to be correct by Luciani and Giusberti

1971 (2014), who therefore considered the last occurrence of *Morozovella subbotinae* as ~~happened~~

1972 happening near the top of C23n, an assumption that was also made for the revision of Eocene

1973 foraminiferal biozones (Wade et al., 2011).

1974   These age assignments, however, cannot be correct, because calcareous nannofossil

1975 biohorizons that lie below or within C22n (top of *T. orthostylus*, top of *Toweius*, base of *D.*

1976 *sublodoensis*) occur above 388 mbsf (Mita, 2001). Instead, there must be a significant hiatus

1977 or condensed interval at the chert horizon, and the above noted intervals of normal polarity

1978 are C23n and C24n.1n.

1979

1980 **4 Methods**

1981

1982 **4.1 Samples for isotopes and foraminifera**

1983

1984 The three sites provide a good stratigraphic background and key existing data for

1985 understanding the temporal link between the EECO, carbon isotope perturbations and

1986 planktic foraminiferal evolution. Our analytical aim was to obtain comparable data sets

1987 across the sites. More specifically, a need existed to generate stable isotope and planktic

1988 foraminiferal assemblage records at the Possagno section, to generate stable isotope records

1989   at DSDP Site 577, and to generate planktic foraminiferal assemblage records at ODP Site

1990   1051.

1991   A In total, of 298 samples were collected from the originally exposed Possagno section

1992   in 2002-2003 for isotope analyses. The sampling interval was 2 to 5 cm for the basal 0.7 m,

1993   50 cm, and 20 cm and at variable spacing from 20 to 50 cm for the interval between 0.7 m

1994   and 66 m. Bulk sediment samples previously were examined for their calcareous nannofossil

1995   assemblages (Agnini et al., 2006). One hundred and ten of these samples were selected for

1996   the foraminiferal study.

1997   Aliquots of the 110 samples were weighed, and then washed to obtain foraminifera using

1998   two standard procedures, depending on lithology. For the indurated marly limestones and

1999   limestones, the cold-acetolyse technique was used (Lirer, 2000; Luciani and Giusberti, 2014).

2000   This method disaggregates strongly lithified samples, in which foraminifera otherwise can be

2001   analyzed only with thin sections (Fornaciari et al., 2007; Luciani et al., 2007). For the marls,

2002   samples were disaggregated using 30 % hydrogen peroxide and subsequently washed and

2003   sieved at 63 μm. In most cases, gentle ultrasonic treatment (e.g., low-frequency at 40 kHz for

2004   30–60 seconds) improved the cleaning of the tests.

2005   Relative abundance data of planktic foraminiferal samples were generated for 65 samples

2006   at Site 577 (Lu, 1995; Lu and Keller, 1995). We collected new samples for stable isotope

2007   (below) measurements that span their previous effort.

2008   Fifty samples of Eocene sediment were obtained from Hole 1051A between 452 to 353

2009   mbsf. Sample spacing varied from 2.0 m to 0.5 m. As the samples are ooze and chalk, they

2010   were prepared using disaggregation using distilled water and washing over 38 μm and 63 μm

2011   sieves. Washed residues were dried at <50°C.

2012

2013   **4.2 Stable Isotopes**

2014

2015   Carbon and oxygen stable isotope data of bulk sediment samples from the Possagno section

2016   and Site 577 were analysed using a Finnigan MAT 252 mass spectrometer equipped with a

2017   Kiel device at Stockholm University. Precision is within ±0.06 ‰ for carbon isotopes and

2018   within ±0.07 ‰ for oxygen isotopes. Stable isotope values were calibrated to the Vienna Pee

2019   Dee Belemnite standard (VPDB) and converted to conventional delta notation (δ^{13}C and

2020 δ^{18}O).

2021

2022   **4.3 Foraminifera analyses**

2023

2024   The mass percent of the >63 μm size fraction relative to the mass of the bulk sample,

2025   typically 100 g/sample was calculated for the 110 Possagno samples. This is referred to as the

2026   weight percent coarse fraction, following many previous works. (Hancock and Dickens,

2027   2005). Due to the consistent occurrence of radiolarians at Site 1051, the coarse fraction

2028   cannot give information on foraminiferal productivity.

2029   Relative abundances for both Possagno and Site 1051 have been determined from about

2030   300 complete specimens extracted from each of the 110 samples investigated in the >63 μm

2031   size fraction from random splits.

2032   The degree of dissolution, expressed as the fragmentation index (*F* index) was evaluated

2033   according to Petrizzo et al. (2008) on ca. 300 elements, by counting planktic foraminiferal

2034   fragments or partially dissolved tests versus complete tests. These data are expressed in

2035   percentages. Fragmented foraminifera include specimens showing missing chambers and

2036   substantial breakage. The taxonomic criteria for identifying planktic foraminifera follows the

2037   work by Pearson et al. (2006).

2038

5 Results

5.1 Carbon isotopes

Possagno

Carbon isotopes of bulk carbonate at Possagno vary between +1.8 and -0.3 ‰ (**Figure 4, Table S1**). Overall, $\delta^{13}C$ decreases from 1.8 ‰ at the base of the section to about 0.6 ‰ at 14 m. Generally, values then increase to 1.5 ‰ at 24 m, and remain between 1.5 ‰ and 0.8 ‰ for the remainder of the studied interval.

Superimposed on these trends are a series of negative CIEs. The most prominent of these (~1.5 ‰) occurs at the 0 m level, and marks the PETM (Agnini et al., 2009). However, other negative CIEs lie above this marker and within the lowermost 21.4 m, albeit some are only defined by one data point (**Figure 4, Table S1**). The lower two at ~8 m and ~12.5 m probably represent the H-1/ETM-2 and J event, respectively, as they lie at the appropriate stratigraphic horizons in relation to polarity chrons. The K/X event may lie at 14.8 m, although this height marks the start of the condensed interval.

The complex interval between 15.5 m and 24 m broadly corresponds to all of Chron C23n and the bottom half of Chron C22r. A series of CIEs occur in that interval on the order of 1.4 ‰, superimposed on a background trend of increasing $\delta^{13}C$ values (about 0.7 ‰). We tentatively label these CIEs with even numbers for internal stratigraphic purposes (**Figure 4**), as will become obvious below; their magnitudes range between 0.9 and 0.3 ‰ (**Table S1**). However, the sample spacing through this interval varies from 20 to 50 cm. The precise magnitudes and positions certainly could change with higher sample resolution, given the estimated compacted sedimentation rate of ~0.5 cm/kyr for this part of the section (Agnini et al., 2006).

2064   Above Chron C22r, the Possagno δ^{13}C record contains additional minor CIEs (**Figure 4**).

2065   The most prominent of these CIEs, at least relative to baseline values (~1.2 ‰), occurs within

2066   Chron C21n. More important to understanding the EECO, a ~0.6 ‰ CIE nearly coincides

2067   with the base of *D. sublodoensis* within the lower part of Chron C22n.

2068

2069   *DSDP Site 577*

2070   The δ^{13}C record of bulk carbonate at DSDP Site 577 from just ~~prior to~~ below the PETM

2071   through Chron C22n ranges between 2.3 and 0.6 ‰ (**Figure 5; Table S2**). Overall, δ^{13}C

2072   decreases from 1.4 ‰ at 84.5 mcd to about 0.6 ‰ at ~76 mcd. Values then generally increase

2073   to 2.1 ‰ at ~68 mcd, and remain between 2.3 ‰ and 1.6 ‰ for the rest of the studied

2074   interval. Thus, the ranges and general trends in δ^{13}C for the two sections are similar, but

2075   skewed at DSDP Site 577 relative to Possagno by about +0.6 ‰.

2076   Like at Possagno, the early Eocene δ^{13}C record at DSDP Site 577 exhibits a series of

2077   CIEs (**Figure 5**). The portion of this record from the PETM through the K/X event has been

2078   documented and discussed elsewhere (Cramer et al., 2003; Dickens and Backman, 2013). The

2079   new portion of this record, from above the K/X event through Chron C22n, spans the

2080   remainder of the EECO. Within this interval, where background δ^{13}C values rise by ~1.5 ‰,

2081   there again occur a series of minor CIEs with magnitudes between 0.3 and 0.5 ‰ (**Table S2**).

2082   Here, however, multiple data points define most of the CIEs. We again give these an internal

2083   numerical labelling scheme. A ~0.4 ‰ CIE also nearly coincides with the base of *D.*

2084   *sublodoensis* within the lower part of C22n.

2085

2086   **5.2 Oxygen isotopes**

2087

2088   *Possagno*

2089 Oxygen isotopes of bulk carbonate at Possagno range between -3.3 and 0.8 ‰ with a mean

2090 value of -1.7 ‰ (**Figure 4, Table S1**). In general, ~~there exists~~ considerable scatter exists

2091 across the data set with respect to depth, as adjacent samples often ~~having~~ display a

2092 difference in δ^{18}O that exceeds 0.5 ‰. Nonetheless, some of the more prominent lows in δ^{18}O

2093 show a clear correspondence with negative δ^{13}C values (CIEs) and vice versa. This

2094 correspondence occurs across the PETM and other known hyperthermals, as well as within

2095 and after the EECO. Indeed, the main phase of the EECO ~~appears to~~ corresponds with a

2096 broad has the lowest δ^{18}O values.

2097

2098 *DSDP Site 577*

2099 The δ^{18}O record at Site 577 noticeably deviates from that at Possagno (**Figure 5, Table S2**).

2100 This is because values range between ~~0.2 and -1.1 ‰~~ -1.1 ‰ and 0.2 with an average value of

2101 -0.4 ‰. Thus, ~~both records have somewhat similar scatter~~ relative to Possagno, the record at

2102 Site 577 has less scatter, and an overall shift of about -1.3 ‰. There ~~is~~ exists again a modest

2103 correlation between decreases in δ^{18}O and negative δ^{13}C values, as well as a general low in

2104 δ^{18}O across the main phase of the EECO.

2105

2106 **5.3 Coarse fraction**

2107

2108 The coarse fraction of samples from Possagno shows two distinct trends (**Figure 6, Table**

2109 **S3**). Before the EECO, values are 10.4 % ± 2.67 %. However, from the base of the EECO

2110 and up through the section, values decrease to 5.3 ± 1.3 %.

2111

2112 **5.4 Foraminiferal preservation and fragmentation**

2113

2114   Planktic foraminifera are consistently present and diverse throughout the studied intervals at

2115   Possagno and at ODP Site 1051. Preservation of the tests at Possagno varies from moderate

2116   to fairly good (Luciani and Giusberti, 2014). However, planktic foraminiferal tests at

2117   Possagno are recrystallized and essentially totally filled with calcite. Planktic foraminifera

2118   from samples at Site 1051 are readily ~~preserved~~ recognizable throughout the studied interval.

2119   Planktic foraminifera from Site 577, at least as illustrated by published plates (Lu and Keller,

2120   1995), show a very good state of preservation (albeit possibly recrystallized).

2121   The F index record at Possagno (**Figure 6, Table S3**) displays large amplitude variations

2122   throughout the investigated interval. The highest values, up to 70 %, were observed between

2123   16 and 22 m. In general, highs in F index values correspond to lows in the $\delta^{13}C$ record.

2124   The F index record at Site 1051 (**Figure 8 ~~7~~, Table S4**) shows less variability compared

2125   to that at Possagno, although some of this may reflect the difference in the number of samples

2126   examined at the two locations. A maximum value of 60 % is found in Zone E5, just below an

2127   interval of uncertain magnetostratigraphy (Norris et al., 1998), but corresponding to the J

2128   event (Cramer et al., 2003). Relatively high F index values, around 50 %, also occur in

2129   several samples below this horizon. The interval across the EECO generally displays low F

2130   index values (<20 %).

2131

2132   **5.5 Planktic foraminiferal quantitative analysis**

2133

2134   *Possagno*

2135   Planktic foraminiferal assemblages at Possagno show significant changes across the early to

2136   early middle Eocene (**Figure 6, Table S3**). Throughout the entire section, the mean relative

2137   abundance of *Acarinina* is about 46 % of the total assemblage. However, members of this

2138   genus ~~show~~ exhibit peak abundances of 60-80 % of the total assemblage ~~occur~~ across several

2139   intervals, often corresponding to CIEs. Particularly prominent is the broad abundance peak of

2140   *Acarinina* coincident with the main phase of the EECO.

2141   The increases in acarininid relative abundance typically are counterbalanced by transient

2142   decreases of subbotinids (**Figure 6**). This group also shows a general increase throughout the

2143   section. Below the EECO the relative abundances of subbotinids average ~24 %. Above the

2144   EECO, this average rises to ~36 %.

2145   The trends of acarininids and subbotinids contrast with that of morozovellids (**Figure 6**),

2146   which exhibit a major and permanent decline within Zone E5. This group collapses from

2147   mean abundances ~24 % in the 0-15 m interval to <6 % above 15 m. Qualitative examination

2148   of species shows that, in the lower part of Zone E5, where relatively high morozovellids

2149   abundances are recorded, there is no dominance of any species. *M. marginodentata*, *M.*

2150   *subbotinae* and *M. lensiformis* are each relatively common, and *M. aequa, M. aragonensis*,

2151   *M. formosa* and *M. crater* are each less common. By contrast, in the upper part of Zone E5,

2152   where low ~~morozovellids~~ abundances of morozovellids occur, *M. aragonensis, M. formosa,*

2153   *M. crater* and *M. caucasica* are the most common species. The general decrease of

2154   morozovellids abundances appears unrelated to the disappearance of a single, dominant

2155   species.

2156   At Possagno, morozovellids never recover to their pre-EECO abundances. This is true

2157   even if one includes the morphologically and ecologically comparable genus *Morozovelloides*

2158   (Pearson et al., 2006), which first appears in samples above 36 m.

2159   Other planktic foraminiferal genera are always less than 15 % of the total assemblages

2160   throughout the studied interval at Possagno (**Figure S1, Table S3**).

2161

2162   *ODP Site 577*

Samples from Site 577 were disaggregated in water and washed through a >63 sieve (Lu,

1995; Lu and Keller, 1995). They determined relative abundances of planktic foraminifera

from random splits of about 300 specimens (Lu, 1995; Lu and Keller, 1995). The resulting

data are shown in **Figure 7**, placed onto the composite depth scale by Dickens and Backman

(2013). Major changes in planktic foraminiferal assemblages are comparable to those

recorded at Possagno. Such changes include indeed a distinct decrease of morozovellids

within Zone E5. The decrease at Site 577 is from mean values of 26.6 % to 6.7 % (**Table S4**).

This marked drop occurs at ca. 78 mcd close to the J event and at the start of the EECO. Like

at Possagno, morozovellids never recover to their pre-EECO abundances.

The morozovellids decrease is counter balanced by the trend of acarininids abundances

that increase from mean values of 30.4 % to 64.8 % in correspondence to the level of the

morozovellids collapse. Subbotinids fluctuate in abundance throughout the interval

investigated from 1 % to 18 %, with a mean value of ca. 8 %.

ODP Site 1051

Planktic foraminifera show distinct changes in abundance at Site 1051 (**Figure 8, Table S5**).

The changes of the main taxa are similar to the variations observed at Possagno. The genus

Acarinina displays an increase in mean relative abundance from 35 % (base to ca. 450 mbsf)

to around 50 % (ca. 430 mbsf), with maximum values of about 60 %. The relatively low

resolution used here does not permit comparison to the early Eocene CIEs at Site 1051

(Cramer et al., 2003), or how the relative abundance of planktic foraminiferal genera varies

with respect to CIEs.

The abundance of subbotinids shows little small variations around mean values of 20 %

at Site 1051. Like at Possagno, samples from Site 1051 also record a slight increase in

abundance toward the end of the EECO and above (ca. 7%, mean value).

2188   The major change in planktic foraminiferal assemblages at Site 1051 includes a distinct

2189   decrease of *Morozovella*, from mean values around 40 % to 10 % in the middle part of Zone

2190   E5 (**Figure 7**). Similar to Possagno, the lower part of Zone E5 with the higher percentages of

2191   morozovellids does not record the dominance of selected species, but at Site 1051 *M.*

2192   *aragonensis* and *M. formosa* besides *M. subbotinae* are relatively common whereas *M.*

2193   *marginodentata* is less frequent. Within the interval of low morozovellids abundances, *M.*

2194   *aragonensis* and *M. formosa* are the most common taxa. The general decline of

2195   morozovellids does not appear therefore related, both at Possagno and at Site 1051, to the

2196   extinction or local disappearance of a dominant species.

2197

2198   **6 Discussion**

2199

2200   **6.1 Dissolution, recrystallization, and bulk carbonate stable isotopes**

2201

2202   The bulk carbonate stable isotope records within the lower Paleogene sections at Possagno

2203   and at Site 577 need thought, ~~consideraction~~ considering how such records are produced and

2204   modified in much younger strata dominated by pelagic carbonate. In open ocean

2205   environments, carbonate preserved on the seafloor principally consists of calcareous tests of

2206   nannoplankton (coccolithophores) and planktic foraminifera (Bramlette and Riedel, 1954;

2207   Berger, 1967; Vincent and Berger, 1981). However, the total amount of carbonate and its

2208   microfossil composition can vary considerably across locations because of differences in

2209   deep-water chemistry and in test properties (e.g., ratio of surface area to volume;

2210   mineralogical composition). For regions at low to mid latitudes, a reasonable representation

2211   of carbonate components produced in the surface water accumulates on the seafloor at

2212   modest (<2000 m) water depth. By contrast, microfossil assemblages become heavily

2213 modified in deeper water, because of increasingly significant carbonate dissolution (Berger,

2214 1967). Such dissolution preferentially affects certain tests, such as thin-walled, highly porous

2215 planktic foraminifera (Berger, 1970; Bé et al., 1975; Thunell and Honjo, 1981).

2216 The stable isotope composition of modern bulk carbonate ooze reflects the mixture of its

2217 carbonate components, which mostly record water temperature and the composition of

2218 dissolved inorganic carbon (DIC) within the mixed layer (<100 m water depth). The stable

2219 isotope records are imperfect, though, because of varying proportions of carbonate

2220 constituents, and "vital effects", which impact stable isotope fractionation for each

2221 component (Anderson and Cole, 1975; Reghellin et al., 2015). Nonetheless, the stable isotope

2222 composition of bulk carbonate ooze on the seafloor can be related to overlying temperature

2223 and chemistry of surface water (Anderson and Cole, 1975; Reghellin et al., 2015).

2224 Major modification of carbonate ooze occurs during sediment burial. This is because,

2225 with compaction and increasing pressure, carbonate tests begin to dissolve and recrystallize

2226 (Schlanger and Douglas, 1974; Borre and Fabricus, 1998). Typically within several hundred

2227 meters of the seafloor, carbonate ooze becomes chalk and, with further burial, limestone

2228 (Schlanger and Douglas, 1974; Kroencke et al., 1991; Borre and Fabricus, 1998). Carbonate

2229 recrystallization appears to be a local and nearly closed system process, such that mass

2230 transfer occurs over short distances (i.e., less than a few meters) (above references and Matter

2231 et al., 1975; Arthur et al., 1984; Frank et al., 1999).

2232 In pelagic sequences with appreciable carbonate content and low organic carbon content,

2233 bulk carbonate δ^{13}C records typically give information of paleoceanographic significance

2234 (Scholle and Arthur, 1980; Frank et al., 1999). Even when transformed to indurated

2235 limestone, the δ^{13}C value for a given sample should be similar to that originally deposited on

2236 the seafloor. This is because, for such sediments, almost all carbon within small sedimentary

2237 volumes exists as carbonate. Bulk carbonate δ^{18}O records are a different matter, especially in

2238 indurated marly limestones and limestones (Marshall, 1992; Schrag et al., 1995; Frank et al.,

2239 1999). This is because pore water dominates the total amount of oxygen within an initial

2240 parcel of sediment, and oxygen isotope fractionation depends strongly on temperature. Thus,

2241 during dissolution and recrystallization of carbonate, significant exchange of oxygen isotopes

2242 occurs. At first, carbonate begins to preferentially acquire ^{18}O, because shallowly buried

2243 sediment generally has ~~colder~~ lower temperatures than surface water. However, with

2244 increasing burial depth along a geothermal gradient, carbonate begins to preferentially

2245 acquire ^{16}O (Schrag et al., 1995; Frank et al., 1999).

2246

2247 **6.2 Carbon isotope stratigraphy through the EECO**

2248

2249 Stratigraphic issues complicate direct comparison of various records from Possagno and Site

2250 577. The two sections have somewhat similar multi-million year sedimentation rates across

2251 the early Eocene. However, the section at Possagno contains the condensed interval, where

2252 much of C23r spans a very short distance (Agnini et al., 2006), and the section at Site 577 has

2253 a series of core gaps and core overlaps (Dickens and Backman, 2013).

2254 　　　An immediate issue to amend is the alignment of Cores 8H and 9H in Hole 577* and

2255 Core 8H in Hole 577A (**Figure 5**). On the basis of GRAPE density records for these cores,

2256 Dickens and Backman (2013) initially suggested a 2.6 m core gap between Cores 8H* and

2257 9H*. However, a 3.5 m core gap also conforms to all available stratigraphic information. The

2258 newly generated $\delta^{13}C$ (and $\delta^{18}O$) records across these three cores show the latter to be correct.

2259 　　　Once sedimentation rate differences at Possagno are recognized and coring problems at

2260 Site 577 are rectified, early Eocene $\delta^{13}C$ records at both locations display similar trends and

2261 deviations in relation to polarity chrons and key microfossil events (**Figures 4, 5**). Moreover,

2262 the $\delta^{13}C$ variations seemingly can be correlated in time to those found in bulk carbonate $\delta^{13}C$

2263   records at other locations, including Site 1051 (**Figure 8**) and Site 1258 (**Figure 9**). As noted

2264   previously, such correlation occurs because the bulk carbonate $\delta^{13}C$ signals reflect past global

2265   changes in the composition of surface water DIC, even after carbonate recrystallization.

2266   For the latest Paleocene and earliest Eocene, nominally the time spanning from the base

2267   of C24r through the middle of C24n, detailed stable carbon isotope records have been

2268   generated at more than a dozen locations across the globe (Cramer et al., 2003; Agnini et al.,

2269   2009; Galeotti et al., 2010; Zachos et al., 2010; Slotnick et al., 2012; Littler et al., 2014;

2270   Agnini et al., in review). These records can be described consistently as a long-term drop in

2271 $\delta^{13}C$ superimposed with a specific sequence of prominent CIEs that include those

2272   corresponding to the PETM, H-1, and J events. In continuous sections with good

2273   magnetostratigraphy and biostratigraphy, there is no ambiguity in the assignment of CIEs

2274   (Zachos et al., 2010; Littler et al., 2014; Slotnick et al., 2012, 2105a; Lauretano et al., 2015).

2275   This "$\delta^{13}C$ template" can be found at the Possagno section and at Site 577 (**Figure 9**); it is

2276   found at Site 1051 for the depth interval where carbon isotopes have been determined

2277   (**Figure 8**).

2278   After the J event and across the EECO, very few detailed $\delta^{13}C$ records have been

2279   published (Slotnick et al., 2012, 2015a; Kirtland-Turner et al., 2014). Moreover, the available

2280   records are not entirely consistent. For example, the K/X event in Clarence River valley

2281   sections manifests as a prominent CIE within a series of smaller $\delta^{13}C$ excursions (Slotnick et

2282   al., 2012, 2015a), whereas the event has limited expression in the $\delta^{13}C$ record at Site 1258

2283   (Kirtland-Turner et al., 2014; **Figure 9**).

2284   The new records from Possagno and Site 577 emphasize an important finding regarding

2285   bulk carbonate $\delta^{13}C$ records across the EECO. Between the middle of C24n and the upper

2286   part of C23r, there appears to be a sequence of low amplitude, low frequency CIEs. (Note

2287   that this portion of the record is missing at Possagno because of the condensed interval;

2288 **Figure 9**). However, near the C23r/C23n boundary, a long-term rise in δ^{13}C begins, but with

2289 a series of relatively high amplitude, high frequency CIEs (Kirtland-Turner et al., 2014;

2290 Slotnick et al., 2014). The number, relative magnitude and precise timing of CIEs within this

2291 interval remain uncertain. For example, the CIE labelled "4" appears to occur near the top of

2292 C23r at Site 577 but near the bottom of C23n.2n at Site 1258 and at Possagno. Additional

2293 δ^{13}C records across this interval are needed to resolve the correct sequence of CIEs and to

2294 derive an internally consistent labelling scheme for these perturbations. It is also not clear

2295 which of these CIEs during the main phase of the EECO specifically relate to significant

2296 increases in temperature, as clear for the "hyperthermals" in the earliest Eocene. Nonetheless,

2297 numerous CIEs, as well as an apparent change in the mode of these events, characterize the

2298 EECO (Kirtland-Turner et al., 2014; Slotnick et al., 2014).

2299 The causes of δ^{13}C changes during the early Paleogene lie at the crux of considerable

2300 research and debate (Dickens et al., 1995, 1997; Zeebe et al., 2009; Dickens, 2011; Lunt et

2301 al., 2011; Sexton et al., 2011; De Conto et al., 2012; Lee et al., 2013; Kirtland Turner et al.,

2302 2014). Much of the discussion has revolved around three questions: (1) what are the sources

2303 of ^{13}C-depleted carbon that led to prominent CIEs, especially during the PETM? (2) does the

2304 relative importance of different carbon sources vary throughout this time interval? and, (3)

2305 are the geologically brief CIEs related to the longer secular changes in δ^{13}C? One might

2306 suggest, through several papers, a convergence of thought as to how carbon cycled across

2307 Earth's surface during the early Paleogene, at least between the late Paleocene and the K/X

2308 event (Cramer et al., 2003; Lourens et al., 2005; Galeotti et al., 2010; Hyland et al., 2013;

2309 Zachos et al., 2010; Lunt et al. 2011; Littler et al., 2014; Lauretano et al., 2015; Westerhold et

2310 al., 2015). Changes in tectoniesm, volcanism, and weathering drove long-term changes

2311 atmospheric pCO$_2$ (Vogt, 1979; Raymo and Ruddiman, 1992; Sinton and Duncan, 1998;

2312 Demicco, 2004; Zachos et al., 2008), which was generally high throughout the early

2313 Paleogene, but increased toward the EECO (Pearson and Palmer, 2000; Fletcher et al., 2008;

2314 Lowenstein and Demicco, 2006; Smith et al., 2010; Hyland and Sheldon, 2013). However, as

2315 evident from the large range in $\delta^{13}C$ across early Paleogene stable isotope records, major

2316 changes in the storage and release of organic carbon must have additionally contributed to

2317 variability in atmospheric pCO_2 and ocean DIC concentrations (Shackleton, 1986; Kurtz et

2318 al., 2003; Komar et al., 2013). When long-term increases in pCO_2, perhaps in conjunction

2319 with orbital forcing, pushed temperatures across some threshold, such as the limit of sea-ice

2320 formation (Lunt et al., 2011), rapid inputs of ^{13}C-depleted organic carbon from the shallow

2321 geosphere served as a positive feedback to abrupt warming (Dickens et al., 1995; Bowen et

2322 al., 2006; DeConto et al., 2012).

2323   Our new $\delta^{13}C$ records do not directly address the above questions and narrative

2324 concerning early Paleogene carbon cycling. However, they do highlight two general and

2325 related problems when such discussion includes the EECO. First, surface temperatures appear

2326 to stay high across an extended time interval when the $\delta^{13}C$ of benthic foraminifer (**Figure 1**)

2327 and bulk carbonate (**Figure 9**) increase. Second, numerous brief CIEs mark this global long-

2328 term rise in $\delta^{13}C$. Whether the aforementioned views need modification or reconsideration

2329 (Kirtland Turner et al., 2014) is an outstanding issue, one that depends on how long-term and

2330 short-term $\delta^{13}C$ changes relate across the entire early Paleogene.

2331   The overall offset between bulk carbonate $\delta^{13}C$ values at Possagno and Site 577 may hint

2332 at an important constraint to any model of early Paleogene carbon cycling. Throughout the

2333 early Eocene, $\delta^{13}C$ values at Site 577 exceed those at Possagno by nominally 0.8 ‰ (**Figure**

2334 **9**). This probably does reflect recrystallization or lithification, because similar offsets appear

2335 across numerous records independent of post-depositional history but dependent on location

2336 (Schmitz et al., 1996; Cramer et al., 2003; Slotnick et al., 2012, 2015a; Agnini et al.,

2337 submitted). In general, absolute values of bulk carbonate $\delta^{13}C$ records increase from the

North Atlantic and western Tethys (low), through the South Atlantic and eastern

Tethys/Indian, to the Pacific ~~oceans~~ (high), although suggestively with a latitudinal

component to this signature.

6.3 Stable oxygen isotope stratigraphy across the EECO

Bulk carbonate $\delta^{18}O$ values for Holocene sediment across the Eastern Equatorial Pacific

relate to average temperatures in the mixed layer (Shackleton and Hall, 1995; Reghellin et al.,

2015). Indeed, values are close to those predicted from water chemistry ($\delta^{18}O_w$) and

equilibrium calculations for calcite precipitation (e.g., Bemis et al., 1998) if vital effects in

the dominant nannoplankton increase $\delta^{18}O$ by nominally 1‰ (Reghellin et al., 2015).

    Site 577 was located at about 15°N latitude in the eastern Pacific during the early

Paleogene. Given that sediment of this age remains "nannofossil ooze" (Shipboard Scientific

Party, 1985), one might predict past mixed layer temperatures from the $\delta^{18}O$ values with

three assumptions: early Paleogene $\delta^{18}O_w$ was 1.2 ‰ less than that at present-day to account

for an ice-free world; local $\delta^{18}O_w$ was equal to average seawater, similar to modern chemistry

at this off-Equator location (LeGrande and Schmidt, 2006); and, Paleogene nannoplankton

also fractionated $\delta^{18}O$ by 1.0 ‰. With commonly used equations that relate the $\delta^{18}O$ of

calcite to temperature (Bemis et al., 1998), these numbers render temperatures of between

16°C and 21°C for the data at Site 577. Such temperatures seem too cold by at least 10°C,

given other proxy data and modelling studies (e.g., Pearson et al., 2007; Huber and Caballero,

2011; Hollis et al., 2012; Pross et al., 2012; Inglis et al., 2015). At low latitudes, bottom

waters are always much colder than surface waters. Even during the EECO, deep waters

probably did not exceed 12°C (Zachos et al., 2008). The calculated tepid temperatures likely

indicate partial recrystallization of bulk carbonate near the seafloor. Examinations of

2363   calcareous nannofossils in Paleogene sediment at Site 577 show extensive calcite

2364   overgrowths (Shipboard Scientific Party, 1985; Backman, 1986). Relatively low $\delta^{18}O$ values

2365   mark the H-1 and K/X events, as well as the main phase of the EECO (**Figure 5**). Both

2366   observations support the idea that the bulk carbonate $\delta^{18}O$ at Site 577 represents the

2367   combination of a primary surface water $\delta^{18}O$ signal and a secondary shallow pore water $\delta^{18}O$

2368   signal.

2369   Lithification should further impact bulk carbonate $\delta^{18}O$ records (Marshall, 1992; Schrag

2370   et al., 1995; Frank et al., 1999). Because this process occurs well below the seafloor, where

2371   temperatures approach or exceed those of surface water, the $\delta^{18}O$ values of pelagic marls and

2372   limestones should be significantly depleted in ^{18}O relative to partially recrystallized

2373   nannofossil ooze. This explains the nominal 2‰ offset in average $\delta^{18}O$ between correlative

2374   strata at Possagno and at Site 577. While temperature calculations using the $\delta^{18}O$ record at

2375   Possagno render reasonable surface water values for a mid-latitude location in the early

2376   Paleogene (26-31°C, using the aforementioned approach), any interpretation in these terms

2377   more than likely reflects happenstance. The fact that planktic foraminifera are completely

2378   recrystallized and totally filled with calcite at ~~this site~~ Possagno supports this inference.

2379   One might suggest, at least for the Possagno section, that meteoric water might have also

2380   impacted the $\delta^{18}O$ record. This is because rainwater generally has a $\delta^{18}O$ composition less

2381   than that of seawater. However, samples were collected at Possagno in 2002-2003 from fresh

2382   quarry cuts.

2383   As observed at Site 577, however, horizons of lower $\delta^{18}O$ at Possagno may represent

2384   times of relative warmth in surface water. This includes the broad interval between 16 and

2385   22.5 m, which marks the main phase of the EECO, as well as many of the brief CIEs, at least

2386   one that clearly represents the PETM (**Figure 4**). That is, despite obvious overprinting of the

2387   original $\delta^{18}O$ signal, early to early middle Eocene climate variations appear manifest in the

2388   data.

2389

2390   **6.4 The EECO and planktic foraminiferal abundances**

2391

2392   Bulk carbonate $\delta^{13}C$ records, especially in conjunction with other stratigraphic markers,

2393   provide a powerful means to correlate early Paleogene sequences from widely separated

2394   locations (**Figure 9**). They also allow for placement of planktic foraminiferal assemblage

2395   changes into broader context.

2396   The most striking change in planktic foraminiferal assemblages occurred near the start of

2397   the EECO. Over a fairly short time interval and at multiple widespread locations, the relative

2398   abundance of acarininids increased significantly whereas the relative abundance of

2399   morozovellids decreased significantly. This switch, best defined by the decline in

2400   morozovellids, happened just before the condensed interval at Possagno (**Figure 6**), just

2401   above the J event at Site 577 (**Figure 7, Table S4**), and during the J event at Site 1051

2402   (**Figure 8**). At the Farra section, cropping out in the same geological setting of Possagno at

2403   50 km NE of the Carcoselle quarry, it also appears to have occurred close to the J event

2404   (**Figure 10**). Indeed, the maximum turnover in relative abundances may have been coincident

2405   with the J event at all locations. Importantly, the relative abundance of subbotinids only

2406   changed marginally during this time.

2407   The "morozovellid ~~crisis~~" decline across the start of the EECO ~~was irreversible~~ did not

2408   rebound afterward. At Possagno, at Site 1051, and at Site 577, it was coupled with the

2409   gradual disappearances of several species, including *M. aequa, M. gracilis, M. lensiformis,*

2410   *M. marginodentata,* and *M. subbotinae*. Furthermore, the loss of morozovellids was not

2411   counterbalanced by the appearance of the *Morozovelloides* genus, which shared with

2412   *Morozovella* the same ecological preferences. This latter genus appeared in C21r, near the

2413   Ypresian/Lutetian boundary, and well after the EECO (Pearson et al., 2006; Aze et al., 2011),

2414   including at Possagno (Luciani and Giusberti, 2014; **Figure 6**). Though *Morozovelloides*

2415   were morphologically similar to *Morozovella*, they probably evolved from *Acarinina*

2416   (Pearson et al., 2006; Aze et al., 2011; **Figure 1**).

2417   At Possagno, higher abundances of acarininids also correlate with pronounced negative

2418 δ^{13}C perturbations before and after the EECO (**Figure 6**). This includes the H-1 event, as well

2419   as several unlabelled CIEs during C22n, C21r and C21n. Such increases in the relative

2420   abundances of acarininids have been described for the PETM interval at the ~~proximal~~ nearby

2421   Forada section (Luciani et al., 2007), and for the K/X event at the proximal Farra section

2422   (Agnini et al., 2009). Unlike for the main switch near the J event, however, these changes are

2423   transient, so that relative abundances in planktic foraminiferal genera are similar before and

2424   after the short-term CIEs.

2425

2426   **6.5 The impact of dissolution**

2427

2428   Carbonate dissolution at or near the seafloor presents a potential explanation for observed

2429   changes in foraminifera assemblages. Some studies of latest Paleocene to initial Eocene age

2430   sediments, including laboratory experiments, suggest a general ordering of dissolution

2431   according to genus, with acarininds more resistant than morozovellids, and the latter more

2432   resistant than subbotinids (Petrizzo et al., 2008; Nguyen et al., 2009, 2011).

2433   Carbonate solubility horizons that impact calcite preservation and dissolution on the

2434   seafloor (i.e., the CCD and lysocline) also shoaled considerably during various intervals of

2435   the early Eocene. The three most prominent hyperthermals that occurred before the main

2436   phase of the EECO (PETM, H-1, K/X) were clearly marked by pronounced carbonate

2437   dissolution at multiple locations (Zachos et al., 2005; Agnini et al., 2009; Stap et al., 2009;

2438   Leon-Rodriguez and Dickens, 2010). A multi-million year interval characterized by a

2439   relatively shallow CCD also follows the K/X event (Leon-Rodriguez and Dickens, 2010;

2440   Pälike et al., 2012; Slotnick et al., 2015b).

2441   Should changes in carbonate preservation primarily drive the observed planktic

2442   foraminiferal assemblages, it follows that the dominance of acarininids during the EECO and

2443   multiple CIEs could represent a taphonomic artefact. Limited support for this idea comes

2444   from our records of fragmentation (*F* index). In general, intervals with relatively high

2445   abundances of acarininids (and low $\delta^{13}C$) correspond to intervals of fairly high fragmentation

2446   at Possagno and at Site 1051 (**Figures 6, 8**). This can suggest carbonate dissolution, because

2447   this process breaks planktic foraminifera into fragments (Berger, 1967; Hancock and

2448   Dickens, 2005).

2449   Carbonate dissolution can cause the coarse fraction of bulk sediment to decrease (Berger

2450   et al., 1982; Broecker et al., 1999; Hancock and Dickens, 2005). This happens because whole

2451   planktic foraminiferal tests typically exceed 63 μm, whereas the resulting fragments often do

2452   not exceed 63 μm. The decrease in CF values at the start of the EECO at Possagno (**Figure 6**)

2453   may therefore further indicate loss of foraminiferal tests. However, relatively low CF values

2454   continue to the top of the section, independent of changes in the *F* index. The CF record

2455   parallels the trend of morozovellids abundance, and thus might also suggest a loss of larger

2456   morozovellids rather than carbonate dissolution.

2457   The cause of the long-term rise in carbonate dissolution horizons remains perplexing, but

2458   may relate to reduced inputs of ^{13}C-depleted carbon into the ocean and atmosphere (Leon-

2459   Rodriguez and Dickens, 2010; Komar et al., 2013). Should the morozovellids decline and

2460   amplified *F* index at the Possagno section mostly represent dissolution, it would imply

2461   considerable shoaling of these horizons in the western Tethys, given the inferred deposition

2462   in middle to lower bathyal setting. As with open ocean sites (Slotnick et al., 2015b), further

2463 studies on the Eocene lysocline and CCD are needed from Tethyan locations. One idea is that

2464 remineralization of organic matter intensified within the water column, driven by augmented

2465 microbial metabolic rates at elevated temperatures during the EECO; this may have decreased

2466 pH at intermediate water column depths (Brown et al., 2004; Olivarez Lyle and Lyle, 2006;

2467 O'Connor et al., 2009; John et al., 2013, 2014).

2468 Despite evidence for carbonate dissolution, this process probably only amplified primary

2469 changes in planktic foraminiferal assemblages. The most critical observation is the similarity

2470 of the abundance records for major planktic foraminiferal genera throughout the early Eocene

2471 at multiple locations (**Figures 6-8**). This includes the section at Site 1051, where carbonate

2472 appears only marginally modified by dissolution according to the F index values (**Figure 7**).

2473 Subbotinid abundance also remains fairly high throughout the early Eocene. One explanation

2474 is that, in contrast to laboratory experiments (Nguyen et al., 2009, 2011), subbotinids are

2475 more resistant to dissolution than morozovellids (Boersma and Premoli Silva, 1983; Berggren

2476 and Norris, 1997), at least once the EECO has transpired. In the proximal middle-upper

2477 Eocene section at Alano, Luciani et al. (2010) documented a dominance of subbotinids within

2478 intervals of high fragmentation (F index) and enhanced carbonate dissolution. The degree of

2479 dissolution across planktic foraminiferal assemblages may have varied through the early

2480 Paleogene, as distinct species within each genus may respond differently (Nguyen et al.,

2481 2011). So far, data on dissolution susceptibility for different species and genera are ~~lacking~~

2482 limited for early and early middle Eocene times (Petrizzo et al., 2008).

2483 There is also recent work from the Terche section (ca. 28 km NE of Possagno) to

2484 consider. This section is located in the same geological setting as Possagno, but across the H-

2485 1, H-2 and I1 events, there are very low F index values and marked increases of acarininids

2486 coupled with significant decreases of subbotinids (D'Onofrio et al., 2014). Therefore,

2487 although the Possagno record may be partially altered by dissolution, an increase of warm

2488 water acarininids concomitant with decrease of subbotinids seems to be a robust finding

2489 during early Paleogene warming events in Tethyan settings.

2490

2491 **6.6 A record of mixed water change**

2492

2493 The switch in abundance between morozovellids and acaraninids at the start of the EECO

2494 supports a hypothesis whereby environmental change resulted in a geographically widespread

2495 overturn of planktic foraminiferal genera. During the PETM and K/X events, acarininids

2496 became dominant over morozovellids in a number of Tethyan successions ~~of northeast Italy~~.

2497 This has been interpreted as signifying enhanced eutrophication of surface waters near

2498 continental margins (Arenillas et al., 1999; Molina et al., 1999; Ernst et al., 2006; Guasti and

2499 Speijer, 2007; Luciani et al., 2007; Agnini et al., 2009; ~~Arenillas et al., 1999; Luciani et al.,~~

2500 ~~2007; Molina et al., 1999~~), an idea consistent with evidence for elevated (albeit more

2501 seasonal) riverine discharge during these hyperthermals (Schmitz and Pujalte, 2007;

2502 Giusberti et al., 2007; Schulte et al., 2011; Slotnick et al., 2012; Puḷjalte et al., 2015).

2503 Increased nutrient availability may also have occurred at Possagno during the early part of the

2504 EECO, given the relatively high concentration of radiolarians, which may reflect

2505 eutrophication (Hallock, 1987).

2506   However, the fact that the major switch at the start of the EECO can be found at Sites

2507 1051 (western Atlantic) and Site 577 (central Pacific) suggests that local variations in

2508 oceanographic conditions, such as riverine discharge, was not the primary causal mechanism.

2509 Rather, the switch must be a consequence of globally significant modifications related to the

2510 EECO, most likely sustained high temperatures, elevated pCO$_2$, or both. Given model

2511 predictions for our Earth in the coming millennia (IPCC, 2014), indirect effects also could

2512 have contributed, especially including increased ocean stratification and decreased pH.

2513   An explanation for the shift may lie in habitat differences across planktic foraminifera

2514   genera. Although both morozovellids and acaraninids likely had photsymbionts,

2515   morozovellids may have occupied a shallower surface habitat than the latter genus as

2516   indicated by minor variations in their stable isotope compositions (Boersma et al., 1987;

2517   Pearson et al., 1993; 2001).

2518   One important consideration to any interpretation is the evolution of new species that

2519   progressively appear during the post-EECO interval. In good agreement with studies of lower

2520   Paleogene sediment from other low latitude locations (Pearson et al., 2006), thermocline

2521   dwellers such as subbotinids and parasubbotinids seem to proliferate at Possagno (Luciani

2522   and Giusberti, 2014). These include *Subbotina corpulenta, S. eocena, S. hagni, S. senni, S.*

2523   *yeguanesis, Parasubbotina griffinae,* and *P. pseudowilsoni*. The appearance of the radially-

2524   chambered *Parasubbotina eoclava*, considered to be the precursor of the truly clavate

2525   chambered *Clavigerinella* (Coxall et al., 2003; Pearson and Coxall, 2014), also occurs at 19.8

2526   m, and in the core of the EECO (Luciani and Giusberti, 2014)*. Clavigerinella* is the ancestor

2527   of the genus *Hantkenina* that successfully inhabited the sub-surface and surface waters during

2528   the middle through late Eocene (Coxall et al., 2000).

2529   A second consideration is the change in planktic foraminiferal assemblages during the

2530   Middle Eocene Climate Optimum (MECO), another interval of anomalous and prolonged

2531   warmth ca. 40 Ma (Bohaty and Zachos, 2003). At Alano (**Figure 11**) and other locations

2532   (Luciani et al., 2010; Edgar et al., 2012), the MECO involved the reduction in the abundance

2533   and test size of large acarininids and *Morozovelloides*. This has been attributed to "bleaching"

2534   and the loss of photosymbionts resulting from global warming (Edgar et al., 2012), although

2535   related factors, such as a decrease in pH, a decrease in nutrient availability, or changes in

2536   salinity, may have been involved (Douglas, 2003; Wade et al., 2008). The symbiotic

2537   relationship with algae is considered an important strategy adopted by muricate planktic

2538 foraminifera during the early Paleogene (Norris, 1996; Quillévéré et al., 2001). Considering

2539 the importance of this relationship in extant species (Bé, 1982; Bé et al., 1982; Hemleben et

2540 al., 1989), the loss of photosymbionts may represent a crucial mechanism to explain the

2541 relatively rapid decline foraminifera utilizing this strategy, including morozovellids at the

2542 start of the EECO.

2543   Available data suggest that the protracted conditions of extreme warmth and high pCO$_2$

2544 during the EECO were the key elements inducing a permanent impact on planktic

2545 foraminiferal evolution, and the ~~demise~~ decline of the morozovellids. Even during the PETM,

2546 the most pronounced hyperthermal, did not adversely affect the morozovellids permanently.

2547 While "excursion taxa" appeared, morozovellids seem to have increased in abundance in

2548 open ocean settings (Kelly et al., 1996; 1998, 2002; Lu and Keller, 1995; Petrizzo, 2007);

2549 only in some continental margin settings did a transient decrease in abundance occur (Luciani

2550 et al., 2007).

2551

2552 **6.7 Post-EECO changes at Possagno**

2553

2554 Several small CIEs appear in the δ^{13}C record at Possagno during polarity chrons C22n, C21r,

2555 and C21n. Some of these post-EECO excursions coincide with planktic foraminiferal

2556 assemblage changes similar to those recorded in lower strata. Specifically, there are marked

2557 increases of acarininids (**Figure 6**). These "post-EECO" CIEs are concomitant with δ^{18}O

2558 excursions and coupled to distinct modifications in the planktic foraminiferal assemblages

2559 comparable to those recorded across known hyperthermals in Tethyan settings (Luciani et al.,

2560 2007; Agnini et al., 2009; D'Onofrio et al., 2014). Additional hyperthermals, although of less

2561 intensity and magnitude, may extend through the entirety of the early and middle Eocene, as

2562 suggested previously (Sexton et al., 2006; 2011; Kirtland-Turner et al., 2014). Whether these

2563 imply different forcing and feedback mechanisms compared to the PETM remains an open

2564 discussion.

2565

2566 **7 Summary and conclusions**

2567 The symbiont-bearing planktic foraminiferal genera *Morozovella* and *Acarinina* were

2568 among the most important calcifiers of the early Paleogene tropical and subtropical oceans.

2569 However, a remarkable and permanent switch in the relative abundance of these genera

2570 happened in the early Eocene, an evolutionary change accompanied by species reduction of

2571 *Morozovella* and species diversification of *Acarinina*. We show here that this switch probably

2572 coincided with a carbon isotope excursion (CIE) presently coined J. Although the Early

2573 Eocene Climatic Optimum (EECO), a multi-million year interval of extreme Earth surface

2574 warmth, lacks an accepted definition, we ~~agree~~ propose ~~with others~~ that the EECO is best

2575 defined as the duration of time between the J event and the base of *D. sublodoensis* (about 53

2576 Ma to 49 Ma on the 2012 GTS).

2577 Our conclusion that the planktic foraminferal switch coincides with the start of the

2578 EECO derives from the generation of new records and collation of old records concerning

2579 bulk sediment stable isotopes and planktic foraminiferal abundances at three sections. These

2580 sections span a wide longitude range of the low latitude Paleogene world: the Possagno

2581 section from the western Tethys, DSDP Site 577 from the central Pacific Ocean, and ODP

2582 Site 1051 from the western Atlantic Ocean. Importantly, these locations have robust

2583 calcareous nannofossils and polarity chron age markers, although the stratigraphy required

2584 amendment at Sites 577 and 1051.

2585 An overarching problem is that global carbon cycling was probably very dynamic during

2586 the EECO. The interval appears to have been characterized not only by numerous CIEs, but

2587 also a major switch in the timing and magnitude of these perturbations. Furthermore, there

was a rapid shoaling of carbonate dissolution horizons in the middle of the EECO. A key finding of our study is that the major switch in planktic foraminiferal assemblages happened at the start of the EECO. Significant, though ephemeral, modifications in planktic foraminiferal assemblages coincide with numerous short-term CIEs, before, during and after the EECO. Often, there are marked increases in the relative abundance of acarininids, similar to what happened permanently across the start of the EECO.

Although we show for the first time that the critical turnover in planktic foraminifera clearly coincided with the start of the EECO, the exact cause for the switch (aka the ~~demise~~ decline of morozovellids) remains elusive. Possible causes are multiple, and may include temperature effects on photosymbiont-bearing planktic foraminifera, changes in ocean chemistry, or even interaction with other microplankton groups such as radiolarians, diatoms or dinoflagellates that represented possible competitors in the use of symbionts or as symbiont providers. For some reason, a critical threshold was surpassed at the start the EECO, and this induced an unfavourable habitat for continued morozovellid diversification and proliferation but a favourable habitat for the acarinids.

2621

References

2623

2624 Abels, H. A., Clyde, W. C., Gingerich, P. D., Hilgen, F. J., Fricke, H. C., Bowen, G. J., and
2625   Lourens, L. J.: Terrestrial carbon isotope excursions and biotic change during Palaeogene
2626   hyperthermals, Nat. Geosci., 5, 326-329, doi: 10.1038/ngeo1427, 2012.

2627 Agnini, C., Muttoni, G., Kent, D. V., and Rio, D.: Eocene biostratigraphy and magnetic
2628   stratigraphy from Possagno, Italy: the calcareous nannofossils response to climate
2629   variability, Earth Planet. Sci. Lett., 241, 815-830, 2006.

2630 Agnini, C., Macrì, P., Backman, J., Brinkhuis, H., Fornaciari, E., Giusberti, L., Luciani, V.,
2631   Rio, D., Sluijs, A., and Speranza, F.: An early Eocene carbon cycle perturbation at 52.5
2632   Ma in the Southern Alps: chronology and biotic response, Paleoceanography, 24,
2633   PA2209. doi: 10.1029/2008PA001649, 2009.

2634 Agnini, C., Fornaciari, E., Giusberti, L., Grandesso, P., Lanci, L., Luciani, V., Muttoni, G.,
2635   Plike, H., Rio, D., Spofforth, D.J.A., and Stefani, C.: Integrated biomagnetostratigraphy
2636   of the Alano section (NE Italy): a proposal for defining the middle-late Eocene boundary,
2637   Geol. Soc. Am. Bull., 123, 841-872, 2011.

2638 Agnini, C., Fornaciari, E., Raffi, I., Catanzariti, R., Pälike, H., Backman, J., and Rio, D.:
2639   Biozonation and biochronology of Paleogene calcareous nannofossils from low to middle
2640   latitudes, News. Strat., 47, 131-181, 2014.

2641 Agnini, C., Spofforth, D. J. A., Dickens, G. R., Rio, D., Pälike, H., Backman, J., Muttoni, G.,
2642   and Dallanave, E.: Stable isotope and calcareous nannofossil assemblage records for the

2643   Cicogna section: toward a detailed template of late Paleocene and early Eocene global

2644   carbon cycle and nannoplankton evolution, Clim. Past, sumbitted.

2645 Anderson, T. F., and Cole, S. A.: The stable isotope geochemistry of marine coccoliths: a

2646   preliminary comparison with planktonic foraminifera, J. Foram. Res., 5 (3), 188-192,

2647   1975.

2648 Arthur , M. A., Dean, W. E., Bottjer, D., and Schole, P. A.: Rhythmic bedding in Mesozoic-

2649   Cenozoic pelagic carbonate sequences: the primary and diagenetic origin of

2650   Milankovitch like cycles, in: Milankovitch and Climate, A. Berger, J. Imbrie, J. Hays, G.

2651   Kucla, B. Satzman (eds.), 191-222, D. Reidel Publ. Company, Dordrecht, Holland,

2652   1984.

2653 Arenillas, I., Molina, E., and Schmitz, B.: Planktic foraminiferal and δ^{13}C isotopic changes

2654   across the Paleocene/Eocene boundary at Possagno (Italy), Int. J. Earth Sc., 88, 352–364,

2655   1999.

2656 Aze, T., Ezard, T. H. G., Purvis, A., Coxall, H. K., Stewart, D. R. M, Wade, B. S., and

2657   Pearson, P. N.: A phylogeny of Cenozoic macroperforate planktonic foraminifera from

2658   fossil data, Biol. Rev., 86, 900-927. 900 doi: 10.1111/j.1469-185X.2011.00178.x, 2011.

2659 Backman, J.: Late Paleocene to middle Eocene calcareous nannofossil biochronology from

2660   the Shatsky Rise, Walvis Ridge and Italy, Palaeogeogr. Palaeoclimatol. Palaeoecol., 57

2661   (1), 43-59, 1986.

2662 Bé, A. W. H.: Biology of planktonic foraminifera, in: Foraminifera: notes for a short course,

2663   Broadhead T., Stud. Geol., 6, Univ. Knoxville, Tenn., 51-92, 1982.

2664 Bé, A. W. H., John, W. M., and Stanley, M. H.: Progressive dissolution and ultrastructural

2665   breakdown of planktic foraminifera, Cushman Foundation for Foraminiferal Research

2666   Special Publication, 13, 27-55, 1975.

2667 Bé, A. W. H., Spero, H. J., and Anderson O. R.: Effects of symbiont elimination and

2668   reinfection on the life processes of the planktonic foraminifer *Globigerinoides sacculifer,*

2669   Marine Biol. 70, 73-86, 1982.

2670 Bemis, B. E., Spero, H. J., Bijma, J., and Lea, D. W.: Reevaluation of the oxygen isotopic

2671   composition of planktonic foraminifera: Experimental results and revised

2672   paleotemperature equations, Paleoceanography, 13 (2), 150-160, 1998.

2673 Berger, W. H.: Foraminiferal ooze: Solution at depth, Science, 156: 383-385, 1967.

2674 Berger, W. H.: Planktonic foraminifera - selective solution and lysocline, Marine Geol., 8(2),

2675   111-138, 1970.

2676 Berger, W. H., Bonneau, M.-C., and. Parker, F. L.: Foraminifera on the deep-sea floor:

2677 lysocline and dissolution rate, Oceanol. Acta, 5 (2), 249-258, 1982.

2678 Berggren, W. A., and Norris, R. D.: Biostratigraphy, phylogeny and systematics of Paleocene

2679 trochospiral planktic foraminifera, Micropaleont., 43 (Suppl. 1), 1-116, 1997.

2680 Berggren, W. A., and Pearson, P. N.: A revised tropical to subtropical Paleogene planktic

2681 foraminiferal zonation: J. Foram. Res., v. 35, p. 279-298, 2005.

2682 Berggren, W. A., Kent, D. V., Swisher, C. C. III, and Aubry, M-P.: A revised Cenozoic

2683 geochronology and chronostratigraphy, in: Berggren W. A, Kent D. V., Aubry M-P.,

2684 Hardenbol J. (Eds.), Geochronology, time scales and global stratigraphic correlation.

2685 SEPM Special Publication 54, 129-212, 1995.

2686 Bijl, P. K., Schouten, S., Sluijs, A., Reichart, G.-J., Zachos, J. C., and Brinkhuis, H.: Early

2687 Paleogene temperature evolution of the southwest Pacific Ocean. Nature, 461, 776–

2688 779, doi:10.1038/nature08399, 2009.

2689 Bleil, U.: The magnetostratigraphy of northwest Pacific sediments, Deep Sea Drilling Project

2690 Leg 86, Initial Reports Deep Sea Drilling Project, 86, 441-458.

2691 Boersma, A., and Premoli Silva, I.: Paleocene planktonic foraminiferal biogeography and the

2692 paleoceanography of the Atlantic-Ocean, Micropaleont., 29, 355-381, 1983.

2693 Boersma, A., Premoli Silva, I., and Shackleton, N.: Atlantic Eocene planktonic foraminiferal

2694 biogeography and stable isotopic paleoceanography, Paleoceanography, 2, 287-331,

2695 1987.

2696 Bohaty, S. M., and J. C. Zachos: A significant Southern Ocean warming event in the late

2697 middle Eocene, Geology, 31, 1017–1020, doi:10.1130/G19800.1, 2003.

2698 Bohaty, S. M., Zachos, J. C., Florindo, F., and Delaney, M. L.: Coupled greenhouse warming

2699 and deep-sea acidification in the middle Eocene, Paleoceanography, 24, PA2207,

2700 doi:10.1029/2008PA001676, 2009.

2701 Bolli, H. M.: Monografia micropaleontologica sul Paleocene e sull'Eocene di Possagno,

2702 Provincia di Treviso, Italia. Mémoires Suisses de Paléontologie 97: 222 pp., 1975.

2703 Borre, M. and Fabricus, I.L.: Chemical and mechanical processes during burial diagenesis of

2704 chalk: an interpretation based on specific surface data of deep-sea sediments,

2705 Sedimentology, 45, 755-769, 1998.

2706 Bosellini, A.: Dynamics of Tethyan carbonate platform, in: Controls on Carbonate Platform

2707 and Basin Platform, Crevello, P.D., Wilson, J.L., Sarg, J.F., Read, J.F., (Eds.), SEPM

2708 Spec. Publ., 44, 3-13, 1989.

2709 Bowen, G. J., Bralower, T. J., Delaney, M. R., Dickens, G. R., Kelly, D. C., Koch, P. L.,

2710 Kump, L. R., Meng, J., Sloan, L. C., Thomas, E., Wing, S. L., and Zachos, J. C.: Eocene

Hyperthermal Event Offers Insight Into Greenhouse Warming, EOS, 87 (17), 165-169, DOI: 10.1029/2006EO170002, 2006.

Braga G.: L'assetto tettonico dei dintorni di Possagno (Trevigiano occidentale). Rendiconti dell'Accademia Nazionale dei Lincei, 8/48: 451-455, 1970.

Bramlette, M. N., and Riedel, W. R.: Stratigraphic value of discoasters and some other microfossils related to recent coccolithophores, J. Paleont., 28: 385-403, 1954.

Broecker, W. S., Clark, E., McCorkle D. C., Peng, T-H., Hajadas, I., and Bonani, G.: Evidence of a reduction in the carbonate ion content of the deep see during the course of the Holocene, Paleoceanography, 14 (6), 744-752, 1999.

Brown, J. H., Gillooly, J. F., Allen, A. P., Savage, V. M., and West, G. B.: Toward a metabolic theory of ecology, Ecology, 85(7), 1771-1789, 2004.

Cita, M. B.: Stratigrafia della Sezione di Possagno, in: Bolli, H. M. (Ed.), Monografia Micropaleontologica sul Paleocene e l'Eocene di Possagno, Provincia di Treviso, Italia, Schweiz. Palaeontol. Abhandl., 97, 9–33, 1975.

Clyde, W. C., Gingerich, P. D., Wing, S. L., Röhl, U., Westerhold, T., Bowen, G., Johnson, K., Baczynski, A. A., Diefendorf, A., McInerney, F., Schnurrenberger, D., Noren, A., Brady, K., and the BBCP Science Team: Bighorn Basin Coring Project (BBCP): A continental perspective on early Paleogene hyperthermals, Scientific Drilling, 16, 21-31, 2013.

Coccioni, R., Bancalà, G., Catanzariti, R., Fornaciari, E., Frontalini, F., Giusberti, L., Jovane, L., Luciani, V., Savian, J., and Sprovieri, M.: An integrated stratigraphic record of the Palaeocene–lower Eocene at Gubbio (Italy): new insights into the early Palaeogene hyperthermals and carbon isotope excursions, Terra Nova, 24, 380-386, 2012.

Coxall, H. K., Pearson, P. N., Shackleton, N.J., Hall, M.A.: Hantkeninid depth adaptation: An evolving life strategy in a changing ocean, Geology, 28, 87-90, doi:10.1130/0091-7613(2000)28<87:HDAAEL>2.0.CO;2, 2000.

Coxall, H. K., Huber, B. T., and Pearson, P. N.: Origin and morphology of the Eocene planktic foraminifera *Hantkenina,* J. Foram. Res., 33, 237-261, 2003.

Cramer, B. S., Wright, J. D., Kent, D. V., and Aubry, M.-P.: Orbital climate forcing of $\delta^{13}C$ excursions in the late Paleocene–early Eocene (chrons C24n–C25n), Paleoceanography, 18, 21-1. doi:10.1029/2003PA000909, 2003.

Cramer, B. S., Toggweiler, J. R., Wright, M. E., Katz, J. D., and Miller, K. G.: Ocean overturning since the Late Cretaceous: Inferences from a new benthic foraminiferal isotope compilation, Paleoceanography, 24, PA4216, doi:10.1029/2008PA001683, 2009.

2745 Crouch, E. M., Heilmann-Clausen, C., Brinkhuis, H., Morgans, H. E. G, Rogers, K.
2746   M., Egger, H., and Schmitz, B.: Global dinoflagellate event associated with the late
2747   Paleocene thermal maximum, Geology, 29(4), 315-318, 2001.

2748 D'Onofrio, R., Luciani V., Giusberti L., Fornaciari E., and Sprovieri, M.: Tethyan planktic
2749   foraminiferal record of the early Eocene hyperthermal events ETM2, H2 and I1 (Terche
2750   section, northeastern Italy), Rendiconti Online della Società Geologica Italiana, 31, 66-
2751   67, doi: 10.3301/ROL.2014.48, 2014.

2752 Dallanave, E., Agnini, C., Bachtadse, V., Muttoni, G., Crampton J. S., Strong, C. P., Hines,
2753   B. H., Hollis, C. J., and Slotnick, B. S.: Early to middle Eocene magneto-biochronology
2754   of the southwest Pacific Ocean and climate influence on sedimentation: Insights from the
2755   Mead Stream section, New Zealand, Geol. Soc. Am. Bull., 127 (5-6), 643-660, 2015.

2756 DeConto, R. M., Galeotti, S., Pagani, M., Tracy, D., Schaefer, K., Zhang, T., Pollard, D., and
2757   Beerling, D. J.: Past extreme warming events linked to massive carbon re-lease from
2758   thawing permafrost, Nature, 484, 87-92, http://dx.doi.org/10.1038/nature10929, 2012.

2759 Demicco, R. V.: Modeling seafloor-spreading rates through time, Geology, 32, 485-488,
2760   2004.

2761 Dickens, G. R.: Methane oxidation during the Late Palaeocene Thermal Maximum, B. Soc.
2762   Geol. Fr., 171 (1), 37-49, 2000.

2763 Dickens, G. R.: Down the Rabbit Hole: toward appropriate discussion of methane release
2764   from gas hydrate systems during the Paleocene–Eocene thermal maximum and other past
2765   hyperthermal events. Clim. Past, 7, 831-846. http://dx.doi.org/10.5194/cp-7-831-2011,
2766   2011.

2767 Dickens, G. R., and Backman J.: Core alignment and composite depth scale for the lower
2768   Paleogene through uppermost Cretaceous interval at Deep Sea Drilling Project Site 577,
2769   Newsl. Stratigr., 46, 47-68, 2013.

2770 Dickens, G. R., O'Neil, J. R., Rea, D. K., and Owen, R. M.: Dissociation of oceanic methane
2771   hydrate as a cause of the carbon isotope excursion at the end of the Paleocene,
2772   Paleoceanography, 10, 965-971, doi:10.1029/95PA02087, 1995.

2773 Dickens, G. R., Castillo, M. M., and Walker, J. C. G.: A blast of gas in the latest Paleocene:
2774   simulating first-order effects of massive dissociation of oceanic methane hydrate,
2775   Geology, 25, 259-262, 1997.

2776 Dunkley Jones, T., Lunt, D. J., Schmidt, D. N., Ridgwell, A., Sluijs, A., Valdez, P. J., and
2777   Maslin, M. A.: Climate model and proxy data constraints on ocean warming across the
2778   Paleocene–Eocene Thermal Maximum, Earth Sci. Rev., 125, 123-145, 2013.

2779   Edgar, K. M., Bohaty, S. M., Gibbs, S. J., Sexton, P. F., Norris, R. D., and Wilson, P. A.:
2780   Symbiont 'bleaching' in planktic foraminifera during the Middle Eocene Climatic
2781   Optimum, Geology, 41, 15-18, doi:10.1130/G33388.1, 2012.

2782   Ernst, S.R., Guasti, E., Dupuis, C., and Speijer, R.P.: Environmental perturbation in the
2783   southern Tethys across the Paleocene/Eocene boundary (Dababiya, Egypt): foraminiferal
2784   and clay mineral records. Mar. Micropaleont., 60, 89–111, 2006.

2785   Ezard, T. H. G., Aze, T., Pearson, P.N., and Purvis, A: Interplay between changing climate
2786   and species' ecology drives macroevolutionary dynamics, Science, 332, 349-351, 2011.

2787   Falkowski, P. G., Katz, M. E., Milligan, A. J., Fennel, K., Cramer, B. S., Aubry, M. P.,
2788   Berner, R. A., Novacek, M. J., Zapol, W. M.: Mammals evolved, radiated, and grew in
2789   size as the concentration of oxygen in Earth's atmosphere increased during the past 100
2790   million years, Science, 309 (5744), 2202-2204, 2005.

2791   Figueirido, B., Janis, C. M., Pérez-Claros, J. A., De Renzi, M., and Palmqvist, P.: Cenozoic
2792   climate change influences mammalian evolutionary dynamics, Proc. Natl. Acad. Sci.
2793   USA, 109 (3), 722-727, 2012.

2794   Fletcher, B. J., Brentnall, S. J., Anderson, C. W., Berner, R. A., and Beerling, D.J.:
2795   Atmospheric carbon dioxide linked with Mesozoic and early Cenozoic climate change,
2796   Nature Geoscience, 1, 43-48, 2008.

2797   Fornaciari, E., Giusberti, L., Luciani, V., Tateo, F., Agnini, C., Backman, J., Oddone, M., and
2798   Rio, D.: An expanded Cretaceous–Tertiary transition in a pelagic setting of the Southern
2799   Alps (central–western Tethys), Palaeogeogr. Palaeoclimatol. Palaeoecol., 255, 98-131,
2800   2007.

2801   Fraass, A. J., Kelly, D. K., and. Peters, S. E.: Macroevolutionary history of the planktic
2802   foraminifera, Annual Review of Earth and Planetary Sciences, 43, 139-66, doi:
2803   10.1146/annurev-earth-060614-105059, 2015.

2804   Frank, T. D., Arthur, M. A., and Dean, W. E.: Diagenesis of Lower Cretaceous pelagic
2805   carbonates, North Atlantic: paleoceanographic signals obscured, J. Foramin. Res., 29,
2806   340-351, 1999.

2807   Galeotti, S., Krishnan, S., Pagani, M., Lanci, L., Gaudio, A., Zachos, J. C., Monechi, S.,
2808   Morelli, G., and Lourens, L. J.: Orbital chronology of early Eocene hyperthermals from
2809   the Contessa Road section, central Italy, Earth Planet. Sci. Lett., 290(1-2), 192-200, doi:
2810   10.1016/j.epsl.2009.12.021, 2010.

2811   Gingerich, P. D.: Rates of evolution on the time scale of the evolutionary process, Genetica,
2812   112-113, 127-144, 2001.

2813 Gingerich, P. D.: Mammalian response to climate change at the Paleocene–Eocene boundary:

2814   Polecat Bench record in the northern Bighorn Basin, Wyoming, Geol. Soc. Am. Spec.

2815   Pap., 369, 463-478, 2003.

2816 Giusberti, L., Rio, D., Agnini, C., Backman, J., Fornaciari, E., Tateo, E., and Oddone, M.:

2817   Mode and tempo of the Paleocene–Eocene thermal maximum in an expanded section

2818   from the Venetian pre-Alps, Geol. Soc. Am. Bull., 119, 391-412, 2007.

2819 Guasti, E., and Speijer, R.P.: The Paleocene–Eocene thermal maximum in Egypt and

2820   Jordan: an overview of the planktic foraminiferal record. Geol. Soc. Spec. Pap., 424, 53–

2821   67, 2007.

2822 Hallock, P.: Fluctuations in the trophic resource continuum: a factor in global diversity

2823   cycles? Paleoceanography, 2, 457–471, 1987.

2824 Hancock, H. J. L., and Dickens, G. R.: Carbonate dissolution episodes in Paleocene and

2825   Eocene sediment, Shatsky Rise, west-central Pacific, Proc. Ocean Drill. Progr., Sci.

2826   Results 198, 24 pp., doi:10.2973/odp.proc.sr.198.116., 2005.

2827 Hemleben, C, Spindler, M., and Anderson, O. R (Eds.).: Modern planktonic foraminifera,

2828   Springer-Verlag, New York, 1-363, ISBN-13: 9780387968155, 1989.

2829 Hilgen, F. J., Abels, H. A., Kuiper, K. F., Lourens, L. J., and Wolthers, M.: Towards a stable

2830   astronomical time scale for the Paleocene: aligning Shatsky Rise with the Zumaia –

2831   Walvis Ridge ODP Site 1262 composite, Newsl. Stratigr., 48, 91-110, doi:

2832   10.1127/nos/2014/0054, 2015.

2833 Hollis, C. J., Taylor, K. W. R., Handley, L., Pancost, R. D., Huber, M., Creech, J. B., Hines,

2834   B. R., Crouch, E. M., Morgans, H. E. G., Crampton, J. S., Gibbs, S., Pearson, P. N., and

2835   Zachos, J. C.: Early Paleogene temperature history of the Southwest Pacific Ocean:

2836   Reconciling proxies and models: Earth Planet. Sci. Lett., 349-350, 53–66, doi:

2837   10.1016/j.epsl.2012.06.024, 2012.

2838 Huber, M., and Caballero, R.: The early Eocene equable climate problem revisited. Clim.

2839   Past, 7, 603-633, 2011.

2840 Hyland, E. G., and Sheldon, N. D.: Coupled CO2-climate response during the Early Eocene

2841   Climatic Optimum, Palaeogeogr. Palaeoclimatol. Palaeoecol., 369, 125-135, 2013.

2842 Hyland, E. G., Sheldon, N. D., and Fan, M.: Terrestrial paleoenvironmental reconstructions

2843   indicate transient peak warming during the early Eocene climatic optimum, Geol. Soc.

2844   Am. Bull., 125 (7-8), 1338-1348, 2013.

2845 IPCC, 2014: Climate Change 2014: Synthesis Report. Contribution of Working Groups I, II

2846   and III to the Fifth Assessment Report of the Intergovernmental Panel on Climate

Change [Core Writing Team, R.K. Pachauri and L.A. Meyer (eds.)]. IPCC, Geneva, Switzerland, 151 pp, 2014.

Inglis, G. N., Farnsworth, A., Lunt, D., Foster, G. L., Hollis, C. J., Pagani, M., Jardine, P. E., Pearson, P. N., Markwick, P., Galsworthy, A. M. J., Raynham, L., Taylor, K. W. R., and Pancost, R. D.: Descent toward the icehouse: Eocene sea surface cooling inferred from GDGT distributions. Paleoceanography, 30 (7), 100-1020, 10.1002/2014PA002723, 2015.

Ito, G., and Clift, P. D.: Subsidence and growth of Pacific Cretaceous plateaus. Earth Plant. Sci. Lett., 161, 85-100, 1998.

John E. H., Pearson P. N., Coxall H. K., Birch H., Wade B. S., and Foster G. L.: Warm ocean processes and carbon cycling in the Eocene, Phil. Trans. R. Soc., A, 371, 20130099, 2013.

John E. H., Wilson J. D., Pearson P. N., and Ridgwell, A.: Temperature-dependent remineralization and carbon cycling in the warm Eocene oceans, Palaeogeogr. Palaeoclimatol. Palaeoecol., 413, 158-166, 2014.

Kelly, D. C., Bralower, T. J., Zachos, J. C., Premoli Silva, I., and Thomas, E.: Rapid diversification of planktonic foraminifera in the tropical Pacific (ODP Site 865) during the late Paleocene thermal maximum, Geology 24, 423-426, 1996.

Kelly, D. C., Bralower, T. J., and Zachos, J. C.: Evolutionary consequences of the latest Paleocene thermal maximum for tropical planktonic foraminifera, Palaeogeogr., Palaeoclimatol., Palaeoecol., 141, 139-161, 1998.

Kennett, J. P., and Stott, L. D.: Abrupt deep-sea warming, palaeoceanographic changes and benthic extinctions at the end of the Palaeocene, Nature 353, 225-229, 1991.

Kirtland-Turner, S., Sexton P. F., Charled C. D., and Norris R. D.: Persistence of carbon release events through the peak of early Eocene global warmth, Nature Geoscience, 7, 748-751, doi: 10.1038/NGEO2240, 2014.

Komar, N., Zeebe, R. E., and Dickens, G. R.: Understanding long-term carbon cycle trends: the late Paleocene through the early Eocene, Paleoceanography, 28, 650-662, doi: 10.1002/palo.20060, 2013.

Kroenke, L. W., Berger, W. H., Janecek, T. R., et al.: Ontong Java Plateau, Leg 130: synopsis of major drilling results, Proceedings of the Ocean Drilling Program, Initial Reports, 130, 497-537, 1991.

Kurtz, A. C., Kump, L. R., Arthur, M. A., Zachos, J. C., and Paytan, A.: Early Cenozoic decoupling of the global carbon and sulfur cycles, Paleoceanography, 18, 1090, doi:

2881   10.1029/2003PA000908, 2003.

2882 Lauretano, V., Littler, K., Polling, M., Zachos, J. C., and Lourens, L. J.: Frequency,

2883   magnitude and character of hyperthermal events at the onset of the Early Eocene

2884   Climatic Optimum, Clim. Past, 11, 1313-1324, doi: 10.5194/cp-11-1313-2015, 2015.

2885 Lee C. T., Shen B., Slotnick B. S., Liao K., Dickens G. R., Yokoyama Y., Lenardic A.,

2886   Dasgupta R., Jellinek M., Lackey J. S., Schneider T., and Tice M. M.: Continental arc-

2887   island arc fluctuations, growth of crustal carbonates, and long-term climate change,

2888   Geosphere, 9, 21-36, 2013.

2889 LeGrande, A. N. and Schmidt, G. A.: Global gridded data set of the oxygen isotopic

2890   composition in seawater, Geophys. Res. Lett., 33, L12604, doi: 10.1029/2006GL026011,

2891   2006.

2892 Leon-Rodriguez, L. and Dickens, G. R.: Constraints on ocean acidification associated with

2893   rapid and massive carbon injections: The early Paleogene record at ocean drilling

2894   program site 1215, equatorial Pacific Ocean, Palaeogeogr. Palaeoclimatol. Palaeoecol.,

2895   298 (3-4), 409-420, doi: 10.1016/j.palaeo.2010.10.029, 2010.

2896 Lirer, F.: A new technique for retrieving calcareous microfossils from lithified lime deposits.

2897   Micropaleontol., 46, 365–369, 2000.

2898 Littler, K., Röhl, U., Westerhold, T., and Zachos, J. C.: A high-resolution benthic stable-

2899   isotope for the South Atlantic: implications for orbital-scale changes in Late Paleocene-

2900   early Eocene climate and carbon cycling, Earth Planet. Sci. Lett., 401, 18-30.

2901   http://dx.doi.org/10.1016/j.epsl.2014.05.054, 2014.

2902 Lourens, L. J., Sluijs, A., Kroon, D., Zachos, J. C., Thomas, E., Röhl, U., Bowles, J., and

2903   Raffi, I.: Astronomical pacing of late Palaeocene to early Eocene global warming events,

2904   Nature, 7045, 1083-1087, 2005.

2905 Lowestein, T. K., and Demicco R. V.: Elevated Eocene atmospheric CO_2 and its subsequent

2906   decline, Science, 313 (5795), doi: 10.1126/science.1129555, 2006.

2907 Lu, G.: Paleocene-Eocene transitional events in the ocean: Faunal and isotopic analyses of

2908   planktic foraminifera, Ph.D. Thesis, Princeton University, pp. 1-284, 1995.

2909 Lu, G., and Keller, G.: Planktic foraminiferal faunal turnovers in the subtropical Pacific

2910   during the late Paleocene to early Eocene, J. Foramin. Res., 25 (2), 97-116, 1995.

2911 Lu, G., Keller, G. and Pardo, A.: Stability and change in Tethyan planktic foraminifera across

2912   the Paleocene-Eocene transition, Mar. Micropaleont., 35 (3-4), 203-233, 1998.

2913 Luciani, V., Giusberti, L., Agnini, C., Backman, J., Fornaciari, E., and Rio., D.: The

2914   Paleocene–Eocene Thermal Maximum as recorded by Tethyan planktonic foraminifera

2915   in the Forada section (northern Italy), Mar. Micropaleont., 64, 189-214, 2007.

2916 Luciani, V., Giusberti, L., Agnini, C., Fornaciari, E., Rio, D., Spofforth, D. J. A., and Pälike

2917   H.: Ecological and evolutionary response of Tethyan planktonic foraminifera to the

2918   middle Eocene climatic optimum (MECO) from the Alano section (NE Italy),

2919   Palaeogeogr. Palaeoclimatol. Palaeoecol., 292, 82-95, doi: 10.1016/j.palaeo.2010.03.029,

2920   2010.

2921 Luciani, V., and Giusberti, L.: Reassessment of the early–middle Eocene planktic

2922   foraminiferal biomagnetochronology: new evidence from the Tethyan Possagno section

2923   (NE Italy) and Western North Atlantic Ocean ODP Site 1051, J. Foram. Res., 44, 2, 187-

2924   201, 2014.

2925 Lunt, D. J., Ridgwell, A., Sluijs, A., Zachos, J., Hunter, S., and Haywood, A.: A model for

2926   orbital pacing of methane hydrate destabilization during the Palaeogene, Nat. Geosc., 4,

2927   775-778, doi: 10.1038/NGEO1266, 2011.

2928 Marshall, J. D.: Climatic and oceanographic isotopic signals from the carbonate rock records

2929   and their preservation, Geol. Mag., 129, 143-160, 1992.

2930 Matter, A., Douglas, R. G., and Perch-Nielsen, K: Fossil preservation, geochemistry and

2931   diagenesis of pelagic carbonates from Shatsky Rise, northwest Pacific, Initial Reports

2932   Deep Sea Drilling Project, 32, 891-922, doi: 10.2973/dsdp.proc.32.137, 1975.

2933 Martini, E.: Standard Tertiary and Quaternary calcareous nannoplankton zonation. In:

2934   Farinacci, A., Ed., Proceedings of the 2nd Planktonic Conference, 739–785. Roma:

2935   Edizioni Tecnoscienza, vol. 2, 1971.

2936 McInerney, F. A. and Wing, S. L.: The Paleocene–Eocene thermal maximum: a perturbation

2937   of carbon cycle, climate, and biosphere with implications for the future, Ann. Rev. Earth

2938   Planet. Sci., 39, 489-516, doi: 10.1146/annurev-earth-040610-133431, 2011.

2939 Mita, I.: Data Report: Early to late Eocene calcareous nannofossil assemblages of Sites 1051

2940   and 1052, Blake Nose, Northwestern Atlantic Ocean, Proc. Ocean Drilling Program, Sci.

2941   Results, 171B, 1-28, 2001.

2942 Molina, E., Arenillas, I., Pardo, A.: High resolution planktic foraminiferal biostratigraphy

2943   and correlation across the Palaeocene Palaeocene/Eocene boundary in the Tethys, B.

2944   Soc. Géol. Fr., 170, 521–530, 1999.

2945 Monechi, L., Bleil, U., and Backman, J.: Magnetobiochronology of Late Cretaceous-

2946   Paleogene and late Cenozoic pelagic sedimentary sequences from the northwest Pacific

2947   (Deep Sea Drilling Project, Leg 86, Site 577. Proceedings of the Ocean Drilling Program

2948   86, Initial Reports, Ocean Drilling Program, College Station, TX,

2949   doi:10.2973/dsdp.proc.86.137.1985.

2950 Nguyen, T. M. P., Petrizzo, M.-R., and Speijer, R. P.: Experimental dissolution of a fossil

2951   foraminiferal assemblage (Paleocene–Eocene Thermal Maximum, Dababiya, Egypt):

2952   implications for paleoenvironmental reconstructions, Mar. Micropaleont., 73 (3-4), 241-

2953   258, doi: 10.1016/j.marmicro.2009.10.005, 2009.

2954 Nguyen, T. M. P., Petrizzo, M.-R., Stassen, P., and Speijer, R. P.: Dissolution susceptibility

2955   of Paleocene–Eocene planktic foraminifera: Implications for palaeoceanographic

2956   reconstructions, Mar. Micropaleont., 81, 1-21, 2011.

2957 Nicolo, M. J., Dickens, G. R., Hollis, C. J., and Zachos, J. C.: Multiple early Eocene

2958   hyperthermals: their sedimentary expression on the New Zealand continental margin and

2959   in the deep sea, Geology, 35, 699-702, 2007.

2960 Norris, R.D.: Biased extinction and evolutionary trends, Paleobiology, 17 (4), 388-399, 1991.

2961 Norris, R.: Symbiosis as an evolutionary innovation in the radiation of Paleocene planktic

2962   foraminifera, Paleobiology, 22, 461-480, 1996.

2963 Norris, R. D., Kroon, D., and Klaus, A.: Proceedings of the Ocean Drilling Program, Initial

2964   Reports, 171B, Proc. Ocean Drill. Progr. Sci. Results, 1-749, 1998.

2965 O'Connor, M., Piehler, M. F., Leech, D. M., Anton, A., and Bruno, J. F.: Warming and

2966   resource availability shift food web structure and metabolism, PLOS Biol., 7(8), 1-6. doi:

2967   10.1371/journal.pbio.1000178, 2009.

2968 Ogg, J. G., and Bardot, L.: Aptian through Eocene magnetostratigraphic correlation of the

2969   Blake Nose Transect (Leg 171B), Florida continental margin, Proc. Ocean Drill. Progr.,

2970 Sci. Results, 171B, 1-58, doi: 10.2973/odp.proc.sr.171B.104.2001

2971 Okada, H. and Bukry, D.: Supplementary modification and introduction of code numbers to

2972   the low-latitude coccolith biostratigraphic zonation (Bukry, 1973;1975). Mar.

2973   Micropaleont., 5, 321-325, 1980.

2974 Olivarez Lyle, A., and Lyle, M. W.: Missing organic carbon in Eocene marine sediments: Is

2975   metabolism the biological feedback that maintains end-member climates?

2976   Paleoceanography, 21, PA2007, doi: 10.1029/2005PA001230, 2006.

2977 Oreshkina, T. V.: Evidence of late Paleocene - early Eocene hyperthermal events in

2978   biosiliceous sediments of Western Siberia and adjacent areas, Austrian Journal of Earth

2979   Science, 105, 145-153, 2012.

2980 Pälike, H., Lyle, M. W., Nishi, H., Raffi, I., Ridgwell, A., Gamage, K., Klaus, A., Acton, G.,

2981   Anderson, L., Backman, J., Baldauf, J., Beltran, C., Bohaty S. M., Bown, P., Busch, W.

2982   Channell, J. E. T., Chun, C. O. J., Delaney, M., Dewangan, P., Dunkley Jones, T., Edgar,

2983   K. M., Evans, H., Fitch, P. L., Foster, G. L., Gussone, N., Hasegawa, H., Hathorne, E. C.,

2984   Hayashi, H., Herrle, J. O., Holbourn, A., Hovan, S., Hyeong, K., Iijima, K., Ito, T.,

2985   Kamikuri, S., Kimoto, K., Kuroda, J., Leon-Rodriguez, L., Malinverno, A., Moore, T. C.,

2986   Brandon, H., Murphy, D. P., Nakamura, H., Ogane, K., Ohneiser, C. Richter, C.,

2987   Robinson, R., Rohling, E. J., Romero, O., Sawada, K., Scher, H., Schneider, L., Sluijs,

2988   A., Takata, H., Tian, J., Tsujimoto, A., Wade, B. S., Westerhold, T., Wilkens, R.,

2989   Williams, T., Wilson, P. A., Yamamoto, Y., Yamamoto, S., Yamazaki, T., and Zeebe, R.

2990   E.: Cenozoic record of the equatorial Pacific carbonate compensation depth, Nature, 488,

2991   609-614, doi: 10.1038/nature11360, 2012, 2012.

2992 Pearson P.N., Coxall H.K.: Origin of the Eocene planktonic foraminifer *Hantkenina* by

2993   gradual evolution, Palaeontology, 57, 243-267, 2014.

2994 Pearson, P. N., and Palmer, M. R.: Atmospheric carbon dioxide concentrations over the past

2995   60 million years, Nature, 406, 695-699, doi: 10.1038/35021000, 2000.

2996 Pearson, P. N., Shackleton, N.J., Hall, M.A.: Stable isotope paleoecology of middle Eocene

2997   planktonic foraminifera and multi-species isotope stratigraphy, DSDP Site 523, south

2998   Atlantic, J. Foram. Res., 23, 123-140, 1993.

2999 Pearson, P.N., Ditchfield, P.W, Singano, J., Harcourt-Brown, K.G., Nicholas, C.J., Olsson,

3000   R.K, Shackleton, N.J., Hall, M.A.: Warm tropical sea surface temperatures in the Late

3001   Cretaceous and Eocene epochs, Nature, 413, 481-487, 2001. doi:10.1038/35097000,

3002   2001.

3003 Pearson, P. N., Olsson, R. K., Huber, B. T., Hemleben, C., and Berggren, W.A. (Eds.): Atlas

3004   of Eocene planktonic foraminifera, Cushman Found. Foram. Res., Spec. Publ., 41, 1-514,

3005   2006.

3006 Pearson, P. N., Van Dongen, B. E., Nicholas, C. J., Pancost, R. D., Schouten, S., Singano, J.

3007   M. and Wade, B. S.: Stable warm tropical climate through the Eocene Epoch, Geology,

3008   35, 211-214, 2007.

3009 Petrizzo, M.R.: The onset of the Paleocene–Eocene Thermal Maximum (PETM) at Sites 1209

3010   and 1210 (Shatsky Rise, Pacific Ocean) as recorded by planktonic foraminifera, Mar.

3011   Micropaleont., 63, 187–200, 2007.

3012 Petrizzo, M.-R., Leoni, G., Speijer, R. P., De Bernardi, B., and Felletti, F.: Dissolution

3013   susceptibility of some Paleogene planktonic foraminifera from ODP Site 1209 (Shatsky

3014   Rise, Pacific Ocean), J. Foram. Res. 38, 357-371, 2008.

3015 Pross, J., Contreras, L., Bijl, P. K., Greenwood, D. R., Bohaty, S. M., Schouten, S., Bendle J.

3016   A., Röhl, U., Tauxe, L., Raine, J. I., Claire E., Huck, C. E., van de Flierdt, T., Stewart S.

R. Jamieson, S. S. R., Stickley, C. E., van de Schootbrugge, B., Escutia, C., and Brinkhuis, H.: Persistent near-tropical warmth on the Antarctic continent during the early Eocene Epoch: Nature, v. 488, 73-77, doi: 10 .1038 /nature11300, 2012.

Pujalte, V., Baceta, J. G., and Schmitz, B.: A massive input of coarse-grained siliciclastics in the Pyrenean Basin during the PETM: the missing ingredient of a coeval abrupt change in hydrological regime, Clim. Past, Climatic and biotic events of the Paleogene, Special issue, G. R. Dickens, V. Luciani, and A. Sluijs, (Eds.), 11, 1653-1672, doi:10.5194/cp-11-1653-2015, 2015.

Quillévéré, F., Norris, R. D., Moussa, I., and Berggren, W. A.: Role of photosymbiosis and biogeography in the diversification of early Paleogene acarininids (planktonic foraminifera), Paleobiology, 27, 311-326, 2001.

Raffi, I., and De Bernardi, B.: Response of calcareous nannofossils to the Paleocene-Eocene Thermal Maximum: observations on composition, preservation and calcification in sediments from ODP Site 1263 (Walvis Ridge-SW Atlantic). Mar. Micropaleont. 69, 119–138, 2008.

Raymo, M. E., and Ruddiman W. F.: Tectonic forcing of late Cenozoic climate, Nature, 359, 117-122, 1992.

Reghellin, D., Coxall, H. K., Dickens, G. R., and Backman, J.: Carbon and oxygen isotopes of bulk carbonate in sediment deposited beneath the eastern equatorial Pacific over the last 8 million years. Paleoceanography, 30: 1261-1286. doi: 10.1002/2015PA002825, 2015.

Röhl, U., Westerhold, T., Monechi, S., Thomas, E., Zachos, J. C., and Donner, B.: The third and final early Eocene Thermal Maximum: characteristics, timing, and mechanisms of the "X" event, Geol. Soc. Am. Abstracts with Program, 37(7), 264, 2005.

Schlanger, S.O. and Douglas, R.G.: The pelagic ooze-chalk-limestone transition and its implications for marine stratigraphy, In: Pelagic Sediments: on Land and under the Sea, K.J. Hsü and H.C. Jenkyns (Eds.), Spec. Publs. Ass. Sediment., 1, 117–148, 1974.

Scholle, P. A., and Arthur, M. A.: Carbon isotope fluctuations in Cretaceous pelagic limestones: potential stratigraphic and petroleum exploration tool, American Association of Petroleum Geologists Bulletin, 64, 67-87, 1980.

Schmitz, B., and Puljate, V.: Abrupt increase in seasonal extreme precipitation at the Paleocene-Eocene boundary, Geology, 35, 215-218, 2007.

Schmidt, D. N., Thierstein, H. R., and Bollmann, J.: The evolutionary history of size variation of planktic foraminiferal assemblages in the Cenozoic, Palaeogeogr. Palaeoclimatol.

3051   Palaeoecol., 212, 159-180, doi: 10.1016/j.palaeo.2004.06.002, 2004.

3052   Scheibner, C., and Speijer, R.P.: Decline of coral reefs during the late Paleocene to early

3053   Eocene global warming, eEarth, 3, 19-26, www.electronic-earth.net/3/19/2008/, 2008.

3054   Schneider, L. J. Bralower, T. J., and Kump, L. J.: Response of nannoplankton to early Eocene

3055   ocean destratification, Palaeogeogr. Palaeoclimatol. Palaeoecol., 310, 152-162, 2011.

3056   Schrag, D. P., DePaolo, D. J., and Richter, F. M.: Reconstructing past sea surface

3057   temperatures: correcting for diagenesis of bulk marine carbonate, Geochim. Cosmochim.

3058   Ac., 59, 2265-2278, 1995.

3059   Schulte, P., Scheibner, C. and Speijer, R.C.: Fluvial discharge and sea-level changes

3060   controlling black shale deposition during the Paleocene–Eocene Thermal Maximum in

3061   the Dababiya Quarry section, Egypt, Chem. Geol., 285, 167-183,

3062   doi:10.1016/j.chemgeo.2011.04.004, 2011.

3063   Schmitz, B., Speijer, R. P., and Aubry M.-P.: Latest Paleocene benthic extinction event on

3064   the southern Tethyan shelf (Egypt): Foraminiferal stable isotopic (δ^{13}C, δ^{18}O) records,

3065   Geology, 24, 347-350, 1996.

3066   Self-Trail, J. M., Powars, D. S., Watkins, D. K., Wandless, G. A.: Calcareous nannofossil

3067   assemblage changes across the Paleocene–Eocene Thermal Maximum: Evidence from a

3068   shelf setting, Mar. Micropaleont., 92–93, 61–80, 2012.

3069   Sexton, P.F., Wilson, P.A., Norris, R.D.: Testing the Cenozoic multisite composite δ^{18}O and

3070 δ^{13}C curves: New monospecific Eocene records from a single locality, Demerara Rise

3071   (Ocean Drilling Program Leg 207), Paleoceanography, 21, PA2019, 2006.

3072   Sexton, P. F., Norris R. D., Wilson, P. A., Pälike, H., Westerhold, T., Röhl, U., Bolton, C. T.,

3073   and Gibbs, S.: Eocene global warming events driven by ventilation of oceanic dissolved

3074   organic carbon, Nature 471, 349-353, doi: 10.1038/nature09826, 2011.

3075   Shackleton, N. J.: Paleogene stable isotope events. Palaeogeogr. Palaeoclim. Palaeoecol., 57,

3076   91-102, 1986.

3077   Shackleton, N. J., and Hall, M. A.: Stable isotope records in bulk sediments (Leg 138), Proc.

3078   Ocean Drill. Progr. Sci. Results, 138, 797-805, doi:10.2973/odp.proc.sr.138.150.1995.

3079   Shamrock, J. L., Watkins, D. K., and Johnston, K. W.: Eocene bio-geochronology of ODP

3080   Leg 122 Hole 762C, Exmouth Plateau (northwest Australian Shelf), Stratigraphy, 9, 55-

3081   76, 2012.

3082   Shipboard Scientific Party, 1985, Site 577: Initial Reports Deep Sea Drilling Project, 86, in:

3083   Heath, G.R., Burckle, L.H., et al. (Eds.), Washington (U.S. Government Printing Office),

3084   91–137. doi:10.2973/dsdp.proc.86.104.1985, 1995.

3085 Shipboard Scientific Party, 1998, Site 1051: Proceeding Ocean Drilling Program, Initial

3086   Reports, 171B, in: Norris, R.D., Kroon, D., Klaus, A., et al (Eds.), Ocean Drilling

3087   Program, College Station, TX, 171–239. doi:10.2973/odp.proc.ir.171b.105.1998, 1998.

3088 Sims, P. A., Mann, D. G., and Medlin, L. K.: Evolution of the diatoms: insights from fossil,

3089   biological and molecular data, Phycologia, 45, 361-402, 2006.

3090 Sinton, C. W., and Duncan R. A.: ^{40}Ar-^{39}Ar ages of lavas from the southeast Greenland

3091   margin, ODP Leg 152, and the Rockall Plateau, DSDP Leg 81, Ocean Drill. Progr., Sci.

3092   Res., 152, 387-402, doi:10.2973/odp.proc.sr.152.234.1998, 1998.

3093 Slotnick, B. S., Dickens, G. R., Nicolo, M. J., Hollis, C. J., Crampton, J. S., Zachos, J. C., and

3094   Sluijs, A.: Large-amplitude variations in carbon cycling and terrestrial weathering during

3095   the latest Paleocene and earliest Eocene: The Record at Mead Stream, New Zealand, J.

3096   Geol., 120, 487-505, 2012.

3097 Slotnick, B. S., Dickens, G. R., Hollis, C. J., Crampton, J. S., Percy Strong, C., and Zachos, J.

3098   C.: Extending lithologic and stable carbon isotope records at Mead Stream (New

3099   Zealand) through the middle Eocene, in: Dickens G.R., Luciani V. eds. Climatic and

3100   biotic events of the Paleogene 2014 CBEP 2014 Volume 31, Roma, Società Geologica

3101   Italiana, 201-202, 2014.

3102 Slotnick, B. S., Dickens, G. R., Hollis, C. J., Crampton, J. S., Strong, P. S. and Phillips, A.:

3103   The onset of the Early Eocene Climatic Optimum at Branch Stream, Clarence River

3104   valley, New Zealand, New Zeal. J. Geol. Geop., doi: 10.1080/00288306.2015.1063514,

3105   2015a.

3106 Slotnick, B. S., Laurentano, V., Backman, J., Dickens, G. R., Sluijs, A., and Lourens, L.:

3107   Early Paleogene variations in the calcite compensation depth: new constraints using old

3108   borehole sediments from across Ninetyeast Ridge, central Indian Ocean, Clim. Past, 11,

3109   472-493, 2015b.

3110 Sluijs, A., and Dickens, G. R.: Assessing offsets between the δ^{13}C of sedimentary

3111   components and the global exogenic carbon pool across early Paleogene carbon cycle

3112   perturbations, Global Biogeochem. Cy., 26 (4), GB4019, doi: 10.1029/2011GB004094,

3113   2012.

3114 Sluijs, A., Schouten, S., Pagani, M., Woltering, M., Brinkhuis, H., Sinninghe Damsté, J. S.,

3115   Dickens, G. R., Huber, M., Reichart, G., Stein, R., Matthiessen, J., Lourens, L. J.,

3116   Pedentchouk, N., Backman, J., Moran, K., and the Expedition 302 Scientists: Subtropical

3117   Arctic Ocean temperatures during the Palaeocene/Eocene thermal maximum, Nature,

3118   441, 610-613, doi: 10.1038/nature04668, 2006.

3119 Sluijs, A., Bowen, G. J., Brinkhuis, H., Lourens, L. J., and Thomas, E.: The Paleocene–

3120   Eocene thermal maximum super greenhouse: biotic and geochemical signatures, age

3121   models and mechanisms of global change, in: Deep-Time Perspectives on Climate

3122   Change, Williams, M., Haywood, A. M., Gregory, F. J., and Schmidt, D. N., (Eds.),

3123   Micropalaeont. Soc. Spec. Publ., Geological Society, London, 323-350, 2007.

3124 Smith, R. Y., Greenwood, D. R., and Basinger, J. F.: Estimating paleoatmospheric pCO_2

3125   during the Early Eocene Climatic Optimum from stomatal frequency of Ginkgo,

3126   Okanagan Highlands, British Columbia, Canada, Palaeogeogr. Palaeoclimatol.

3127   Palaeoecol., 293, 120-131, 2010.

3128 Stap, L., Sluijs, A., Thomas, E., and Lourens L. J.: Patterns and magnitude of deep sea

3129   carbonate dissolution during Eocene Thermal Maximum 2 and H2, Walvis Ridge,

3130   southeastern Atlantic Ocean, Paleoceanography, 24, 1211, doi: 10.1029/2008PA001655,

3131   2009.

3132 Thomas, E.: Biogeography of the late Paleocene benthic foraminiferal extinction, in: Late

3133   Paleocene-early Eocene climatic and biotic events in the marine and terrestrial Records,

3134   Aubry, M.-P., Lucas, S., and Berggren, W. A., (Eds.), Columbia University Press, New

3135   York, 214-243, 1998.

3136 Thomas, E., Brinkhuis, H., Huber, M., and Röhl, U.: An ocean view of the early Cenozoic

3137   Greenhouse world, Oceanography, 19, 94-103, 2006.

3138 Thunell R. C. and Honjo, S.: Calcite dissolution and the modification of planktonic

3139   foraminiferal assemblages, Mar. Micropaleont., 6, 169-182, 1981.

3140 Vandenberghe N., Hilgen F. J., Speijer R. P., Ogg J. G., Gradstein F. M., Hammer O., Hollis

3141   C. J., and Hooker J. J.: The Paleogene Period, in: Gradstein, F., Ogg, J.G., Schmitz,

3142   M.D., Ogg, G.M., (Eds.), The Geologic Time Scale 2012, 855-921, Elsevier,

3143   Amsterdam, 2012.

3144 Vincent, E., and Berger, W. H: Planktonic foraminifera and their use in paleoccanography;

3145   in: Emiliani. C (Ed.), The Sea, 7 (25), New York, 1025-1119, 1981.

3146 Vogt, P. R.: Global magmatic episodes: New evidence and implications for the steady state

3147   mid-oceanic ridge, Geology, 7, 93-98, 1979.

3148 Wade, B. S.: Planktonic foraminiferal biostratigraphy and mechanisms in the extinction of

3149   *Morozovella* in the late Middle Eocene, Mar. Micropaleont., 51, 23–38, 2004.

3150 Wade, B. S., Al-Sabouni, N., Hemleben, C., and Kroon, D.: Symbiont bleaching in fossil

3151   planktonic foraminifera, Evol. Ecol., 22, 253-265. doi: 10.1007/s10682-007-9176-6,

3152 2008.

Wade, B. S., Pearson, P. N., Berggren, and W. A., Pälike, H.: Review and revision of Cenozoic tropical planktonic foraminiferal biostratigraphy and calibration to the geomagnetic polarity and astronomical time scale, Earth Sci. Rev., 104, 111-142, doi: 10.1016/j.earscirev.2010.09.003, 2011.

Wade, B.S., Fucek, V.P., Kamikuri, S.-I., Bartol, M., Luciani, V., Pearson, P.N.: Successive extinctions of muricate planktonic foraminifera (*Morozovelloides* and *Acarinina*) as a candidate for marking the base Priabonian, Newsl. Stratigr., 45 (3) 245-262, 2012.

Westerhold, T., Röhl, U., Frederichs, T., Bohaty, S. M., and Zachos, J. C.: Astronomical calibration of the geological timescale: closing the middle Eocene gap, Clim. Past, 11, 1181–1195, doi: 10.5194/cp-11-1181-2015, 2015.

Wilf, P., Cúneo, R. N., Johnson, K. R., Hicks, J. F., Wing, S. L., and Obradovich, J. D.: High plant diversity in Eocene South America: evidence from Patagonia, Science, 300, 122-125, 2003.

Wing, S. L., Bown, T. M., and Obradovich, J. D.: Early Eocene biotic and climatic change in interior western North America, Geology 19, 1189-1192, 1991.

Woodbourne, M. O., Gunnell, G. F., and Stucky, R. K.: Climate directly influences Eocene mammal faunal dynamics in North America, P. Natl. Acad. Sci. USA, 106 (32), 13399-13403, 2009.

Yapp, C. J.: Fe(CO$_3$)OH in goethite from a mid-latitude North American Oxisol: Estimate of atmospheric CO$_2$ concentration in the early Eocene "climatic optimum". Geochim. Cosmochim. Ac., 68(5), 935-947. doi: 10.1016/j.gca.2003.09.002, 2004.

Yamaguchi, T., and Norris R. D.: Deep-sea ostracode turnovers through the Paleocene-Eocene thermal maximum in DSDP Site 401, Bay of Biscay, North Atlantic, Mar. Micropaleont., 86-87, 32-44, 2012.

Zachos, J. C., Pagani, M., Sloan, L., Thomas, E., and Billups, K.: Trends, rhythms, and aberrations in global climate 65 Ma to Present, Science, 292, 686-693, 2001.

Zachos, J. C., Röhl, U., Schellenberg, S. A., Sluijs, A., Hodell, D. A., Kelly, D. C., Thomas, E., Nicolo, M., Raffi, I., Lourens, L. J., McCarren, H., and Kroon, D.: Rapid acidification of the ocean during the Paleocene–Eocene thermal maximum, Science, 308, 1611-161, 2005.

Zachos, J. C., Dickens, G. R., and Zeebe, R. E.: An early Cenozoic perspective on greenhouse warming and carbon-cycle dynamics, Nature, 451, 279-283, 2008.

Zachos, J. C., McCarren, H., Murphy, B., Röhl, U., and Westerhold, T.: Tempo and scale of

3186   late Paleocene and early Eocene carbon isotope cycles: Implications for the origin of

3187   hyperthermals, Earth Planet. Sci. Lett., 299, 242-249, doi: 10.1016/j.epsl.2010.09.004,

3188   2010.

3189   Zeebe, R. E., Zachos, J. C., Dickens, G. R.: Carbon dioxide forcing alone insufficient to

3190   explain Palaeocene–Eocene Thermal Maximum warming. Nat. Geosci.2 (8), 576-580,

3191   http://dx.doi.org/10.1038/ngeo578, 2009.

3192   Zonneveld, J. P., Gunnell, G. F., and Bartels, W. S.: Early Eocene fossil vertebrates from the

3193   southwestern Green River Basin, Lincoln and Uinta Counties, Wyoming, Journal of

3194   Vertebrate Paleontology, 20, 369-386, 2000.

3195

3196   **Figure Captions**

3197

3198   **Figure 1.** ~~The~~ Evolution of climate, carbon cycling, and planktic foraminifera across the

3199   middle Paleogene on the GPTS 2012 time scale. ~~The~~ Left side shows polarity chrons, and

3200   smoothed oxygen and carbon isotope records of benthic foraminifera, slightly modified from

3201   Vandenberghe et al. (2012). ~~The~~ Original oxygen and carbon isotope values come from

3202   ~~numerous source~~ compilations by Zachos et al. (2008) and Cramer et al. (2009). ~~The~~ Middle

3203   of the figure indicates planktic foraminiferal biozones by ~~(~~Wade et al. ~~(~~2011), ~~and partly~~

3204   ~~modified by~~ ~~Luciani and Giusberti (2014)~~ with three modifications. The lower boundary for

3205   Zone E7a is now based on the first occurrence of *Astrorotalia palmerae* due to ~~diachronous~~

3206   diachroneity in the first appearance of the previously selected marker ~~A.~~ *Acarinina*

3207   *cuneicamerata* (Luciani and Giusberti, 2014). ~~In addition,~~ The base of Zone E5, identified by

3208   the first appearance of *Morozovella aragonensis,* occurs within the middle of C24n instead of

3209   lower C23r (see text). ~~We add a~~ A question marks the top of *Morozovella subbotinae* because

3210   ~~the present study highlights a remarkable diachronism of this event~~ there is diachroneity for

3211   this occurence (see text). ~~The~~ Right side ~~of the figure~~ shows a partial view of morozovellid

3212   and acarininid evolution as ~~suggested~~ envisioned by Pearson et al. (2006) and Aze et al.

3213   (2011). It does not include several "root taxa" that disappear in the earliest Eocene (e.g., *M.*

3214 *velascoensis*) or "excursion taxa" that appear during the Paleocene-Eocene Thermal

3215 Maximum (PETM) (e.g., *M. allisonensis*). Superimposed on these records are key intervals of

3216 climate change, including the Early Eocene Climatic Optimum (EECO), the Middle Eocene

3217 Climatic Optimum (MECO) and the three well documented early Eocene hyperthermal

3218 events. ~~The shown alignment of these records and~~ The extent of the EECO ~~are~~ is not precise,

3219 because of stratigraphic issues (see text). ~~Nevertheless, there appears a major switch from~~

3220 ~~morozovellids to acarininids at the species level, independent of abundance, sometime within~~

3221 ~~the EECO.~~ Red and blue triangles= top and base of the morozovellid and acarininid zonal

3222 markers.

3223

3224

3225 **Figure 2.** Approximate locations ~~for~~ of the three sites discussed in this work during the early

3226 Eocene. Also shown is Site 1258, which has a bulk carbonate $\delta^{13}C$ record spanning the

3227 EECO. Base map is from http://www.odsn/de/services/paleomap.html.

3228

3229 **Figure 3**. The Possagno section. ~~in northeast Italy when sampled in the Carcoselle quarry~~

3230 ~~between Summer 2002 and Spring 2003 (Photo by Luca Giusberti, Summer 2002).~~ ~~Lower~~

3231 ~~panel shows the then exposed quarry face.~~ Upper panel ~~shows the~~: geological map (modified

3232 from Braga, 1970). 1 = Quaternary deposits; 2, 3 = Calcarenite di Castelcucco (Miocene); 4 =

3233 glauconitic arenites (Miocene); 5 = siltstones and conglomerates (upper Oligocene-lower

3234 Miocene); 6 = Upper Marna di Possagno (upper Eocene); 7 = Formazione di Pradelgiglio

3235 (upper Eocene); 8 = Marna di Possagno (upper Eocene); 9 = Scaglia Cinerea (middle-upper

3236 Eocene); 10 = Scaglia Rossa (upper Cretaceous-lower Eocene); 11 = faults; 12 = traces of

3237 stratigraphic sections originally studied by Bolli (1975); red circle = the Carcoselle quarry.

3238 Lower panel: the exposed quarry face during Summer 2002 (Photo by Luca Giusberti). ~~The~~

3239 ~~outcrop sampled in 2003 was located very close to the outcrops sampled in the sixties (dotted~~

3240 ~~red circle).~~

3241

3242 **Figure 4.** Lithology, stratigraphy, and bulk sediment stable-isotope composition of the

3243 Possagno section aligned according to depth. Lithololologic key: 1 = limestone; 2 = marly

3244 limestone and calcareous marl; 3 = cyclical marl-limestone alternations, 4 = marl; 5= Clay

3245 Marl unit (CMU). Planktic foraminiferal biozones follow those of Wade et al. (2011), as

3246 modified by Luciani and Giusberti (2014). Magnetostratigraphy and key calcareous

3247 nannofossil events come from Agnini et al. (2006); NP-zonation is from Martini (1971).

3248 Nannofossil events are shown as red triangles (tops), blue triangles (bases), and purple

3249 diamonds (evolutionary crossovers); *S. rad*. = *Sphenolithus radians*; T.c./T.o. = *Tribrachiatus*

3250 *contortus/ Tribrachiatus orthostylus; D. lod*. = *Discoaster lodoensis*; Tow. =*Toweius*; *T. orth*.

3251 = *Tribrachiatus orthostylus*; *D. sublod*. = *Discoaster sublodoensis*. ~~The~~ Stable isotope

3252 records ~~come from~~ determined in this study. Established early Eocene "events" are

3253 superimposed in light red; suggested carbon isotope excursions (CIEs) within the EECO are

3254 shown with numbers. ~~1= Limestone, 2= Marly limestones and calcareous marls, 3= cyclical~~

3255 ~~marl-limestone alternations, 4= Marls, 5=Clay marly units (CMU).~~

3256

3257 **Figure 5.** Cores, stratigraphy, and bulk sediment stable isotope composition for the early

3258 Eocene interval at Deep-Sea Drilling Project (DSDP) Site 577 aligned according to

3259 composite depth (Dickens and Backman, 2013). Note the increased length for the gap

3260 between Core 577*-8H and Core 577*-9H (see text). The Wade et al. (2011) E-zonation,

3261 partly modified by Luciani and Giusberti (2014), has been applied to Site 577 ~~on the basis of~~

3262 ~~the events recorded~~ given assemblages presented by Lu (1995) and Lu and Keller (1995).

3263 Note that: (a) the base of Zone E3 ~~has been positioned at the~~ (top of *Morozovella*

velascoensis) lies within a core gap~~; even though this event is uncertain due to the lowest~~

~~core gap. The lowest occurrence of *Morozovella formosa* occurs within C24r in agreement~~

~~with Wade et al. (2011) and defines the E3/E4 zonal boundary.~~ (b) the E4/E5 zonal boundary

(base of M. *aragonensis*) occurs within C24n, in agreement with Luciani and Giusberti

(2014); ~~and The base of M. *aragonensis*, defining the E4/E5 zonal boundary, is recorded~~

~~within C24n.~~ (c) the E5/E6 zonal boundary is problematic because the top of *M. subbotinae*

occurs in middle C24n, much earlier than the presumed disappearance in the upper part of

C23n ~~The boundary between Zones E5 and E6 cannot be placed by means of the *M.*~~

~~*subbotinae* top because this species disappears (at Site 577) much earlier with respect to the~~

~~expected C23n top~~ (Wade et al., 2011). ~~i.e., in middle C24n, even below the base of *M.*~~

~~*aragonensis*. Our new interpretation of the magnetostratigraphy at Site 1051, based on~~

~~calcareous nannofossil events (see text), substantiates the significant diachrony of this~~

~~biohorizon.~~ We have therefore positioned~~, at Site 577,~~ the E5/E6 boundary ~~upper boundary of~~

~~Zone E5~~ at the lowest occurrence of *Acarinina aspensis,* according to the original definition

of Zone E5 ~~by~~ (Berggren and Pearson, 2005); (d) we cannot differentiate between Zone E6

and Zone E7a ~~D~~due to the absence of *Astrorotalia palmerae* ~~at Site 577~~ and to the

diachronous appearance of *A. cuneicametrata* ~~base~~ (Luciani and Giusberti, 2014).

~~Cores are aligned following Dickens and Backman (2013), with an increased gap between~~

~~Core 577*-8H and Core 577*-9H (see text).~~ Magnetostratigraphy and key calcareous

nannofossil events are those summarized by Dickens and Backman (2013). For the latter and

beyond that noted for **Figure 4**: *F.* spp.= *Fasciculithus spp.*; *D. dia.= Discoaster diastypus*;

~~T.c./T.o.= Tribrachiatus contortus/ Tribrachiatus orthostylus; D. lod.= Discoaster lodoensis;~~

~~T. orth.= Tribrachiatus orthostylus; D. sublod.= Discoaster sublodoensis.~~ The stable isotope

records: ~~come from~~ black – Cramer et al. (2003), ~~and~~ red and blue – this study. ~~Established~~

~~E~~arly Eocene "events" are the same as those in **Figure 4**. ~~are superimposed in light red;~~

suggested carbon isotope excursions (CIEs) following the "L event" (yellow band) are shown with numbers.

Figure 6. The Possagno section and its δ^{13}C record (**Figure 4**) with measured relative abundances of primary planktic foraminiferal genera, fragmentation index (*F* index) and coarse fraction. The subbotinid abundance includes both *Subbotina* and *Parasubbotina* genera. Note that a significant increase in *Acarinina* abundance marks the EECO and several carbon isotope excursions (CIEs). before and after it are marked by a significant increase in *Acarinina* abundance.. Note also the major decline in abundance of *Morozovella* at the start of the EECO. Filled yellow circles hexagons show occurrences of abundant radiolarians. Lithological symbols and early Eocene "events" are the same as those in **Figure 4**.

Figure 7. The early Eocene succession at DSDP Site 577 and its δ^{13}C record (**Figure 5**) with measured relative abundances of primary planktic foraminiferal genera (Lu, 1995; Lu and Keller, 1995). The Wade et al. (2011) E-zonation, partly modified by Luciani and Giusberti (2014), has been applied to Site 577 on the basis of the events recorded by Lu (1995) and Lu and Keller (1995). F. spp.= Fasciculithus spp.; D. dia.= Discoaster diastypus; T.c./T.o.= Tribrachiatus contortus/ Tribrachiatus orthostylus; D. lod.= Discoaster lodoensis; T. orth.= Tribrachiatus orthostylus; D. sublod.= Discoaster sublodoensis. Suggested carbon isotope excursions (CIEs) following the "L event" are shown with numbers. The subbotinid abundance includes both *Subbotina* and *Parasubbotina* genera. Note also that the major switch in *Morozovella* and *Acarinina* abundances approximately coincides with the J-event, the top of polarity chron C24n, and the start of the EECO. Early Eocene "events" are the same as those in **Figure 4**.

3314 **Figure 8.** ~~Lithlogy,~~ Stratigraphy, bulk sediment δ^{13}C composition, relative abundances of

3315 primary planktic foraminiferal genera, and fragmentation index (*F* index) for the early

3316 Eocene interval at ODP Site 1051. ~~The~~ Planktic foraminiferal biozones follow those of Wade

3317 et al. (2011), as modified by Luciani and Giusberti (2014; see **Figure 1** caption).

3318 Magnetostratigraphy and positions of key calcareous nannofossil events come from Ogg and

3319 Bardot (2001) and Mita (2001), but with an important modification to polarity chron labelling

3320 (see text and Cramer et al., 2003~~). S. rad.= Sphenolithus radians; D. lod.= Discoaster~~

3321 ~~lodoensis; Tow.= Toweius; T. orth.= Tribrachiatus orthostylus; D.sub.= Discoaster~~

3322 ~~sublodoensis.~~ Calcareous nannofossil horizons are the same as in previous figures.

3323 Foraminferal information comes from this study~~,~~ ; subbotinids include both *Subbotina* and

3324 *Parasubbotina*.

3325 Early Eocene "events" are the same as those in **Figure 4**.

3326

3327 **Figure 9.** Carbon isotope and paleomagnetic records across the early Eocene for the

3328 Possagno section, DSDP Site 577, and ODP Site 1258 (Kirtland-Turner et al., 2014). This

3329 highlights the overall framework of carbon cycling in the early Eocene, but also stratigraphic

3330 problems across the EECO at each of the three sites. At Possagno, the coarse resolution of

3331 δ^{13}C records and the condensed interval makes correlations difficult. At ODP Site 1258, ~~the~~

3332 ~~entire record is compressed in the depth domain~~ the prominent K/X event seems missing. At

3333 DSDP Site 577, the entire record is compressed in the depth domain. Nonetheless, a major

3334 shift in frequency and amplitude of carbon isotope excursions (CIEs) appears to have

3335 happened during the EECO. ~~Suggested~~ ~~Carbon isotope excursions~~ CIEs that suggestively

3336 ~~probably~~ correlate within the EECO are shown with numbers.

3337

3338 **Figure 10.** ~~Abundance patterns of primary planktic foraminiferal taxa from the Farra section,~~

3339 ~~cropping out 50 km NE of Possagno, plotted against bulk sediment δ^{13}C, CaCO₃ content, *F*~~

3340 ~~index and magnetostratigraphy.~~ Records of magnetostratigraphy, bulk sediment δ^{13}C, CaCO₃

3341 content, *F* index and abundance patterns for primary planktic foraminiferal taxa at the Farra

3342 section, which crops out 50 km NE of Possagno. ~~The *Subbotina* group includes besides~~

3343 ~~*Subbotina* the genera *Parasubbotina* and *Globorotaloides*, that constitute the minor~~

3344 ~~components of this group.~~ All data are from Agnini et al. (2009). Note that the switch in

3345 abundance between *Morozovella* and *Acarinina* occurs close the "J event".

3346

3347 **Figure 11**. ~~The~~ Records of ~~warm-indices symbiont-bearing~~ morozovellids and large

3348 acarininids (>200 micron) in the western Tethyan setting from the Possagno section (~~below,~~

3349 this paper) and the Alano section (Luciani et al., 2010), plotted with generalized δ^{13}C and

3350 δ^{18}O curves for benthic foraminiferal on the GTS2012 time scale (as summarized by

3351 Vandenberghe et al., 2012; slightly modified). ~~The original oxygen and carbon isotopic~~

3352 ~~values from Cramer et al. (2009) are recalibrated to GTS2012 (Vandenberghe et al., 2012).~~

3353 ~~The Tethyan~~ These records suggest that the long-lasting EECO and MECO intervals of

3354 anomalous ~~intense~~ warmth mark two main steps in the decline of morozovellids and

3355 acarininids. ~~within this group of important early Paleogene calcifiers, which almost~~

3356 ~~completely disappeared at about 38 Ma, near the Bartonian/Priabonian boundary (Agnini et~~

3357 ~~al., 2011; Luciani et al., 2010; Wade, 2004; Wade et al., 2012).~~ ~~E-Zones~~ The planktic

3358 foraminferal biozones follow those presented by Wade et al. (2011), as partly modified by

3359 Luciani and Giusberti (2014).

3360

3361 **Supplementary material**

3362

3363 **Table S1**. Carbon and oxygen isotopes from the Possagno section.

3364

3365   **Table S2**. Carbon and oxygen isotopes from DSDP Site 577.

3366

3367   **Table S3**. Foraminiferal abundances, fragmentation index (%) and coarse fraction (%) from

3368   the Possagno section.

3369

3370   **Table S4**. Foraminiferal abundances from DSDP Site 577.

3371

3372   **Table S5**. Foraminiferal abundances from ODP Site 1051.

3373

3374   **Figure S1.** The Possagno δ^{13}C data and relative abundance of minor planktic foraminiferal

3375   genera and selected species plotted against lithology and fragmentation index (*F* index) data.

3376   Magnetostratigraphy is from Agnini et al. (2006). ~~The biozonal scheme is from Wade et al.~~

3377   ~~(2011), modified by Luciani and Giusberti (2014).~~ The planktic foraminferal biozonal

3378   scheme is from Wade et al. (2011), as modified by Luciani and Giusberti (2014). ~~Established~~

3379   ~~early Eocene "events" are superimposed in light red; suggested carbon isotope excursions~~

3380   ~~(CIEs) within the EECO are shown with numbers. Lithological~~ Various symbols are the same

3381   as in **Figure 4**.

3382

3383   **Appendix A: Taxonomic list of planktic ~~forainiferal~~ foraminiferal species cited in text**

3384   **and figures**

3385

3386   *Globanomalina australiformis* (Jenkins, 1965)

3387   *Morozovella aequa* (Cushman and Renz, 1942)

3388   *Morozovella gracilis* (Bolli, 1957)

3389   *Morozovella lensiformis* (Subbotina, 1953)*,*

3390   *Morozovella marginodentata* (Subbotina, 1953)

3391   *Morozovella subbotinae* (Morozova, 1939)

3392   *Parasubbotina eoclava* Coxall*,* Huber and Pearson, 2003

3393   *Parasubbotina griffinae* (Blow, 1979)

3394   *Parasubbotina pseudowilsoni* Olsson and Pearson, 2006

3395   *Subbotina corpulenta* (Subbotina, 1953)

3396   *Subbotina eocena* (Gümbel, 1868)

3397   *Subbotina hagni* (Gohrbandt, 1967)

3398   *Subbotina senni* (Beckmann, 1953)

3399   *Subbotina yeguanesis* (Weinzierl and Applin, 1929*)*

3400   *Planoglobanomalina pseudoalgeriana* Olsson & and Hemleben, 2006

3401

3402   **Appendix B: Taxonomic list of calcareous nannofossil taxa cited in text and figures**

3403

3404   *Discoaster diastypus* Bramlette and Sullivan, 1961

3405   *Discoaster lodoensis* Bramlette and Sullivan, 1961

3406   *Discoaster sublodoensis* Bramlette and Sullivan, 1961

3407   *Fasciculithus* Bramlette and Sullivan, 1961

3408   *Fasciculithus tympaniformis* Hay and Mohler in Hay et al., 1967

3409   *Sphenolithus radians* Deflandre in Grassé, 1952

3410   *Toweius* Hay and Mohler, 1967

3411   *Tribrachiatus contortus* (Stradner, 1958) Bukry, 1972

3412   *Tribrachiatus orthostylus* (Bramlette and Riedel, 1954) Shamrai, 1963

3413

Figure 1
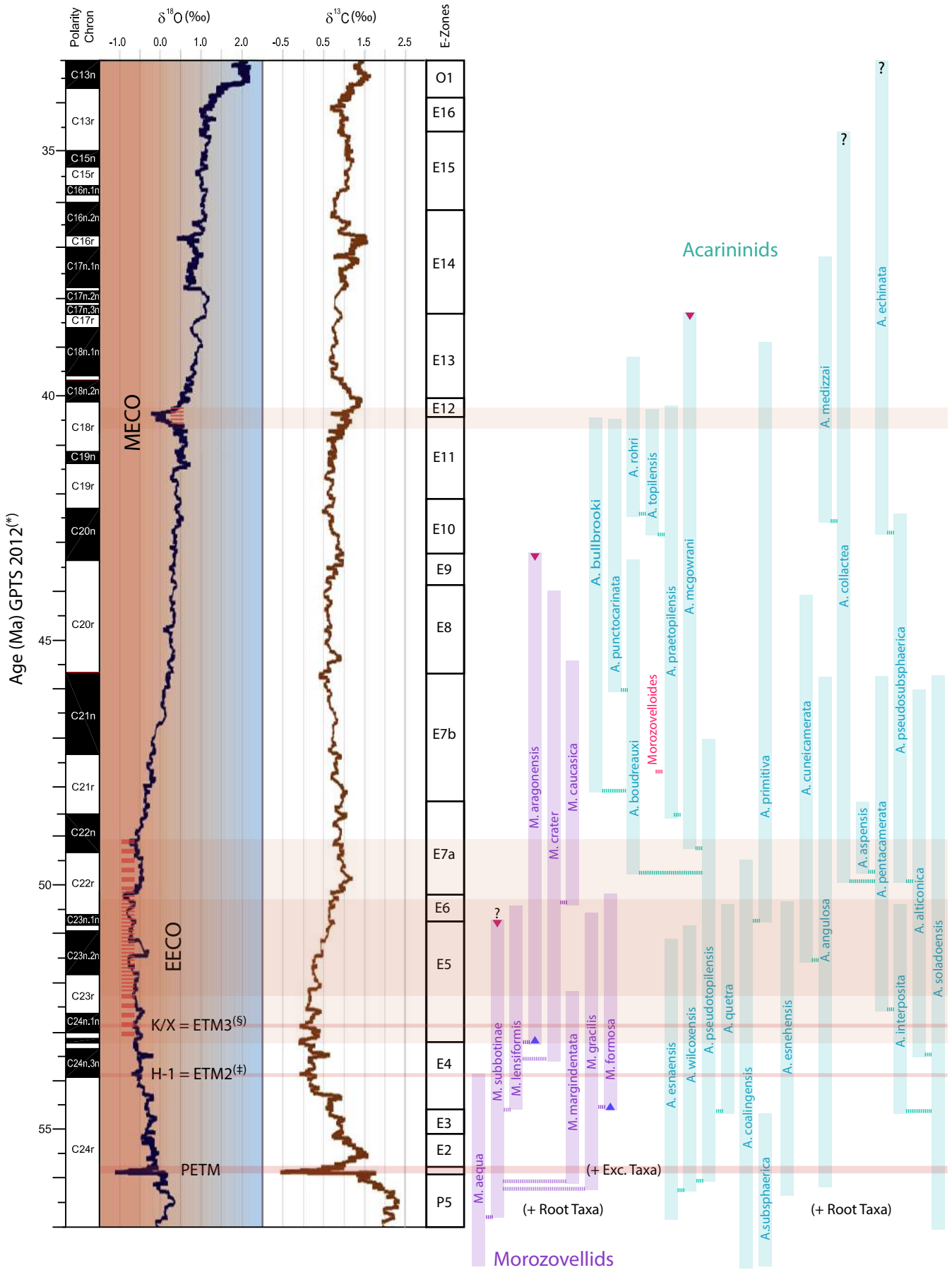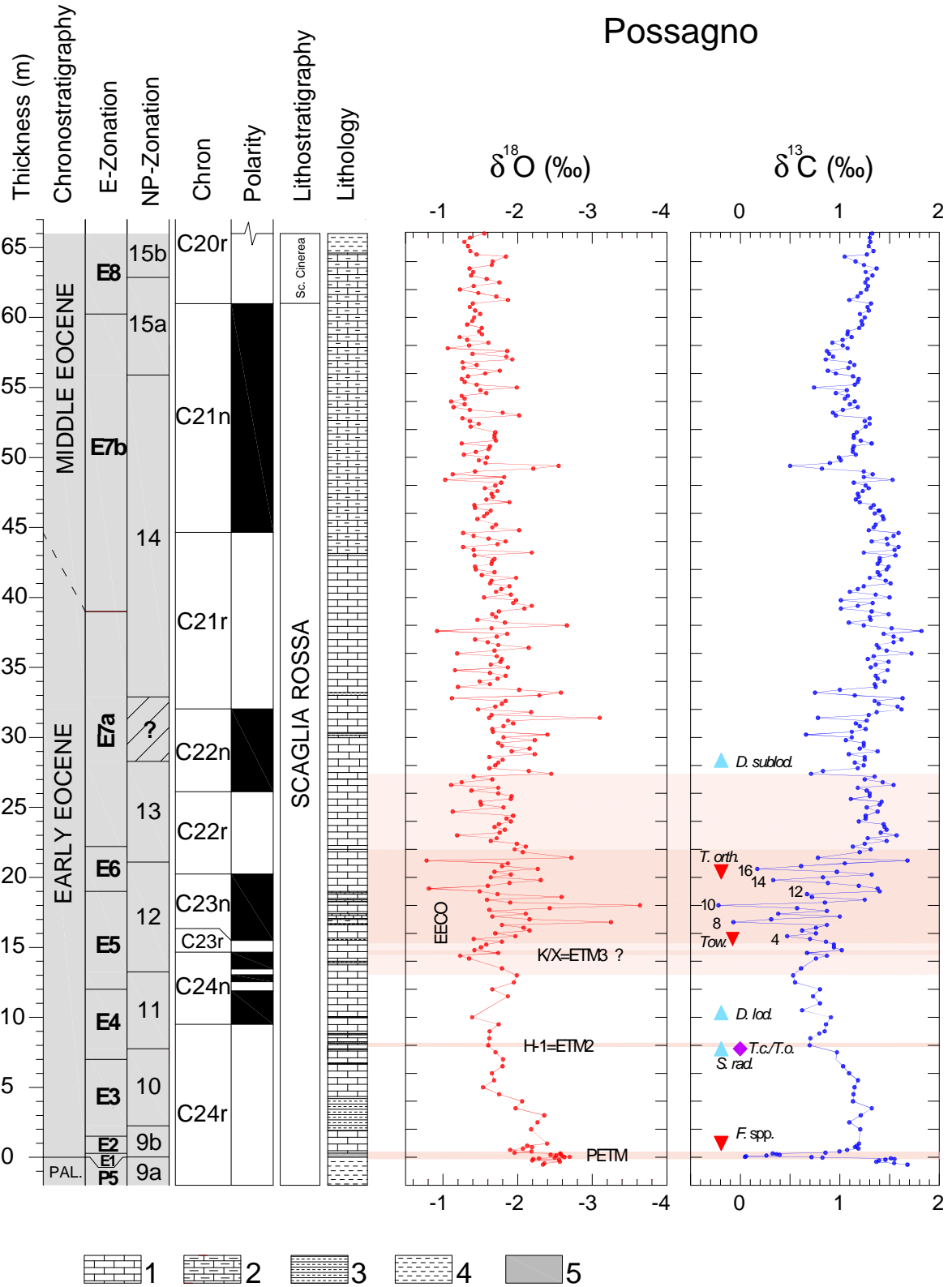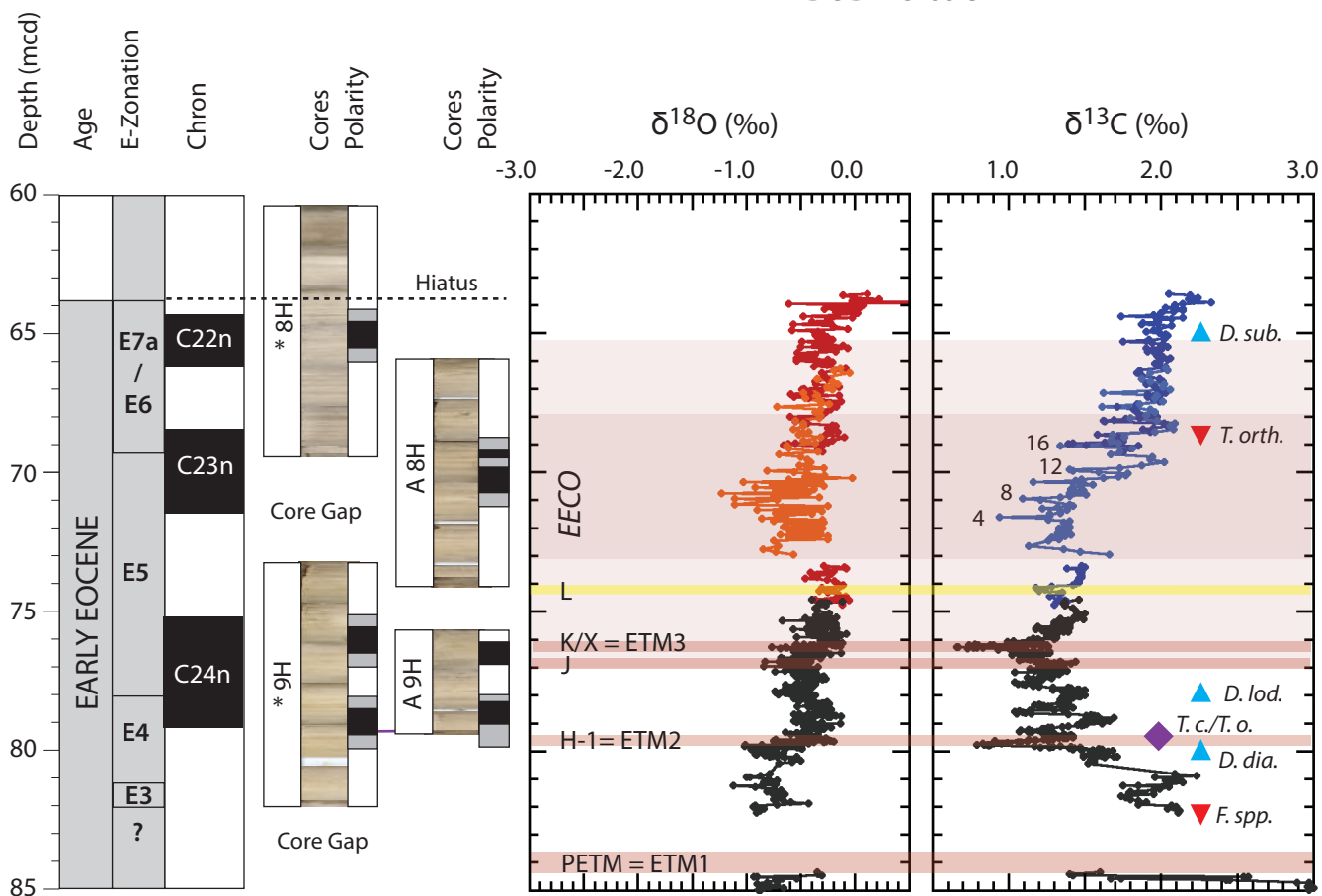
Figure 2
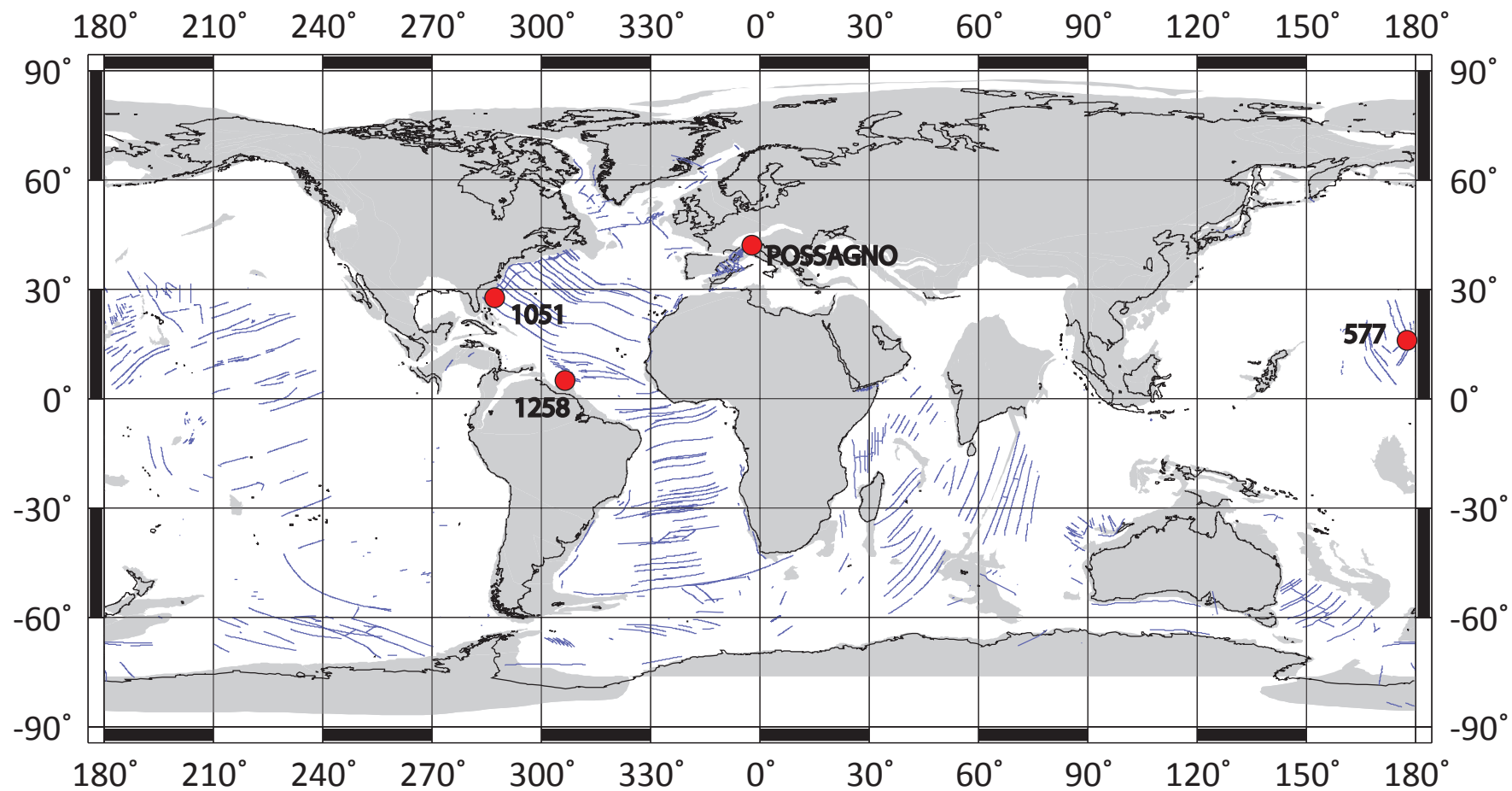
50 Ma Reconstruction
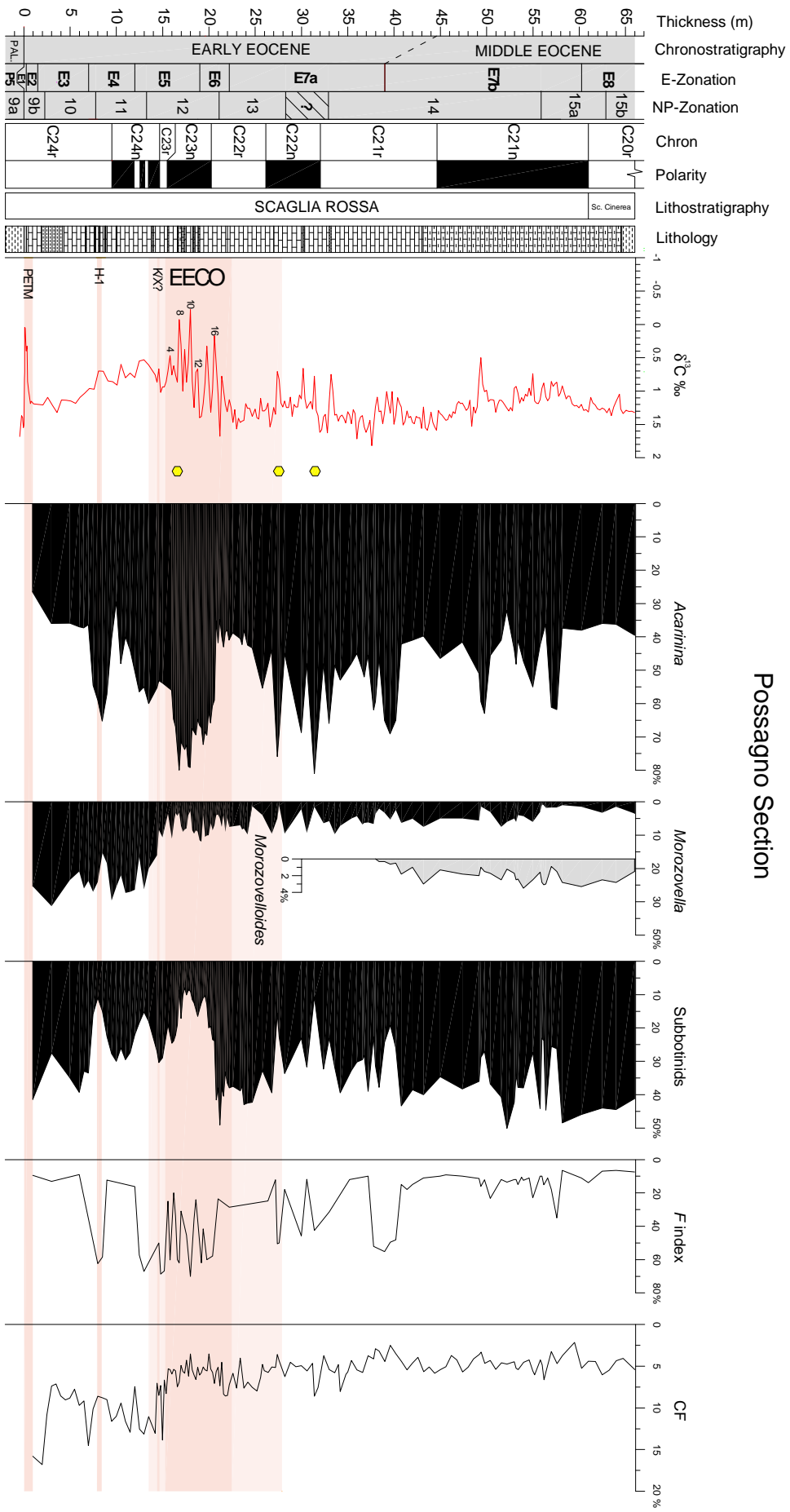
Figure 3
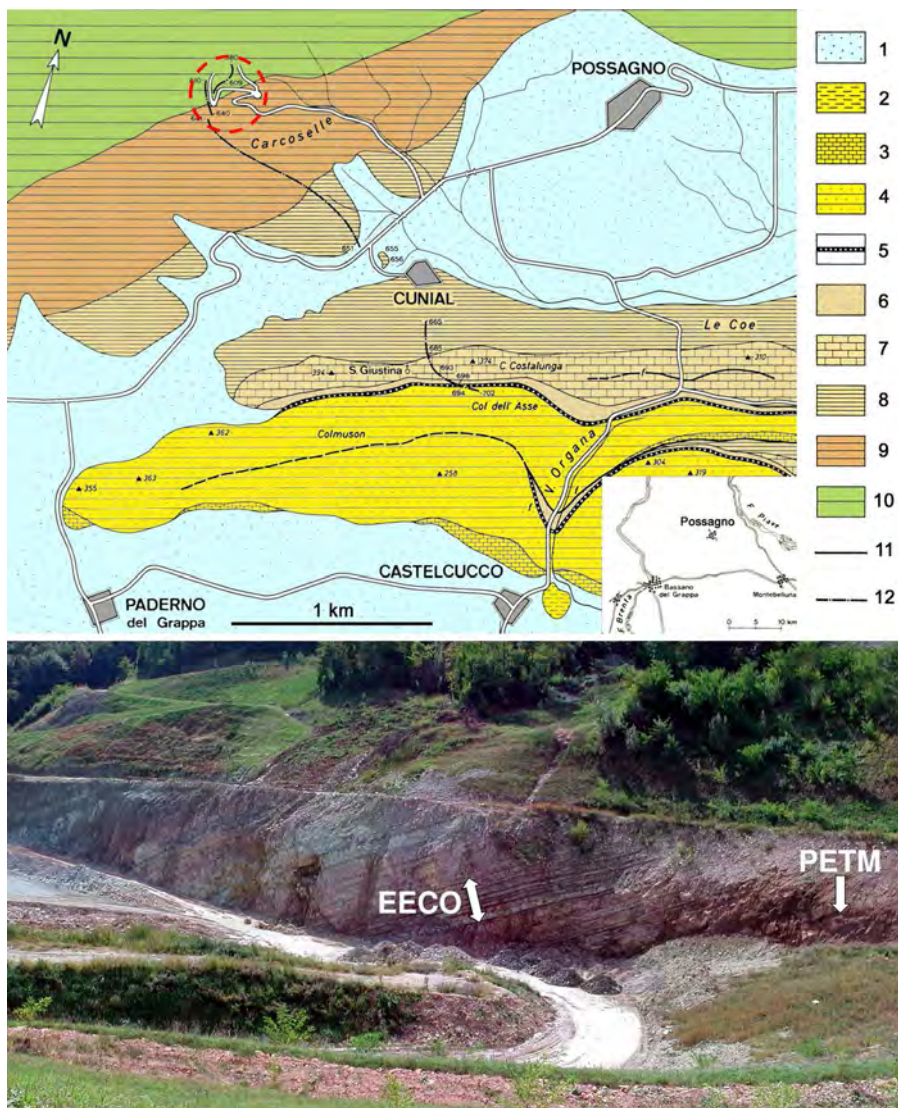
Figure 4

Figure 5

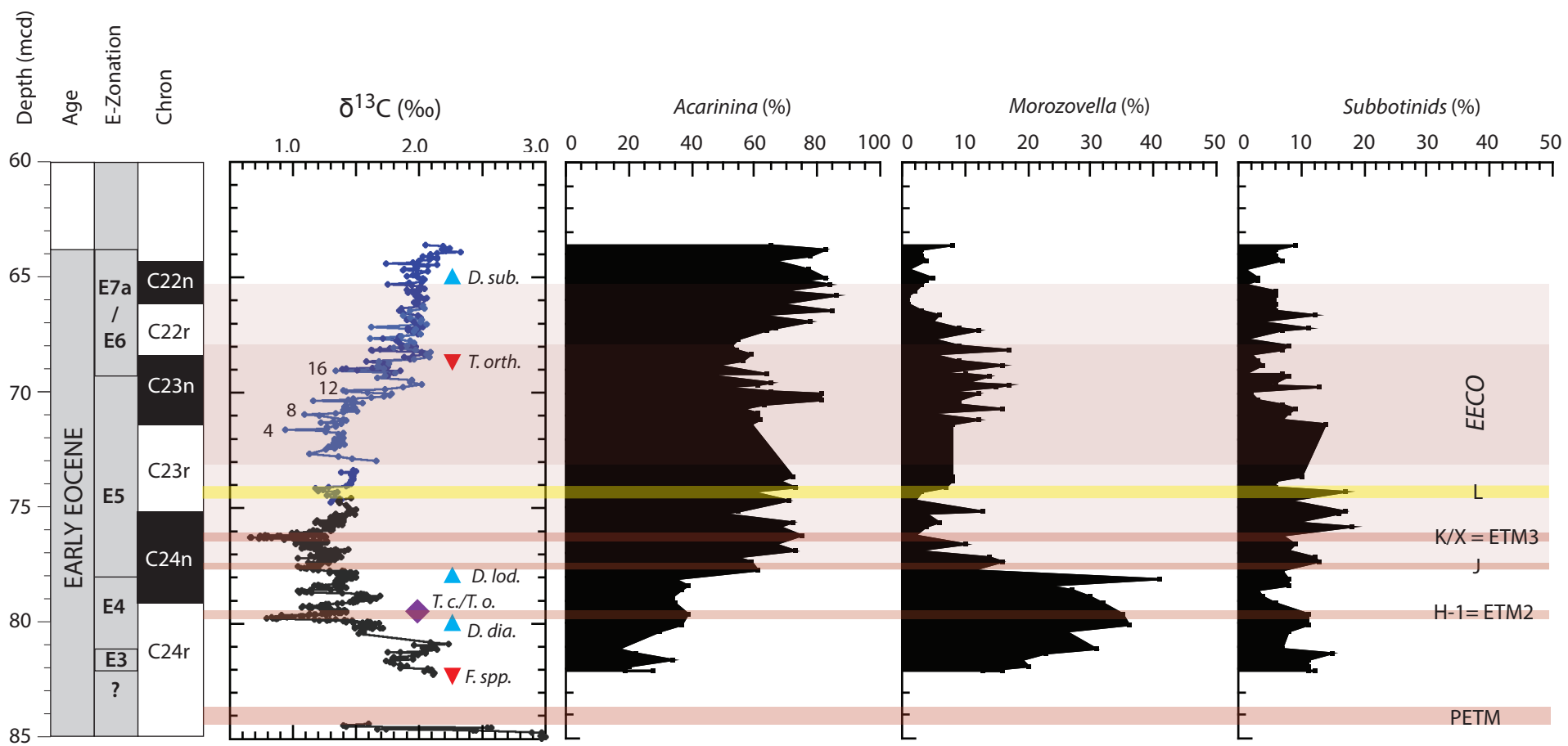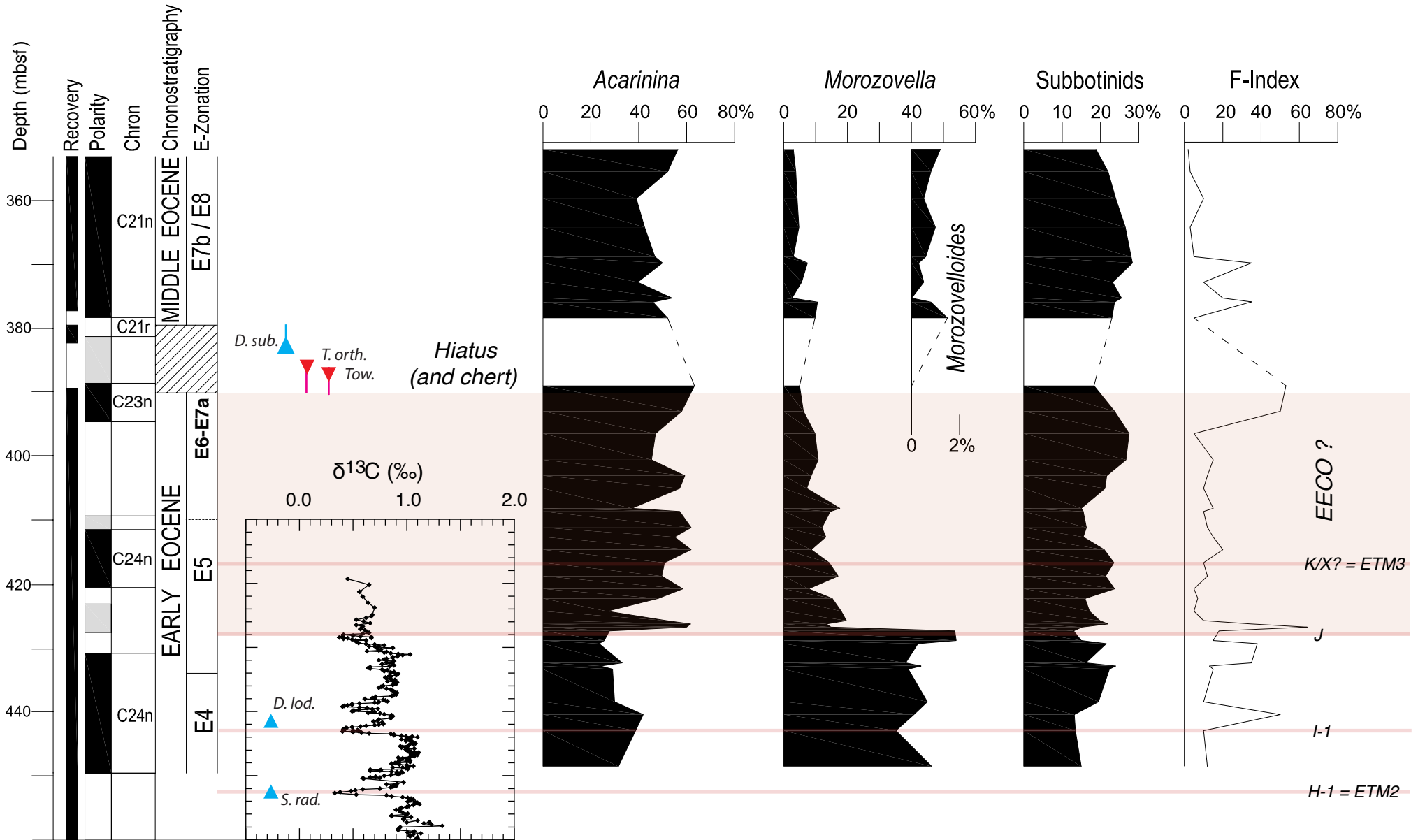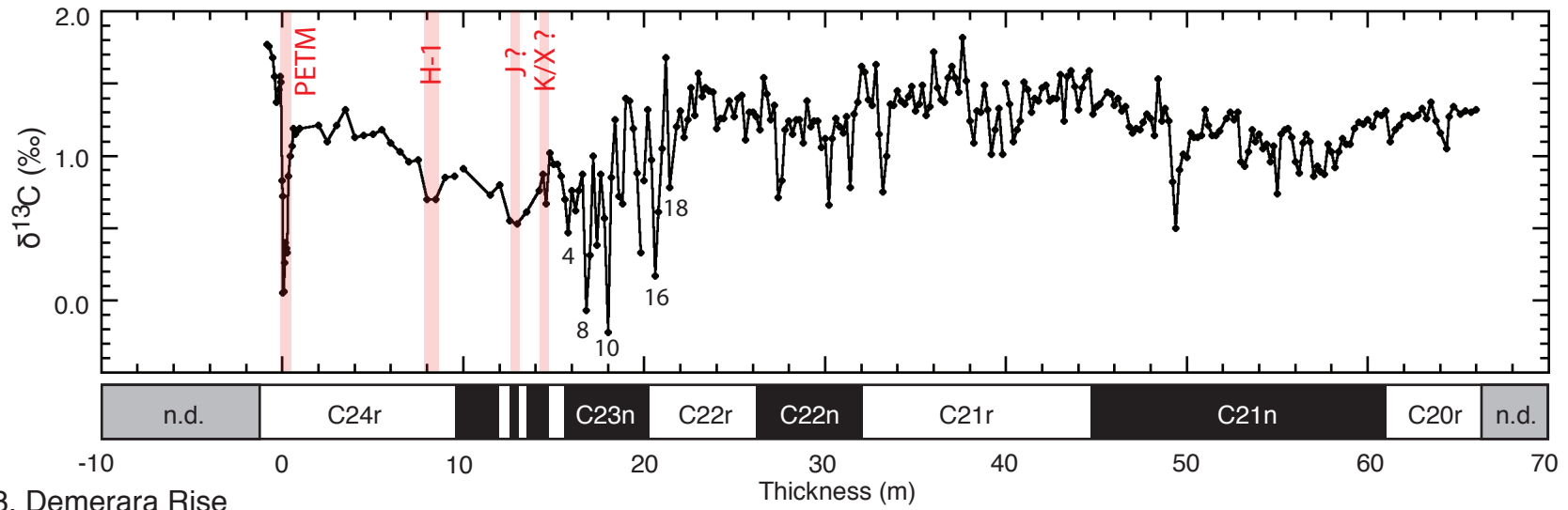DSDP Site 577

Figure 6
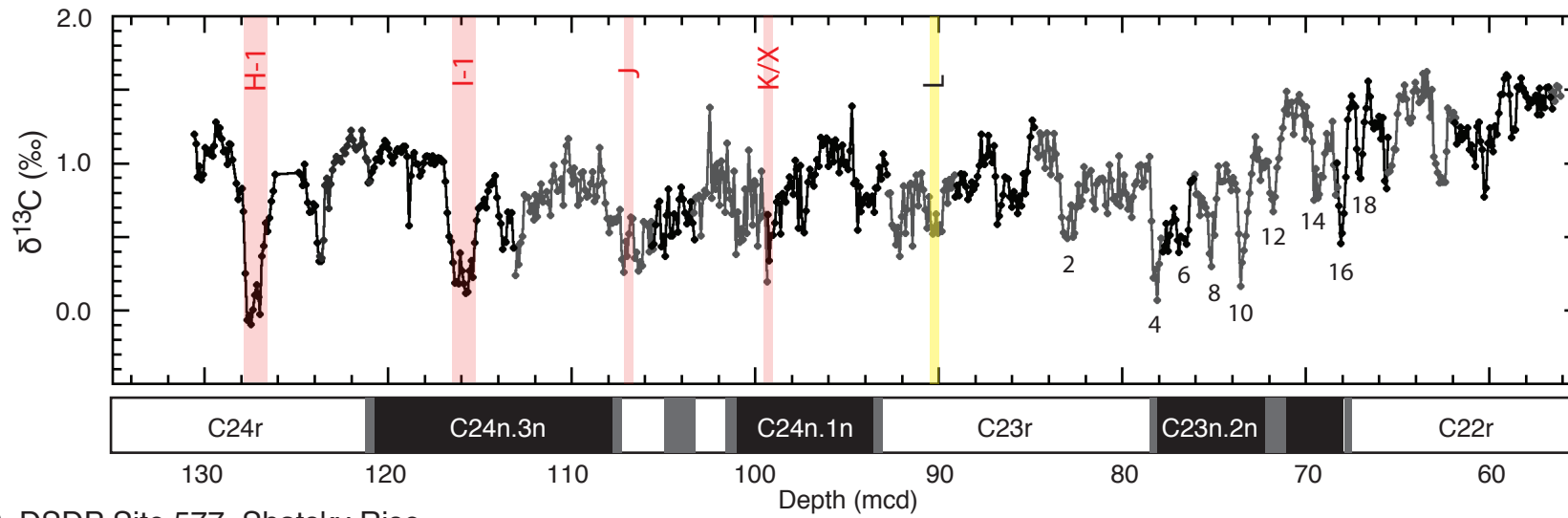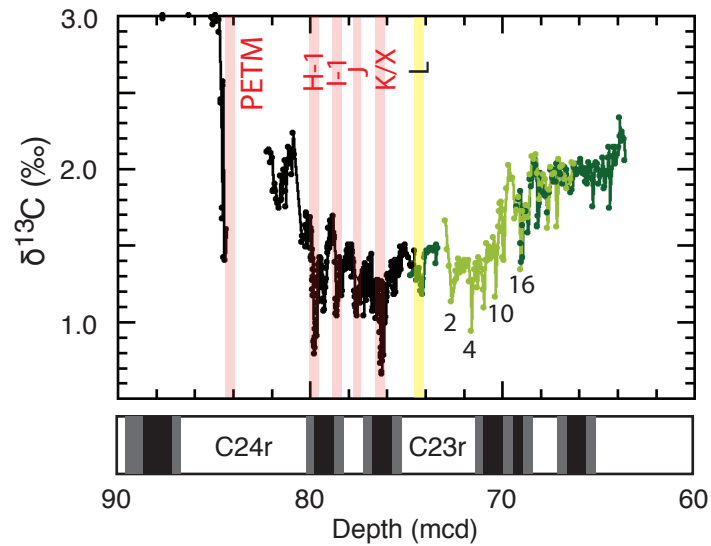
Possagno Section

Figure 7

DSDP Site 577

Figure 8

ODP Site 1051

A. Possagno, northeast Italy

B. ODP Site 1258, Demerara Rise
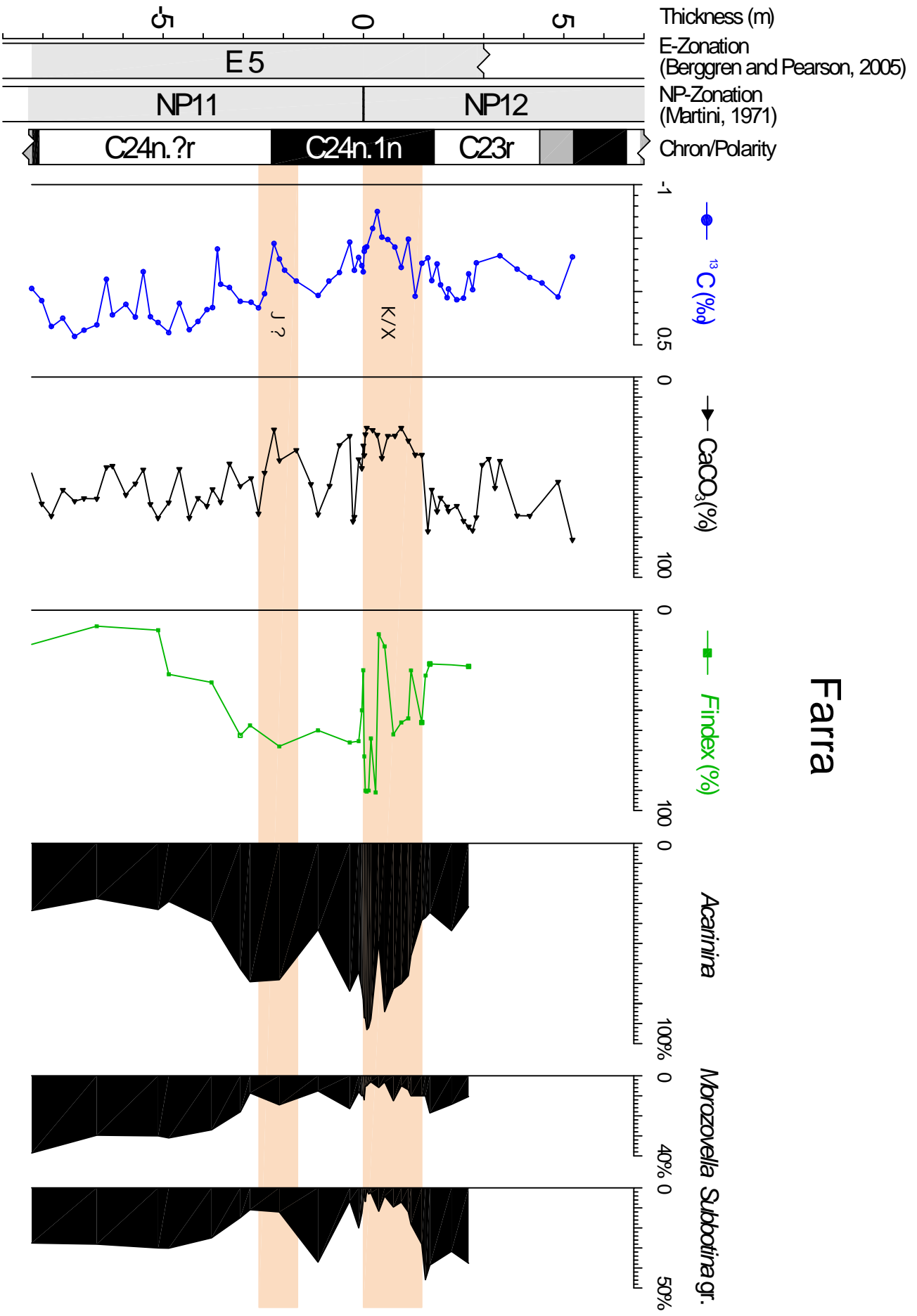
C. DSDP Site 577, Shatsky Rise

Figure 9

Figure 10

Farra

Thickness (m)

E-Zonation (Berggren and Pearson, 2005)

NP-Zonation (Martini, 1971)

Chron/Polarity

E 5

NP11   NP12

C24n.?r   C24n.1n   C23r

^{13}C (‰)

J ?   K/X

CaCO$_3$ (%)

F index (%)

Acarinina

Morozovella

Subbotina gr.

Figure 11